AN ABSTRACT OF THE DISSERTATION OF

Yung Hae Kim for the degree of Doctor of Philosophy in Animal Science presented on September 4, 2002.
Title: Role of Post-translational Modifications to Lens Proteins in Cataract Formation.

Abstract approved: Redacted for Privacy
Thomas R. Shearer

Cataract is a leading cause of blindness throughout the world, yet the fundamental biochemical causes are unknown. A rodent model of the biochemical processes is selenite cataract. This cataract shows some of the features of human cataracts such as increased lens calcium, proteolysis of proteins, and insolubilization leading to lens opacity. The goals of the current experiments were: (1) To measure changes in transcript levels for calpains and caspase 3 and oxidation of epithelial proteins in selenite cataract. (2) To elucidate changes in calpain 10 and its interaction with other calpains in selenite cataract. (3) To investigate changes in stability of βB1-crystallin caused by deamidation and truncation. These data would provide roles for apoptosis, protein insolubilization, proteolysis and deamidation observed in cataract.

To induce cataract, 12-day old rats were injected with an overdose of Na_2SeO_3. Epithelium was analyzed by competitive RT-PCR, zymography, and thiol-blotting. Calpains were detected by western-blotting. For βB1-crystallin stability studies, recombinant βB1-crystallins were denatured by urea or heat. Urea stability was

measured by circular dichroism and fluorescence spectrometry, and heat stability was measured by light scattering at 405 nm.

During selenite cataract formation, calpains in epithelium were activated resulting in increased proteolysis of crystallins, but mRNA levels for calpains did not show appreciable changes. Oxidation of sulfhydryls in epithelial proteins was minimal during cataract formation. These results suggested that calpain-induced proteolysis in the epithelium contribute to selenite cataract. In selenite cataract, calpain 10 proteins disappeared, which appeared to be due to degradation by calpain 2 and Lp82 calpain.

Deamidated βB1-crystallin was less stable in urea and heat, compared to wild-type. When the terminal extensions were removed, βB1-crystallin was as stable as wild-type. However, without the extensions, truncated βB1-crystallin caused accelerated precipitation in a complex with αA-crystallin, suggesting that the extensions may contribute to proper association with other crystallins and to stability of the soluble complexes.

In summary, proteolysis of proteins by calpains was more pronounced than protein oxidation in lens epithelium of selenite cataract. Deamidation and truncation caused instability of βB1-crystallin and abnormal association with αA-crystallin. Thus, proteolysis and deamidation may increase susceptibility of lenses to cataract.

Role of Post-translational Modifications to Lens Proteins in Cataract Formation

by
Yung Hae Kim

A DISSERTATION

Submitted to

Oregon State University

in partial fulfillment of
the requirements for the
degree of

Doctor of Philosophy

Presented September 4, 2002
Commencement June 2003

Doctor of Philosophy dissertation of Yung Hae Kim presented on September 4, 2002.

APPROVED:

Redacted for Privacy

Major Professor, representing Animal Science

Redacted for Privacy

Head of the Department of Animal Sciences

Redacted for Privacy

Dean of the Graduate School

I understand that my dissertation will become part of the permanent collection of Oregon State University libraries. My signature below authorizes release of my dissertation to any reader upon request.

Redacted for Privacy

Yung Hae Kim, Author

ACKNOWLEDGEMENTS

It has been a great period of learning and growing not only scientifically but personally as well. I have come to realize that this was all possible because of so much support and love from many different people around me. Without them, I would not be the person I am today.

First of all, I express my sincere appreciation to Dr. Tom Shearer, my major advisor, for his guidance, encouragement, patience, and support throughout my studies and during the preparation of this dissertation. Whenever needed, he was never too busy to see me. Especially, his prompt response to my requests and the thesis drafts helped this process be done in a timely manner.

Special thanks are due to Dr. Kirsten Lampi for her critique and advice on the βB1-crystallin studies, and to Dr. Larry David for his advice and assistance in mass spectrometry and chromatography. Both Dr. Lampi and Dr. David helped me enormously in carrying on the research projects. Much gratitude goes to Dr. Hans Peter Bachinger, whose expertise on protein biophysics was essential for the βB1-crystallin studies, and to Dr. Steven King for letting us use the spectrofluorimeter.

I also owe many thanks to our lab members, Dr. Hong Ma, Mrs. Marjorie Shih and Mrs. Deborah Kapfer, and a previous member Dr. Yoji Ueda for their assistance and friendship. My special thanks go to a great friend of mine, Dr. Chiho Fukiage, for her devotion, support, and patience over my silliness. I deeply

appreciate her time spent on lens dissections under the microscope and discussions as a scientist, as well as time spent as a friend.

I express sincere gratitude to Dr. Neil Forsberg, my previous advisor, for his support, understanding, and recommendation, and to Mr. Mike Beilstein for his support and friendship. I also thank Dr. Mitsuyoshi Azuma from Senju Pharmaceutical Co. for his support and recommendation. In addition, warm appreciation goes to the program committee members, Drs. Phil Whanger, Fred Menino, and Mina McDaniel for their time and support.

I thank my parents, sisters, brothers, the twins and friends, Bong Im and Soo-Lyon for their love, support and prayers. Finally I thank God my Lord for letting me meet great people and making me keep learning and growing.

The studies were supported by grants from the National Institute of Health, EY03600 to Dr. Shearer, EY12239 to Dr. Lampi, and EY07755 to Dr. David at the Oregon Health & Science University.

TABLE OF CONTENTS

TABLE OF CONTENTS (Continued)

TABLE OF CONTENTS (Continued)

LIST OF FIGURES

LIST OF FIGURES (Continued)

LIST OF FIGURES (Continued)

Role of Post-translational Modifications to Lens Proteins in Cataract Formation

1 INTRODUCTION

1.1 LENS OF THE EYE

The lens is a unique organ distinguished by its transparency and high protein content. Lens contains approximately 35% protein, the bulk of which is contributed by the soluble proteins called crystallins (Berman, 1991). The water content decreases significantly from the peripheral region to the center of the lens. The lens is comprised of two cell types: the outer layer of epithelial cells and the underlying differentiated lens fiber cells. Unlike other organs; blood, connective tissue and nerve cells are not present in the lens (McAvoy, 1981). The mature lens is separated from surrounding aqueous and vitreous humors by a thin basement membrane termed the lens capsule (Figure 1.1). The capsule controls lens shape while allowing the passage of small molecules (Harding, 1991a). A single layer of epithelial cells is located at the anterior pole of the lens. The epithelial cells divide at the germinative zone and move toward the lens equator. In the equatorial region, the epithelial cells differentiate into elongated fiber cells and surround mature fiber cells. During the differentiation, cell organelles, cell nuclei, mitochondria, and

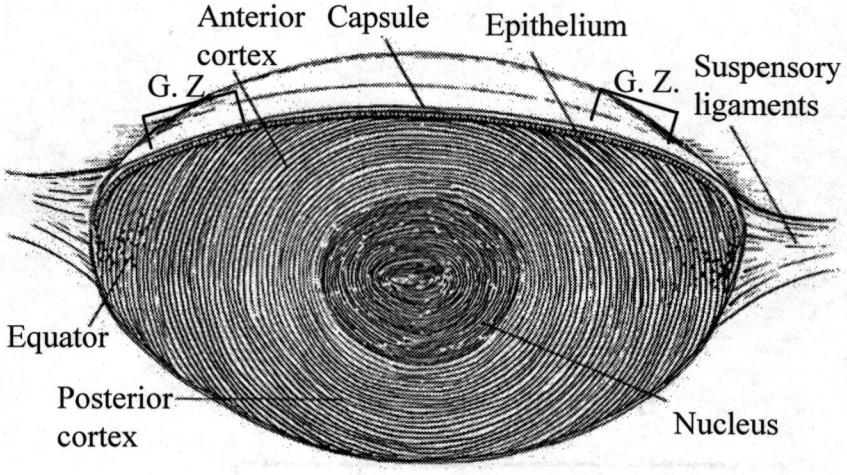

Figure 1.1: Anatomical overview of lens of the eye in cross section. G. Z., Germinative zone. Modified from Harding, J. J. (1997) *Biochemistry of the Eye*.

ribosomes are degraded. Terminally differentiated fibers are pushed toward the center of the lens as more superficial fiber cells differentiate into the cortex. The lens nucleus is the center region of the lens, and the fiber cells in the central nucleus are formed during embryonic development.

1.1.1 Lens transparency

The main function of the lens is to provide an adjustable refractive body to focus images onto the retina (Berman, 1991). For this function, the lens must be transparent and flexible with minimal light scattering. Lens transparency is achieved by structural regularity of the fiber cytoplasmic matrix composed of crystallins and cytoskeleton, and by uniform alignment of the fiber cell plasma membranes (Alcala, and Maisel, 1985). The absence of cell organelles in the fiber cell facilitates lens transparency. Delaye, and Tardieu (1983) reported from their small-angle X-ray study that the major proteins in lens are not in a crystalline array, but are relatively free as in a dense liquid, indicating a short-range order of proteins. This short-range order of the protein molecules was proven to be sufficient to ensure lens transparency (Veretout, Delaye, and Tardieu, 1989). With age, light transmission by lens decreases, and cataractous lenses scatter light significantly. Loss of transparency is the result of many types of physical and/or biochemical changes. These changes include formation of water-insoluble

aggregates from soluble proteins, membrane disintegration, and changes in the cytoskeletal organization (Berman, 1991). Therefore, any modification that disrupts transparency leads to light scattering and cataract.

1.1.2 Role of epithelium in lens metabolism

An important regulator of lens homeostasis is the single outer layer of epithelial cells, because the bulk of fiber cells underneath are devoid of cell organelles (Berman, 1991). Since the lens is an avascular tissue, it depends on the aqueous humor as the main source of nutrients needed for normal metabolism. The epithelium contains the majority of enzymes involved in cell division and growth, active transport of cations, amino acids, and myoinositol, and protein and lipid synthesis (Cheng, and Chylack, 1985). Transportation of intracellular materials between the epithelium and fiber cells is achieved via gap junctions along the plasma membranes (Rafferty, 1985). The primary purpose of the metabolism in lens is to maintain lens transparency, and abnormal metabolism in lens may result in loss of lens transparency.

Approximately 80% of the energy production in lens is provided by glucose metabolism mainly via glycolysis (Berman, 1991). Oxidative metabolism through the tricarboxlyic acid cycle provides only 5% of the energy for the lens. The pentose phosphate pathway is an important system for NADPH production and

accounts for approximately 10 to 15% of glucose metabolism. NADPH is used in several key metabolic systems in the lens, especially for maintaining high levels of reduced glutathione. Another notable carbohydrate metabolic pathway in lens is the sorbitol pathway. This pathway is responsible for formation of sugar cataracts (Cheng, and Chylack, 1985). Increased glucose level in the lens epithelium from a disease such as diabetes leads to accumulation of cell-impermeable sorbitol due to reduction of glucose via aldose reductase in the sorbitol pathway. This increases the osmotic pressure within the lens fibers, leading to cellular swelling, rupture, and disintegration.

Lens contains relatively high concentrations (average 4-6 mM) of glutathione, γ-glutamyl-cysteinyl-glycine tripeptide (Giblin, 2000). The lens epithelium contains the highest concentration of reduced glutathione (GSH). The GSH concentration decreases in the cortex and is much lower in the nucleus. Interestingly, lens cortex in rabbit and guinea pig contains over 20 mM GSH, and the epithelium may contain even higher concentrations (Giblin, 2000). Glutathione in lens epithelium exists mainly in a reduced form (GSH), and oxidized glutathione (GSSG) can hardly be detected. Glutathione plays an important role as an antioxidant in the lens for major functions such as (1) maintenance of protein sulfhydryl groups in the reduced state, (2) protection of cell components from oxidative damage by H_2O_2, (3) removal of xenobiotics through a reaction catalyzed by glutathione S-transferase, and (4) participation in amino acid transport (Berman, 1991). Reduction of disulfide bonds and maintenance of protein sulfhydryl groups by GSH

are probably the most important functions of GSH. Maintenance of Na-K-ATPase by preventing thiol oxidation is an indirect role of GSH in ion transport (Cheng, and Chylack, 1985).

Maintenance of ionic balance is essential for lens function, especially for calcium, sodium, and potassium balance. In many cataracts, increases in lens calcium and sodium concentrations have been reported (Harding, 1991b). The epithelium is essential for ion transport, since ion channels are mainly located in the epithelial cell membranes. Active transport of sodium and potassium is controlled by Na-K-ATPase located exclusively in anterior epithelial cells (Patmore and Duncan, 1981). Calcium tends to leak into the lens from the aqueous humor. Active efflux of calcium is regulated by Ca-ATPase located predominantly in the epithelium and cortex, and it is not dependent on sodium or potassium levels (Harding, 1991a).

Protein synthesis in the lens occurs in the epithelium and peripheral cortex throughout life (Berman, 1991; Harding, 1991a). Remarkably, protein synthesis and turnover of protein is minimal in the nucleus of the lens. However, the pattern of protein synthesis in lens cells is different depending on the developmental stage of the cell (Graw, 1997). α-crystallins are synthesized in epithelium, but β- and γ-crystallins are synthesized during or after elongation of the fiber cell. In addition, synthesis of individual subunits of β- and γ-crystallins depends on the developmental stage. During aging of the lens, lens proteins also undergo

modifications such as proteolysis and deamidation and accumulation of modified proteins, which may contribute to loss of lens transparency.

1.1.3 Crystallins of the lens

Crystallins are the principal soluble structural proteins in the lens. They are highly organized and are maintained without turnover throughout the lifetime of the host (Slingsby and Clout, 1999). The important physiological function of crystallins is maintenance of lens transparency by their short-range spatial order (Delaye and Tardieu, 1983). The solubility of crystallins is a critical factor for lens transparency. Insolubilization of crystallins resulting in light scattering occurs during aging and cataract formation (Berman, 1991; Graw 1997).

Crystallins in the mammalian lens are divided into three major classes: α-, β-, and γ-crystallins (Reviewed by Berman, 1991; Graw, 1997; Slingsby and Clout, 1999). α-crystallins form very large oligomers (~800 kDa) composed of the 20 kDa αA and αB subunits. α-crystallins are related to small heat-shock proteins and have chaperone-like activity. β-crystallins form oligomers ranging in size from 50 to 200 kDa. They are composed of seven different subunits ranging in size from 20 to 30 kDa. The β-crystallin subunits are divided into acidic (βA1, βA2, βA3, βA4) and basic (βB1, βB2, βB3) families. The basic β-crystallins have the N- and C-terminal peptides extending from their core globular domain structures, whereas the

acidic β-crystallins lack the C-terminal extensions. γ-crystallins are comprised of six 21 kDa monomers, γA-γF, and they are concentrated in the lens nucleus (Lindley et al., 1985). β- and γ-crystallins share sequence homologies and a similar two-domain folding structure. The difference between β- and γ-crystallins is the presence of long N-terminal extensions on the β-crystallin subunits. This suggests a possible role of the N-terminal extensions in oligomerization of β-crystallins.

Lens crystallins are modified during aging. The major post-translational modifications of crystallins are truncation and deamidation. The N-terminal extensions of β-crystallins are most susceptible to proteolysis (David et al., 1996; Lampi et al., 1998; Ma et al., 1998; Hanson et al., 2000). During cataract formation in animal models, the rate of proteolysis is increased leading to insolubilization of crystallins (David, Wright, and Shearer, 1992; Shearer et al., 1997).

Deamidation has been detected in α-, β-, and γS-crystallins during aging (Lund, Smith and Smith, 1996; Lampi et al., 1998; Ma et al., 1998; Takemoto and Bolye, 1998; Hanson et al., 2000; Takemoto and Boyle, 2000; Takemoto, 2001). Takemoto and Boyle (2000) found increased deamidation in γS-crystallin during human senile cataract formation. The mechanism of deamidation was suggested to be non-enzymatic (Takemoto, Fujii and Bolye, 2001).

βB1-crystallin is a major subunit among the family of β-crystallins in man. βB1-crystallin forms tetramers or octamers identified from size exclusion

chromatography (Ajaz et al., 1997). Human βB1-crystallin contains an N-terminal extension of 57 amino acids and C-terminal extension of 18 amino acids (David et al., 1996). The N-terminal extension on βB1-crystallin was reported to be missing 15 amino acids in the newborn human lens (David et al., 1996). During maturation, truncation of the N-terminus increases, and by early adulthood, βB1-crystallin is extensively degraded (David et al., 1996; Lampi et al., 1998; Ma et al., 1998; Hanson et al., 2000). As the βB1-crystallin is degraded by age, it also undergoes deamidation (Lampi et al., 1998; Ma et al., 1998; Hanson et al., 2000). We recently showed that truncation of βB1-crystallin *in vitro* caused retarded elution of βB1-crystallin on size exclusion chromatography (Lampi et al., 2001). Bateman et al. (2001) also showed similar results with several truncated βB1-crystallin mutants. On size exclusion chromatography deamidated βB1-crystallin (Q204E) eluted earlier than WT, even though multi-angle light scattering showed both proteins to be dimers. Since dramatic changes in the secondary structure were not observed (Lampi et al., 2001), we concluded that deamidation altered the shape of the dimer.

However, it is not known if truncation and deamidation cause changes in protein stability. Also, we do not know if the truncation of the N-terminal extension affects the secondary structure of protein. Both truncation and deamidation are most likely to occur on the crystallins during lens maturation or senile cataract formation. It is important to investigate if concurrent truncation and deamidation cause a synergistic effect on protein stability or behavior. Thus, a goal of the

studies presented below was to determine how stability of βB1-crystallin is affected by deamidation and/or truncation as measured by urea-induced and heat-induced denaturation.

1.2 LOSS OF LENS TRANSPARENCY AND CATARACT FORMATION

1.2.1 Causes of lens opacity

Cataract is the major cause of blindness throughout the world (Harding, 1991b). Although cataract can occur as a result of disease or congenital abnormalities, the majority of human cataract is associated with the aging process.

During aging, many changes occur in lens, and many of these changes can lead to opacification and cataract formation. The changes in the aging lens include increases in lens weight, increased thickness and yellow coloring, and a decrease in accommodative power (Harding, 1991c). Less obvious changes include increases in minor, peripheral opacities, increased fluorescence, post-translational modifications of proteins, and decreased activities of enzymes. Lens opacity is a result of complex multi-factorial processes, and significant changes in lens usually occur before the appearance of lens opacity. Aged human lens epithelium exhibits decreased intracellular organelles, condensation of chromatin, accumulation of

cytoplasmic granules, and an increase in cytoplasmic filaments (Cheng, and Chylack, 1985).

In human and a variety of animal cataract models, three major mechanisms are known to cause cataract: UV radiation, oxidation and osmotic stress (Graw, 1997). Osmotic imbalance is present in sugar cataract such as in diabetes or galactosaemia (Berman, 1991; Chylack, 1981; Harding, 1991b). Excessive amounts of glucose, galactose, or xylose are converted to the corresponding sugar alcohol (glucose to sorbitol; galactose to dulcitol; xylose to xylitol). Accumulation of these sugar alcohols in the epithelial and fiber cells causes a hypertonic intracellular environment relative to the extracellular fluid. The osmotic disequilibrium then causes influx of water to the cells and results in swelling, formation of interfibrillar and intracytoplasmic foci of light scattering, and later cataract formation (Chylack, 1981).

Cataract can be produced in experimental animals by many types of radiation, including X-rays, β- and γ-radiations, neutron radiation, protons and heavy ions, infrared, microwave, ultraviolet (UV), sunlight, and visible radiation (Harding, 1991b). Oxidative insults are associated with epithelial cell damages, followed by lens opacification. The main targets of radiation-induced, free radical, and oxidative damage in the lens are proteins such as crystallins and membrane proteins (Ottonello et al., 2000). UV-radiation is the most extensively studied cataractogenic agent. UV is believed to induce generation of oxidative free radicals (Ottonello et al., 2000). UV-radiation can also cause yellowing of lens by altering

tryptophan residues (Berman, 1991). The effects of oxidative insults on the lens have been studied in numerous animal cataract models. Animal experiments are performed because human cataract also shows evidence for oxidative changes, such as loss of reduced glutathione and protein thiols, increases in mixed disulfides, protein-protein crosslinks, and methionine sulfoxide formation in proteins (Harding, 1991b). Selenite cataract model is one of the animal models thought to be caused by oxidative stress and will be discussed below.

1.2.2 Selenite cataract model

Selenite cataract is a rapid and convenient model of nuclear cataract. Several morphological and biochemical changes occurring in human cataractous lenses have also been reported in selenite cataract: (1) cytosolic lipid membrane structures become discontinuous with the plasma membrane (Boyle, Blunt, and Takemoto, 1997; Boyle, and Takemoto, 1997), (2) decreased amounts of reduced glutathione (Rao, Sadasivudu, and Coltier, 1983; David, and Shearer, 1984a; Shearer, David, and Anderson, 1987; Harding, 1991d; Chakrapani et al., 1995; Mitton, Hess, and Bunce, 1997), (3) elevated calcium (Shearer, and David, 1982; Bunce, Hess, and Batra, 1984; Harding, 1991d), (4) increased water insoluble proteins (Shearer, and David, 1982; Shearer, David, and Anderson, 1987; Harding, 1991d), and (5) decreased water soluble proteins (Spector, 1984; Harding, 1991d).

Selenite cataract is produced in suckling rat pups by an overdose of sodium selenite (Na_2SeO_3). A single subcutaneous injection of selenite into 10-14 day old rats produces the nuclear cataract within 3-5 days (reviewed in Shearer et al., 1997). Multiple, lower doses of selenite by injection or by mouth also can induce nuclear cataract in rat pups (Huang et al., 1992). Selenite is cataractogenic only when administered to young rats within the critical maturation period of the lens up to approximately 16 days of age (Ostadalova, Babicky, and Kopoldova, 1988).

Development of selenite cataract is probably initiated by an oxidative stress caused by selenite, since a rapid decrease of reduced glutathione was observed during selenite cataract formation (David, and Shearer, 1984a). Treatment with anti-oxidants can prevent or delay selenite cataract formation *in vivo* (Gupta, and Joshi, 1994; Blunt, and Takemoto, 2000; Yilmaz et al., 2000) and *in vitro* (Ito et al., 2001a). These anti-oxidant treatments also prevented the deleterious biochemical changes from occurring during selenite cataract formation. These included decreases in reduced glutathione and protein thiol content and an increase in lipid peroxidation levels (Ito et al., 2001a). Such observations suggested that oxidative damage may be one of the earlier biochemical alterations in selenite cataractous lenses. Interestingly, Ito et al. (2001b) reported involvement of nitric oxide in selenite cataract development. Nitric oxide is a reactive nitrogen species radical, and it is produced by nitric oxide synthase from oxidation of L-arginine (Drew and Leeuwenburgh, 2002). Nitric oxide is known to play a significant role in cell signaling, vasodilation, immune response, and aging, as well as numerous disease

developments (Becquet, Courtois, and Goureau, 1997; Drew and Leeuwenburgh, 2002). In selenite cataract, nitric oxide was detected at one day after injection before cataract appeared. Inducible nitric oxide synthase seemed to be responsible for elevated nitric oxide in selenite cataract formation (Ito et al., 2001b).

During the cataract formation by selenite, numerous biochemical changes have been observed, including altered epithelial metabolism, calcium accumulation, calpain-induced proteolysis, crystallin precipitation, phase transition, and cytoskeletal loss (Figure 1.2; Shearer et al., 1997).

Lens epithelium is the first layer exposed to the oxidative insult of selenite during selenite cataract formation, and metabolic changes occur before the lens opacity appears. Altered metabolic changes in the epithelium include (1) suppressed mitosis and cell nuclear fragmentation in the germinative zone (Anderson, Shearer, and Claycomb, 1986), (2) increases in DNA damage, repair, and replication (Huang, Hess, and Bunce, 1990), (3) decreased rate of epithelial cell differentiation (Cenedella, 1987), (4) loss of calcium homeostasis resulting in increased calcium influx and decreased calcium pump activity (Wang, Bunce, and Hess, 1993), and (5) apoptosis (Tamada et al., 2001).

As seen in most cataracts (Harding, 1991b), massive accumulation of calcium was observed in selenite cataract, especially in nuclear region of lens where the opacity occurs (David, and Shearer, 1984b; Hightower, David, and Shearer, 1987). Proteolysis and insolubilization of crystallins in the nucleus region is pronounced in selenite cataract (David, and Shearer, 1984b). The massive increase in calcium

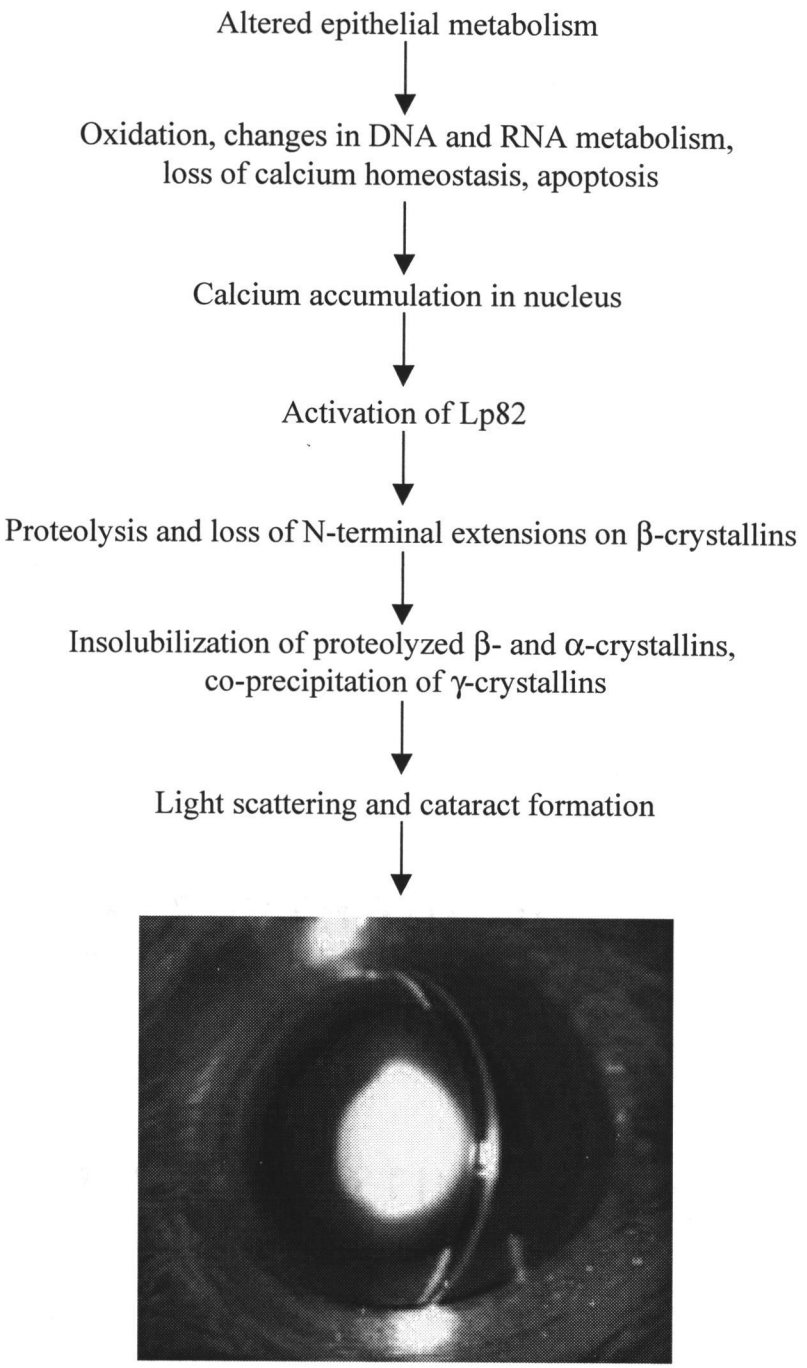

Figure 1.2: Mechanism of selenite nuclear cataract formation (Shearer et al., 1997).

may activate calcium-activated protease, calpain, during selenite cataract formation. Calpains comprise a family of calcium-dependent non-lysosomal, cysteine proteases (reviewed in Huang, and Wang, 2001). Calpain 1 (calpain I, μ-calpain, and CAPN1) and calpain 2 (calpain II, m-calpain, CAPN2) are ubiquitously distributed mammalian calpains. To date, at least 12 additional mammalian calpains have been identified, including tissue-specific calpains and atypical calpains with calcium-binding domain replaced or missing. The typical four-domain structure of calpain catalytic subunit is comprised of domain I (autolytic activation), domain II (cysteine catalytic site), domain III (electrostatic switch), and domain IV (calmodulin-like calcium binding sites) (Figure 1.3; Huang, and Wang, 2001).

Lens-specific calpain Lp82 is found in most lenses except human lenses (Ma et al., 1998a; Ma et al., 1998b) along with ubiquitous calpains 1 and 2 (David, and Shearer, 1986; Ma et al., 1997). Lp82 is a splice variant of skeletal muscle-specific calpain p94 (Ma et al., 1998a) with deletions of NS, IS-1 and IS-2 regions. A rodent-specific isozyme Lp85 also exists in lens (Ma et al., 2000a). Until Lp82 was discovered, calpain 2 was thought to be the major calpain involved in rat lens maturation and cataract formation (David, Wright, and Shearer, 1992; David, Shearer, and Shih, 1993; Azuma et al., 1997). Similar cleavage sites on β-crystallins produced by calpain 2 *in vitro* were found in selenite cataract (David, Wright, and Shearer, 1992; David, Shearer, and Shih, 1993; Shearer et al., 1995). However, Lp82 shows major proteolytic activity in nuclear region of young rats,

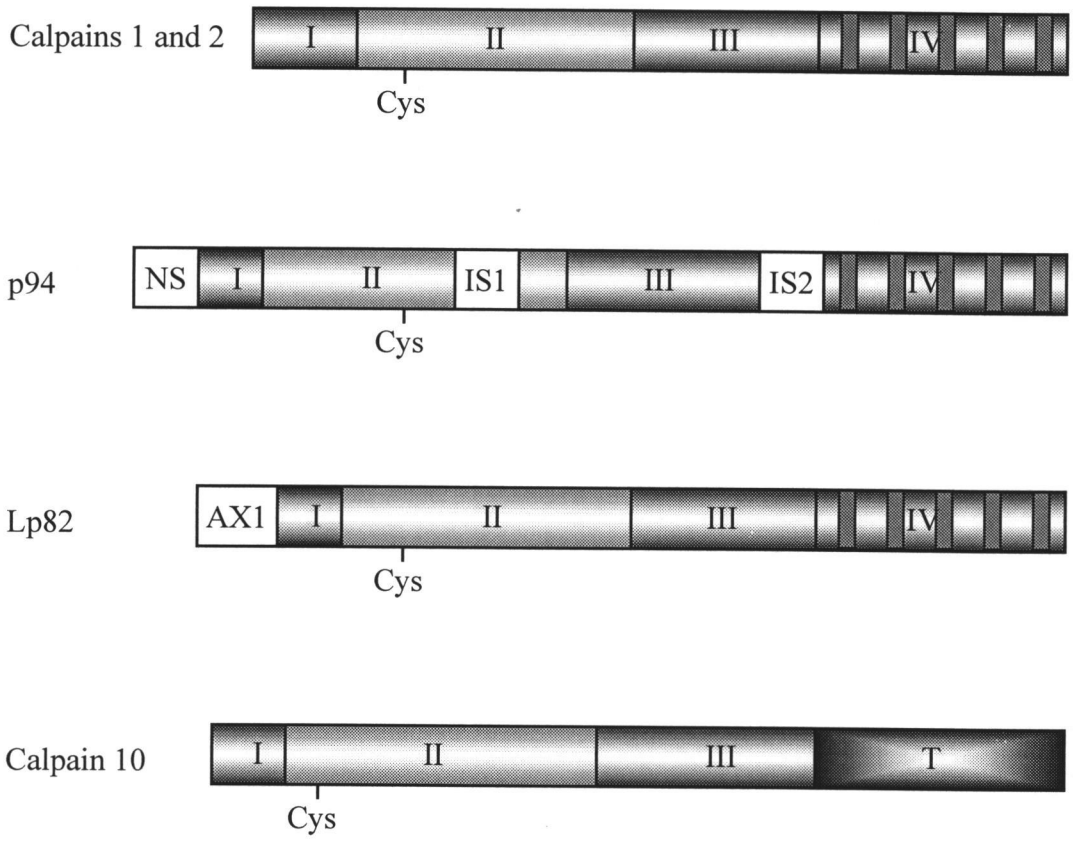

Figure 1.3: Domain structure of calpains. I, II, III, and IV or T are the main domains in calpain family.

while calpain 2 is concentrated in epithelium and cortex (Ma et al., 1998b; Shearer et al., 1998). Similar localization patterns of Lp82 and calpain 2 were observed in lenses from mouse (Ma et al., 1999; Ma et al., 2000b). Recently, a major cleavage site on αA-crystallin in the nucleus from selenite cataract was identified to be Lp82-specific (Ueda et al., 2002), suggesting activation of Lp82 in nucleus during selenite cataract formation, rather than calpain 2.

Another newly characterized calpain in lens is calpain 10 (Ma et al., 2001). Calpain 10 has domains I, II and III, but the C-terminal T domain has no EF-hand motifs (Figure 1.3). Interestingly, Horikawa et al. (2000) recently reported that genetic variation in calpain 10 gene was associated with an increased risk for type 2 diabetes mellitus in certain human population groups. The calpain 10 gene was ubiquitously expressed and at least eight alternative splice variants exist, some of which would lack the proteolytic domain II. The function of calpain 10 is not known yet, and further study is needed to elucidate the role of calpain 10 in selenite cataract.

Calpains cause rapid proteolysis, precipitation of lens crystallins and cataract in young rodent lenses. The insoluble pellet in selenite cataract is massive, comprising 17% of the total protein in the nucleus (David, and Shearer, 1984b). The mechanism for insolubilization of truncated crystallins is not clear. We hypothesize that the truncation of crystallins by calpain decreases the solubility of crystallins. Covalent associations between crystallins or truncated crystallins are not the cause of selenite cataract. Contrary to human cataracts (Harding, 1991d),

selenite cataract showed no additional protein-protein disulfide bonds in the insoluble pellet (David, and Shearer, 1984a). High molecular weight aggregates were not found after size exclusion chromatography of proteins in selenite cataract (David, Wright, and Shearer, 1992). In addition, a shift from the βH-crystallin to the βL-crystallin fraction was observed, as has been found in truncated βB1-crystallins from aged human lens (Ajaz et al., 1997). This indicates the high susceptibility of βB1-crystallin to proteolysis and loss of the ability to assemble into highly ordered aggregates. Simple insolubilization of truncated crystallins was supported by the observed decrease in phase separation temperature in selenite cataract lenses (Shearer, David, and Anderson, 1986). Selenite cataract was prevented by phase separation inhibitors (Clark, and Steele, 1992; Hiraoka et al., 1996).

Loss of cytoskeletal proteins was also observed in selenite cataract lenses (Matsushima et al., 1997; Clark et al., 1999). Selenite accelerated the loss of actin, tubulin/vimentin, and spectrin as well as several unidentified nuclear proteins. In normal lens, the relative amounts of cytoskeletal proteins decreased as crystallin synthesis accelerated during differentiation (Clark et al., 1999). After initial organization of lens proteins, decreases in cytostructural proteins may facilitate lens transparency. In addition, lens cytoskeletal proteins and selected crystallins appear to be substrates for the same proteases that result in post-translational modification and altered interactions between proteins (Truscott et al., 1989; Sanderson, Marcantonio, and Duncan, 2000). However, the rapid loss of cytoskeletal proteins

in selenite cataract may cause morphological instability of fiber cells and disrupt associations between crystallins and the cytoskeletal structures, and subsequently lead to opacity.

Selenite cataract is a useful model for understanding the mechanism of cataract formation caused by an oxidative stress and to screen potential anti-cataract agents. The rapid and reproducible occurrence of cataract allows repeated experiments in a brief time period. The model also provides insights on the effect of post-translational modification to crystallins. Selenite cataract has been especially useful for studying the effects of truncation, the role of calpains in lens, and insolubilization and precipitation of crystallins. Extensive studies have reported the morphological and biochemical changes in selenite cataract, but the exact biochemical mechanism of selenite cataract has yet to be elucidated.

1.3 PURPOSE OF STUDIES

As described above, lens epithelium is important for maintaining lens homeostasis. The epithelium is first exposed to selenite when young rats are treated with sodium selenite. The major observations in selenite cataract are massive elevation of intracellular calcium, activation of calpains, and proteolysis of crystallins and cytoskeletal proteins leading to lens opacity. The purpose of our studies on epithelium was to elucidate changes in lens epithelium during cataract

formation as related to: (1) changes in expression of calpains and caspase 3 involved in apoptosis, (2) changes in epithelial proteins and calpain activities, and (3) changes in oxidation of lens epithelial proteins.

During lens maturation and selenite cataract formation, calpains play an important role in post-translational modification of crystallins. The function of newly characterized calpain 10 is not known yet. Thus, in the second section of the studies, we investigated (1) changes in calpain 10 protein level during aging and selenite cataract formation, and (2) hydrolysis of calpain 10 by other calpains in lens.

During the normal aging process, lens crystallins undergo post-translational modifications, yet some lenses with modified proteins remain transparent. However, progressive changes in crystallins in cataract lead to insolubilization, aggregation, and opacity. Thus, it is important to characterize how the post-translational modifications affect the physical properties of crystallins. βB1-crystallin is an abundant subunit comprising approximately 9% of total crystallins in human lens (Lampi et al., 2001). Modifications to βB1-crystallin cause loss in ability to assemble into high-ordered aggregates (David, Wright, and Shearer, 1992; Ajaz et al., 1997). In the third part of our studies, we investigated the effects of post-translational modifications on βB1-crystallins on stability as related to: (1) changes in behavior and structure of modified βB1-crystallins, and (2) changes in protein stability induced by urea and heat.

2 MATERIALS AND METHODS

2.1 STUDIES ON EPITHELIAL CHANGES IN SELENITE CATARACT

2.1.1 Cataract model *in vivo* and tissue collection

An overdose of sodium selenite (Na_2SeO_3, ICN Biochemicals, Inc., Plainview, NY) was used to produce cataract in Sprague-Dawley rats (B & K Universal, Fremont, CA). Cataract was induced by a single subcutaneous injection of 30 μmol of sodium selenite/kg body weight into 12-day old rat pups as previously described (Shearer et al., 1997). All animals were handled in compliance with the "Guiding Principles in Care and Use of Animals" (DHEW publication, NIH 86-23), and according to the tenets of the ARVO Statement for the Use of Animals in Ophthalmic and Vision Research.

Lenses were subsequently removed by a posterior approach, and lens capsule/epithelium dissections were performed under a dissecting microscope by removing the capsule with adhering epithelium. Lens epithelial preparations were pooled to obtain sufficient material. The interface between the cortex and nucleus of the remaining lens mass was determined by the appearance of cold cataract, and cortical and nuclear regions were dissected at approximately 50% of the lens

radius. All lens and soft tissues were chilled on ice throughout the dissection to prevent breakdown of RNA.

2.1.2 Competitive RT-PCR

In order to investigate if changes in gene expression of several enzymes occurred in lens epithelial cells during selenite cataract formation, competitive RT-PCR was performed, and the number of mRNA copies for specific genes was calculated. Total RNA was extracted from lens epithelial cells at 12 hours, 3 and 5 days after selenite injection in TRIzol reagent (Invitrogen, Carlsbad, CA), and RNA quantitation was performed at A_{260}. Gene specific primers were synthesized based on cDNA sequences (accession numbers for calpain 1, U53858; calpain 2, L09120; Lp82, U96367; calpastatin, X56729; caspase 3, U84410) from each mRNA (Table 2.1). Internal RNA standards were constructed by first using a downstream composite primer to delete 100-150 bp in the mRNA templates during reverse transcription. An upstream composite primer containing SP6 RNA polymerase binding region, ATT TAG GTG ACA CTA TAG AAT AC, upstream of each 5' upstream primer was added to the PCR reaction to produce cDNA used as internal standards. These cDNAs for each internal standard were transcribed *in vitro* with SP6 RNA polymerase (MAXIscript SP6 Kit, Ambion, Austin, TX) to produce RNA which could be used competitively in subsequent RT-PCR reactions.

Table 2.1: RT-PCR primers

Primer name	Position within cDNA (Nucleotides)	Primer sequence 5' – 3'	PCR product size (bp)	PCR cycle #
mCal-up	Calpain 2 1436-1465	gggcagaccaacatccacctcagcaaaaac	404	30
mCal-down	Calpain 2 1811-1839	gtctcgatgctgaagccatctgacttgat	404	
mCal-IS-up	SP6/Calpain 2 1436-1465	atttaggtgacactatagaatacgggcagaccaacatccacctcagcaaaaac	310	
mCal-IS-down	Calpain 2 1691-1712/1811-1839	gtctcgatgctgaagccatctgacttgatccatctccaatgtcctcctc	310	
Lp82-up	Lp82 272-302	gaaagccaagatgaaggccatcacttggaag	551	35
Lp82-down	Lp82 797-822	actgcaccggaacaattgtatcaatg	551	
Lp82-IS-up	SP6/Lp82 272-302	atttaggtgacactatagaatacgaaagccaagatgaaggccatcacttggaag	423	
Lp82-IS-down	Lp82 642-662/797-822	actgcaccggaacaattgtatcaatgtttcagagcttcataggaacc	423	
μCal-up	Calpain 1 1257-1270	gtggatgacgcagacgacta	457	33
μCal-down	Calpain 1 1688-1707	cccctgctaacttgctgaac	457	
μCal-IS-up	SP6/Calpain 1 1257-1270	atttaggtgacactatagaatacgtggatgacgcagacgacta	355	
μCal-IS-down	Calpain 1 1560-1579/1688-1707	cccctgctaacttgctgaacaagaagcgcagcagaaagtc	355	
Calpst-up	Calpastatin 1376-1395	tggcactgagaggagagaca	448	35
Calpst-down	Calpastatin 1802-1823	tgcatcttcatccacctttggc	448	
Calpst-IS-up	SP6/Calpastatin 1376-1395	atttaggtgacactatagaatactggcactgagaggagagaca	329	
Calpst-IS-down	Calpastatin 1659-1678/1802-1823	tgcatcttcatccacctttggggcagctatccaagtcttc	329	
Casp-up	Caspase 3 424-443	ggacctgtggacctgaaaaa	463	35
Casp-down	Caspase 3 867-886	taccccactcccagtcattc	463	
Casp-IS-up	SP6/Caspase 3 424-443	atttaggtgacactatagaatacggacctgtggacctgaaaaa	328	
Casp-IS-down	Caspase 3 712-731/867-886	taccccactcccagtcattctgcatgaattccagcttgtg	328	

This copied the same section of cDNA as in each wild-type mRNA but lacking a specific section of known length. The RNA standards were quantitated at A_{260}, and their copy numbers were calculated.

For RT-PCR for calpain 2 and Lp82, 100 ng total RNA was used, and 300 ng was used for calpastatin RT-PCR, and 200 ng was used for caspase 3 and calpain 1. Competitive RT-PCR was performed using a one-step system (Invitrogen). Total RNA and increasing amounts of each internal RNA standard were added in a 1× reaction mixture containing 0.2 mM each dNTP, 2.4 mM $MgSO_4$, 0.2 μM each upstream and downstream primer, and RT/Taq enzyme mix in a total volume of 50 μl. Reverse transcription was performed at 50°C for 30 min, (except for Lp82 at 55°C), and then the mixture was heated at 94°C for 2 min. The PCR reaction was continued for the cycle numbers specific for each mRNA (Table 2.1): denaturation, 94°C for 30 sec (45 sec for Lp82); annealing, 60°C for 30 sec (65°C for 45 sec for Lp82); primer extension, 72°C for 1 min and final primer extension, 72°C for 10 min.

PCR products from wild-type mRNAs and internal standards were visualized on 1.5% ethidium bromide-stained gels, scanned with a flatbed scanner, and digitized. NIH image software (version 1.57) was used to invert the image, and to determine the uncalibrated optical density of the bands corresponding to mRNA-specific products and their competing RNAs. Equivalence point analysis using linear regression was then used to calculate copies of mRNA per μg total RNA. Depending on the availability of pooled epithelial RNA samples, duplicate,

triplicate, 5 or 6 repeats were used for RT-PCR. Percent change in mRNA in lens epithelia from selenite cataract was compared to mRNA in age-matched control epithelia. Control mRNA was expressed as 100%. The data with enough repeats were analyzed statistically using ANOVA as a one-way comparison to age-matched controls.

2.1.3 SDS-PAGE and casein zymography

To investigate protein changes in lens epithelial cells during selenite cataract formation, SDS-PAGE was performed using 12% Novex Tris-Glycine precasted minigels (Invitrogen). For protein preparation, dissected tissues were homogenized in Tris buffer containing 20 mM Tris-HCl, 1 mM EDTA, 1 mM EGTA, 2 mM dithioerythritol (DTE), pH 7.4. Soluble and insoluble proteins were obtained by centrifugation at 13,000× g for 20 minutes at 4°C. Protein concentrations were determined by the Bio-Rad protein assay kit (Hercules, CA) using BSA as standard. For changes in calpain activities in epithelial cells, casein zymography was performed as described by Shearer et al. (2000). 10% native polyacrylamide gels, 1 mm thick, were co-polymerized with 0.05% casein in 225 mM Tris-HCl, pH 7.5. The stacking gels contained 4% acrylamide in 125 mM Tris-HCl, pH 6.8. Gels were run with a buffer containing 25 mM Tris, 192 mM Glycine, 1 mM EGTA, 1 mM DTE, pH 8.3 at 125 V for 150 minutes at 4°C. After electrophoresis,

gels were incubated overnight at room temperature in a calcium incubation buffer containing 20 mM Tris-HCl, 10 mM DTE, 20 mM $CaCl_2$, pH 7.4. Gels were stained with Coomassie Brilliant Blue (Pierce Biotechnology, Inc., Rockford, IL). Bands of caseinolysis appeared white on a blue background.

2.1.4 Isolation of soluble protein from the epithelium of cataractous lenses

3-(N-maleimidopropionyl) biocytin (MPB; Sigma, St. Louis, MO) is a specific thiol-binding compound cross-reacting with avidin. To allow free sulfhydryl groups to bind to MPB, dissected epithelia were homogenized in Tris buffer with no reducing agent containing 20 mM Tris (pH 7.4), 1 mM EDTA, 1 mM EGTA, and MPB at 37.5 μg/mg protein.

2.1.5 *In vitro* alkylation and oxidation of lens epithelial proteins

To verify the thiol-blot protocol, lens epithelial proteins were alkylated *in vitro* using iodoacetamide (IAA), prior to MPB treatment. Epithelial soluble proteins obtained from 12-day old lens were incubated with 5 mM IAA for an hour at 37°C.

To study how selenite affects oxidation of lens epithelial proteins, 100 μM sodium selenite was incubated with epithelial soluble proteins for 1 hour at 37°C.

2.1.6 Two-dimensional (2-D) gel electrophoresis

To study the profiles of lens epithelial proteins after oxidation, 2-D gel electrophoresis was performed prior to thiol-blotting. For first-dimension isoelectric focusing, Immobiline DryStrip, pH 3-10 NL, 13 cm IPG strips (Amersham Biosciences, Piscataway, NJ) were used. Proteins (25 μg) was combined with a rehydration buffer containing 8 M urea, 2% CHAPS, 50 mM dithiothreitol (DTT), 2% IPG buffer for the pH3-10 NL strip (Amersham Biosciences), 2% glycerol, 0.002% bromophenol blue. After reswelling the IPG strip with the sample overnight, isoelectric focusing was performed on a Multiphor II unit at 35°C with a programmed gradient of 0 – 300 V for a minute, 300 – 3500 V for 1.5 hour, and 3500 V constant for 3.5 hours. The strips were then stored at -70°C until second-dimensional gel electrophoresis could be performed.

For the second-dimension, SDS-PAGE was performed with 10% polyacrylamide gels (14×14 cm^2) in a model SE 600 electrophoresis unit (Hoefer, Amersham Biosciences). Before SDS-PAGE, the IPG strips were equilibrated in a SDS-equilibration buffer containing 50 mM Tris, pH 8.8, 6 M urea, 30 % glycerol, 2% SDS, 0.001% bromophenol blue. The IPG strip was equilibrated with reducing equilibration buffer containing 2% DTT at room temperature for 15 minutes, followed by alkylating buffer containing 2.5% IAA. After SDS-PAGE, free

sulfhydryl groups in proteins were visualized using the thiol-blot procedure described below.

2.1.7 Thiol-blot

The protocol for thiol-blotting was adapted from previous publications (Bayer, Safars, and Wilchek, 1987; Rogers, Morris and Blake, 1991). Before homogenization of epithelium, excess MPB was added to the sample buffer to facilitate binding of MPB to free sulfhydryl groups in proteins (Figure 2.1). Proteins were then separated by 2-D gel electrophoresis and blotted onto a PVDF membrane. Since avidin binds to MPB, free sulfhydryl groups were visualized by a colorimetric enzyme-substrate system. During the 2-D electrophoresis, previously oxidized sulfide groups were reduced and only MPB-bound sulfhydryl groups were visualized on the blot. After 2-D gel electrophoresis, thiol-stained protein spots were compared to those of age-matched controls using Melanie 3 software (Genebio, Geneva, Switzerland).

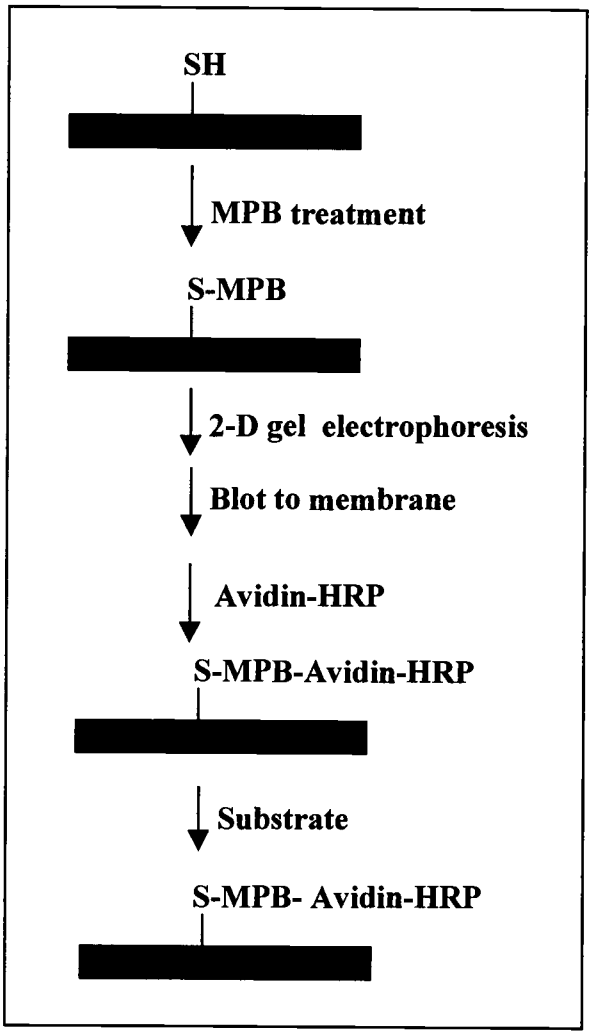

Figure 2.1: Thiol-blot procedure. MPB, 3-(N-Maleimidopropionyl)biocytin; HRP, horse-radish peroxidase. Modified from Rogers, Morris and Blake, 1991.

2.1.8 Identification of protein spots on 2-D gels

MPB-treated, normal, epithelial, soluble proteins from 13-day old lenses were visualized on 2-D gels by negative zinc staining, and the gel image was captured on a flat bed scanner. Protein spots from the gel were excised and digested with trypsin. Briefly, the gel pieces were washed with 50 mM citric acid for 20 minutes, followed by two washes with 20 mM ammonium bicarbonate containing 50% (v/v) acetonitrile for 30 minutes. The washed gel pieces were dried in a vacuum concentrator. Trypsin in 20 mM ammonium bicarbonate was then added to the gel pieces and incubated overnight at 37°C. 1% TFA was added to the incubation mixture, and peptides was extracted by sonication at 37°C followed by centrifugation. Peptides were further extracted by adding 60% acetonitrile to 1% TFA solution. Pooled peptide solutions were vacuum concentrated and injected onto a reversed phase HPLC using a Higgins Targa 0.5 mm×150 mm C18 column (Higgins Analytical, Inc., Mountain View, CA) and analyzed on-line by an electrospray ionization mass spectrometer, model LCQ (ThermoFinnigan, San Jose, CA). Data were processed using SEQUEST software (ThermoFinnigan).

2.2 STUDIES ON CALPAINS IN LENS

2.2.1 SDS-PAGE, and Western blot for calpain

To investigate changes in recently characterized calpain 10 (Ma et al., 2001) in lens during aging and selenite cataract formation, Western blots were performed using 8% Novex Tris-Glycine precasted minigels (Invitrogen) with polyclonal antibody against rat calpain 10 peptide (TriplePoint Biologics, Portland, OR). After separation of 100 μg soluble and 75 μg insoluble proteins, immunoblotting was performed by electrotransferring the proteins from the gels to a polyvinylidene difluoride membrane at 30 V for 90 min at 4°C. The membranes were then incubated in a blocking agent, 5% skim milk in Tris-buffered saline with 0.05% Tween 20 (TTBS) at room temperature for 1 hour. The affinity-purified polyclonal antibody against calpain 10 was used at 1:200 dilution in the blocking agent. After overnight incubation with the primary antibody, and then washing with TTBS three times, the membrane was incubated with alkaline phosphatase conjugated to anti-rabbit IgG secondary antibody for 1 hour. Immunoreactivity was visualized with substrates BCIP/NBT (Bio-Rad). For calpain activity studies, SDS-PAGE with 12% Novex gels, Western blots, and casein zymography were performed as described previously. For SDS-PAGE of crystallins, 10 μg soluble proteins were used in each lane and for zymography, 50 or 75 μg proteins were used. For the

calpain 2 Western blots, 100 μg was used and for Lp82, 80 μg proteins were used in each lane.

2.2.2 Hydrolysis of calpains by recombinant calpains

To investigate if calpains are substrates for other calpains, calcium-dependent incubations of calpains with other calpains were performed. For calpain 10 hydrolysis by endogenous calpains, soluble lens fiber proteins were incubated with 2 mM $CaCl_2$ at 37°C, and samples were collected at 0, 1, 2 hours and overnight. As negative controls, incubations without calcium or with calcium and E64, a cysteine protease inhibitor, were performed in parallel.

For hydrolysis of endogenous calpains with recombinant calpains, endogenous calpains in soluble lens nuclear protein were inactivated by incubation with 5 mM iodoacetamide (IAA) for 30 minutes at 37°C, followed by quenching of excessive IAA using 10 mM DTE for 30 minutes at 37°C. Purified recombinant calpain 2 (rCalpain 2; Calbiochem, La Jolla, CA) and recombinant Lp82 (rLp82; Fukiage et al., 2002) were then added to protein samples in the presence of 2 mM $CaCl_2$ and incubated for 1 hour at 37°C.

2.2.3 Protease activity assay

To obtain similar proteolytic activities for rCalpain 2 and rLp82, an *in vitro* protease activity assay was performed using BODIP FL labeled casein as a substrate (EnzChek protease assay kit, Molecular Probes, Eugene, OR). All protease activity assays were performed in 96-well flat bottom ELISA plates. Each 200 µl reaction solution contained 5 µg/ml casein substrate, 2 mM $CaCl_2$ and different amounts of enzyme solution in Tris buffer with 20 mM Tris, 2 mM DTE, pH 7.4. Calcium-dependent proteolysis was initiated by adding $CaCl_2$ to each well and incubating at 37°C for 1 hour. Fluorescence of the samples was then determined at 535 nm after excitation at 485 nm on a fluorescence spectrometer (HTS 7000 Bio Assay Reader, Perkin Elmer, Norwalk, CT). Free BODIP FL dye (10 mM) was dissolved in methanol and was further diluted serially in Tris buffer and used as a fluorescent standard to determine the activity of calpains. Enzyme activity was determined in the linear range from the *in vitro* activity graph (Figure 2.2).

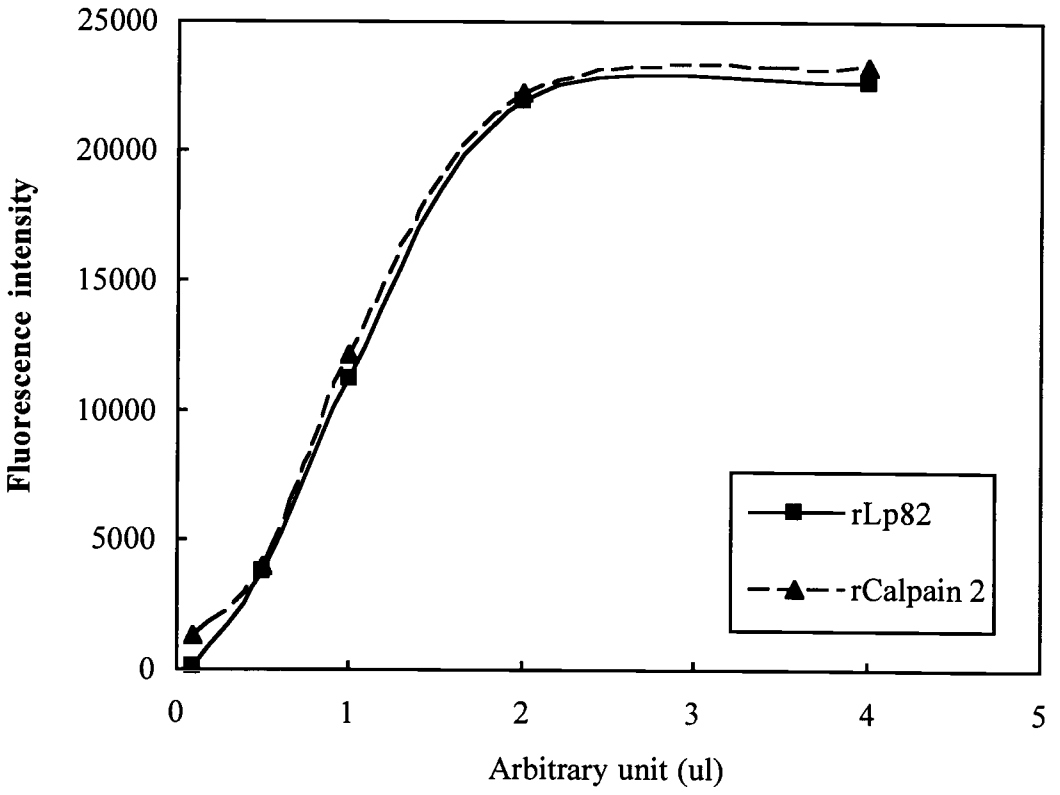

Figure 2.2: *In vitro* activities of recombinant calpains.

2.3 STUDIES ON POST-TRANSLATIONAL MODIFICAITON OF βB1-CRYSTALLIN

2.3.1 Expression and purification of βB1-crystallins

Human wild-type βB1-crystallin (WT) and a deamidated βB1-crystallin (Q204E) were expressed in *E. coli* and purified as described previously (Lampi et al., 2001). The cDNA of WT βB1-crystallin was cloned into the pCR®T7/CT TOPO TA expression vector, and recombinant protein was expressed in BL21 Star™(DE3) cells (Invitrogen). Q204E protein was produced by introducing a point mutation on the WT cDNA by replacing the glutamine at residue 204 with glutamic acid.

Protein expression was induced by addition of 100 mM IPTG when the optical density at 600 nm of cultures was between 0.2 and 0.5. Cells were harvested after 4 hour induction, and pellets were stored at -70°C until later use. The cell pellet was lysed by sonication in a lysis buffer, pH 6.8, containing 4 mM Na_2HPO_4, 4 mM KH_2PO_4, 14 mM KCl, 36 mM NaCl, 0.01 mM EDTA, and protease inhibitor cocktail (Complete Inhibitor Tablets, Roche Molecular Biochemicals, Indianapolis, IN). The lysate was treated with DNase I, RNase A, 1 mM DTT and 1 mM $MgCl_2$. The soluble fraction of cell lysate was obtained by centrifugation at 20,000 g for 30 minutes, and then it was applied to a cation exchange column, SP Sepharose Fast Flow, 2.5 cm × 10 cm (Amersham Biosciences, Piscataway, NJ). The ion exchange

buffer A contained 6.6 mM Na_2HPO_4, 6.6 mM KH_2PO_4, 23 mM KCl, 1 mM DTT, and 0.16 mM EDTA, pH 6.8. The recombinant proteins were eluted with a linear 0.5 M NaCl gradient. After purification, protein solutions were concentrated and buffers were exchanged. Protein concentrations were determined by the Coomassie blue protein assay reagent using BSA as a standard (Pierce Biotechnology, Rockford, IL).

Truncated βB1-crystallins, missing 15 or 47 amino acids from the N-terminus, were expressed in *E. coli*. Truncations were confirmed by Western blot and mass spectrometry. However, the level of protein expression was too low to yield a large quantity of proteins for denaturation experiments. Thus, recombinant calpain 2 (Calbiochem, San Diego, CA) was used to produce truncated βB1-crystallins. This is relevant since calpain 2 is found in human lenses (David et al., 1989). Truncation of purified WT and Q204E was performed with purified calpain 2 (3.87U/mg βB1-crystallin) in the presence of 2 mM $CaCl_2$ for 1-2 hours at 37°C. The reaction was stopped by exchanging buffer lacking calcium at 4°C.

2.3.2 Electrophoresis, mass spectrometry and sequence analysis of trWT and trQ204E

Electrophoresis was performed using pre-cast 10% polyacrylamide mini-gels (NuPAGE from Invitrogen). Proteins were visualized by staining with Coomassie

blue G-250 (SimplyBlue SafeStain, Invitrogen). Mass spectrometry was performed to confirm the truncation sites. Approximately 0.17 nmol of trWT and trQ204E were injected into a 1 mm × 250 mm C4 reverse-phase column (Vydak, Hesperia, CA) in line with an electrospray ionization mass spectrometer (ESI-MS, model LCQ, ThermoFinnigan). The N-terminal amino acid sequence analysis and MALDI-MS was performed in the Genomics and Proteomics Facility at the University of Oregon (Eugene, OR).

2.3.3 Size exclusion chromatography (SEC)

In order to determine the elution properties and apparent size of native βB1-crystallins, SEC was performed. A 7.8 mm × 30 cm TSK-GEL G3000SW$_{XL}$ column (TosoHaas, Montgomeryville, PA) was equilibrated with a buffer containing 29 mM Na_2HPO_4, 29 mM KH_2PO_4, 100 mM KCl, 0.7 mM EDTA, 1 mM EGTA, 1 mM DTT, pH 6.8, with a flow rate of 0.2 ml/min. Gel filtration standards (Bio-Rad) were used to compare elution pattern of samples.

2.3.4 Circular dichroism

Circular dichroism spectra of trWT and trQ204E (0.48 mg/ml) were recorded on a JASCO J-500 A spectrometer in the far UV range. Samples were applied to the size exclusion column to remove autolyzed peptides of calpain 2 using buffer containing 5 mM NaH_2PO_4, 5 mM Na_2HPO_4, 100 mM NaCl, pH 6.8. The samples were then dialyzed against 5 mM NaH_2PO_4, 5 mM Na_2HPO_4, pH 6.8 containing 100 mM NaF. CD measurements were taken in a 0.1 mm cell at 20°C. Secondary structure was calculated using the variable selection method (Compton, Mathews and Johnson, 1987). Protein concentration was determined by amino acid analysis.

For the urea stability study, CD spectra of full length WT and Q204E were measured on an AVIV CD spectrometer, model 202 (Protein Solutions, Lakewood, NJ) from 200 to 260 nm. Ten μM protein (280 μg/ml) was tested in various concentrations of urea for unfolding/refolding studies.

2.3.5 Fluorescence spectrometry

In order to study the stability of WT and modified βB1-crystallins, fluorescence spectroscopy was used to measure protein unfolding and refolding patterns in urea. Proteins at 1 μM (27.9 μg/ml for WT & Q204E, 23.0 μg/ml for trWT & trQ204E) were incubated in varying urea concentrations ranging from 0 to 7 or 8 M. To

prepare buffers containing varying concentrations of urea, a stock solution of 9 M urea (Pierce, Rockford, IL) was prepared and then deionized and filtered. Different concentrations of urea were combined with buffer containing 5 mM Na_2HPO_4, 5 mM NaH_2PO_4, 100 mM NaCl, pH 6.8. Proteins were incubated in urea buffer overnight at 25°C. For refolding experiments, protein samples were incubated in 7 M urea buffer overnight prior to dilution into buffers containing consecutively lower concentrations of urea.

Fluorescence measurements were made on a Photon Technology International Spectrofluorimeter model QM-2000-7 (Lawrenceville, NJ). The absorption scan was measured between 240 and 320 nm, and the emission wavelength was set at 336 nm. For emission scanning, proteins were excited at 283 nm, and the fluorescence emission was recorded between 300 and 400 nm at 25°C with the excitation and emission slit width set to 2 nm. Fluorescence measurements were analyzed with FeliX, a fluorescence analysis software (Photon Technology International, Lawrenceville, NJ). Fluorescence emission spectrum was corrected by subtracting the blank buffer spectrum at each urea concentration and smoothed using the Savitzky-Golay equation.

2.3.6 Folding calculations

Percent folded protein was calculated from fluorescence and CD data by the following equation:

$$\% \text{ Folded protein} = (Vi - Vu)/(Vn - Vu) \times 100,$$

where Vi is the emission or ellipticity data value at a specified urea concentration, Vu is the value of 100% unfolded protein, and Vn is the value of native protein without urea. For fluorescence data, fluorescence intensity at 357 nm was used. For CD measurements, ellipticity at 218 nm was used. These wavelengths were chosen because they produced the largest difference between native and unfolded proteins.

2.3.7 Expression and purification of recombinant αA-crystallin

Human αA-crystallin was expressed in *E. coli*. Gene-specific primers were used for RT-PCR to obtain αA-crystallin cDNA. The RT-PCR product was cloned into pCR®T7/CT TOPO TA expression vector, and the recombinant protein was expressed in BL21 Star™(DE3) cells (Invitrogen).

After cell lysis, αA-crystallin protein was partially purified by $(NH_4)_2SO_4$ precipitation. Briefly, 50% $(NH_4)_2SO_4$ solution (w/v) was added to the cell lysate supernatant to a final concentration of 15% (v/v). The mixture was rocked at room temperature for 5 minutes and then was centrifuged at 20,000 g for 10 min. The supernatant was treated with 50% $(NH_4)_2SO_4$ to yield 25% final concentration and then centrifuged again. Pellet was resolubilized in size exclusion chromatography buffer containing 29 mM Na_2HPO_4, 29 mM KH_2PO_4, 100 mM KCl, 0.7 mM EDTA, 1 mM DTT (pH6.8), and then dialyzed against the buffer. The sample was applied to a 3 cm × 80 cm size exclusion column, S-300 HR Sephacryl (Amersham Biosciences) at 0.4 ml/min flow rate. This was followed by ion exchange in a 2.5 cm × 12 cm Macro Prep DEAE column (Bio-Rad) using a buffer containing 20 mM Tris-HCl, 1 mM EDTA, 1 mM EGTA, 1 mM DTT, pH 7.4 with a linear NaCl gradient from 0 to 750 mM.

2.3.8 Heat turbidity

Heat-induced turbidity was monitored at 405 nm while heating proteins at 55°C. βB1-crystallins at 3.6 μM were heated at 55°C for 725 min in a thermal jacketed cuvette with constant stirring (Cary 4 Bio UV-Visible spectrophotometer, Varian, Palo Alto, CA). Incubations were performed in a buffer containing 5 mM Na_2HPO_4, 5 mM NaH_2PO_4, 100 mM NaCl, pH 6.8. For incubation of βB1-

crystallin with αA-crystallin, various molar amounts of αA-crystallin were added to βB1-crystallin, and the samples were incubated at room temperature for an hour prior to incubation at 55°C for turbidity measurements.

2.3.9 SDS-PAGE

After the heat turbidity measurements, samples were collected, and water soluble and insoluble fractions were separated by centrifugation at 13,000× g for 20 minute. SDS-PAGE was performed with 12% NuPAGE gels (Invitrogen). Proteins were visualized by staining with Coomassie blue G-250.

3 RESULTS

3.1 STUDIES ON EPITHELIAL CHANGES IN SELENITE CATARACT

3.1.1 Transcripts for caspase 3 and calpains in selenite cataract

We first determined if the activation of enzyme activities in lens epithelial cells during selenite cataract formation was coupled to up-regulation of gene expression. mRNA levels for calpains, calpastatin and caspase 3 in epithelial cells from selenite cataract were compared to the levels in normal lens epithelial cells at 12 hours, 3 and 5 days after selenite injection. The mRNA level of caspase 3 in selenite cataract was found to be the same as normal epithelium (Figure 3.1). This indicated that the changes in caspase 3 activity in selenite cataract may be due to activation of caspase 3 rather than up-regulation of gene expression. Expression of calpain 1 mRNA tended to increase (Figure 3.2), and calpain 2 expression tended to decrease throughout selenite cataract formation (Figure 3.3). However, the differences were not statistically significant. Expression of the Lp82 transcript showed a variable pattern over the period (Figure 3.4), and a significant decrease in mRNA was observed after 5 days in selenite cataract ($p<0.05$). Similar to Lp82 calpain, the endogenous inhibitor of ubiquitous calpains, calpastatin, showed a significant decrease in mRNA at 5 days after selenite injection ($p<0.01$; Figure

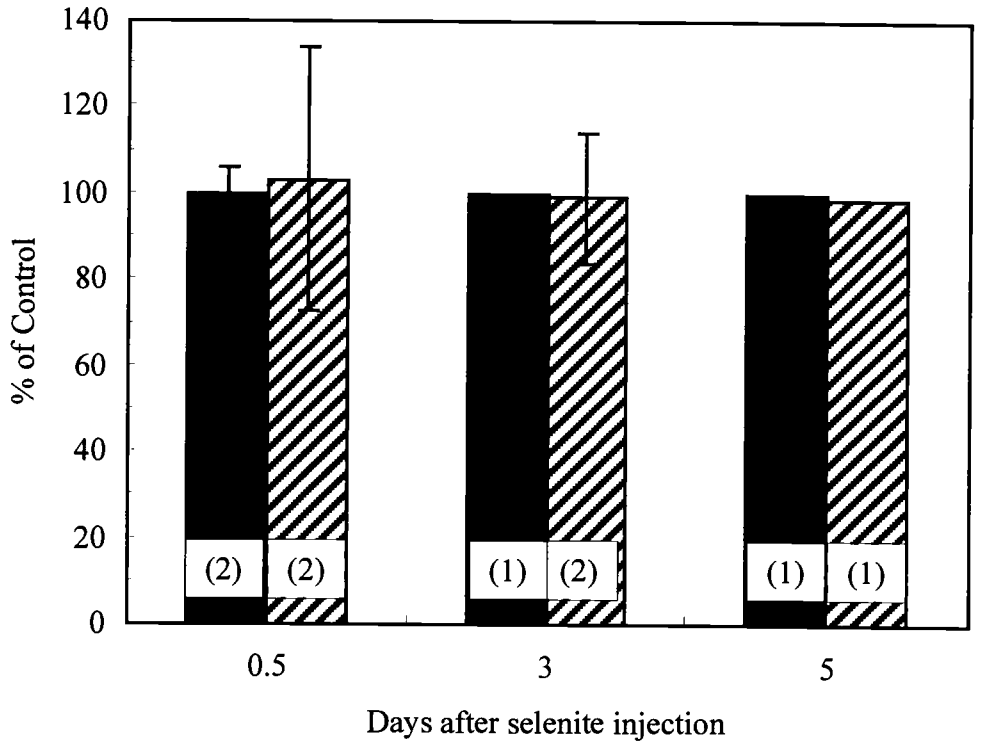

Figure 3.1: Changes in caspase 3 mRNA during selenite cataract formation. Percent change in mRNA in lens epithelia from selenite cataract was compared to mRNA in control epithelia. Control mRNA was expressed as 100 %. Control mRNA, solid bar; cataractous mRNA, stippled bar. Number in parenthesis on each bar indicates the number of replications. Error bars at means represent plus and minus one standard deviation unit.

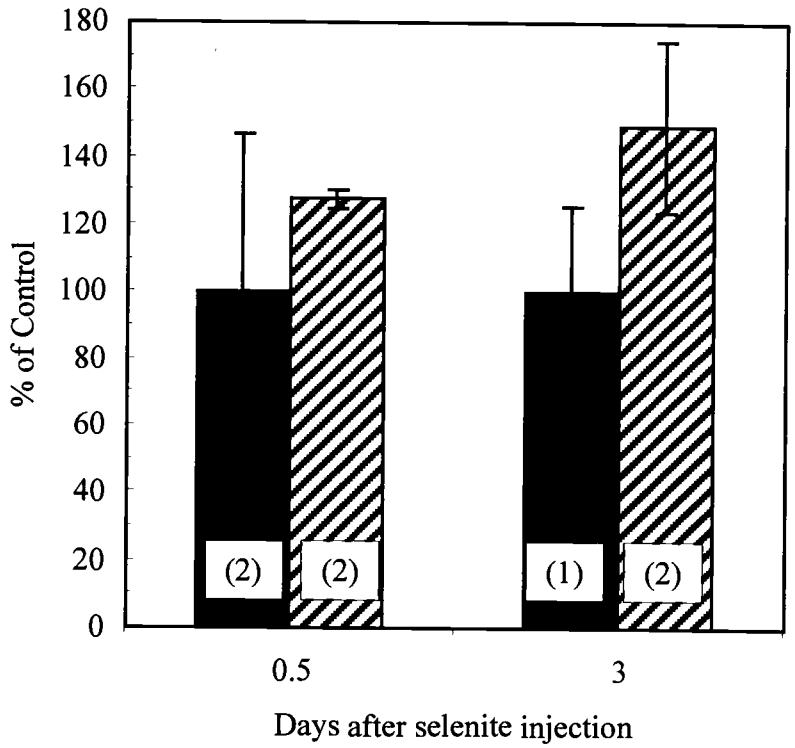

Figure 3.2: Changes in calpain 1 mRNA during selenite cataract formation. Percent change in mRNA in lens epithelia from selenite cataract was compared to mRNA in control epithelia. Control mRNA was expressed as 100 %. Control mRNA, solid bar; cataractous mRNA, stippled bar. Number in parenthesis on each bar indicates the number of replications. Error bars at means represent plus and minus one standard deviation unit.

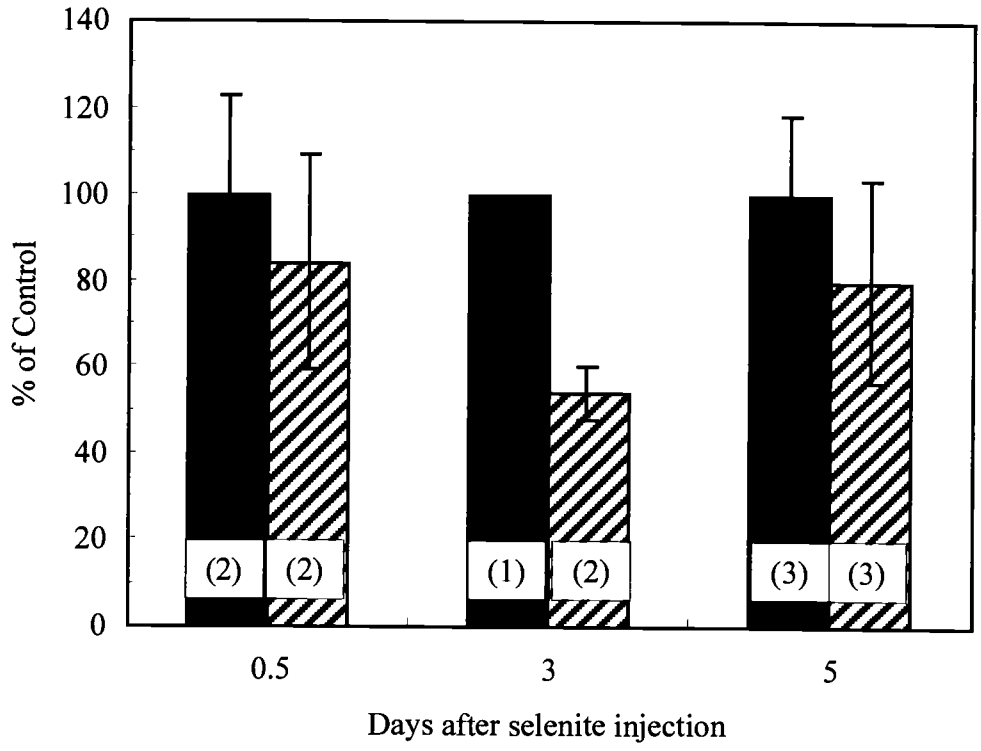

Figure 3.3: Changes in calpain 2 mRNA during selenite cataract formation. Percent change in mRNA in lens epithelia from selenite cataract was compared to mRNA in control epithelia. Control mRNA was expressed as 100 %. Control mRNA, solid bar; cataractous mRNA, stippled bar. Number in parenthesis on each bar indicates the number of replications. Error bars at means represent plus and minus one standard deviation unit.

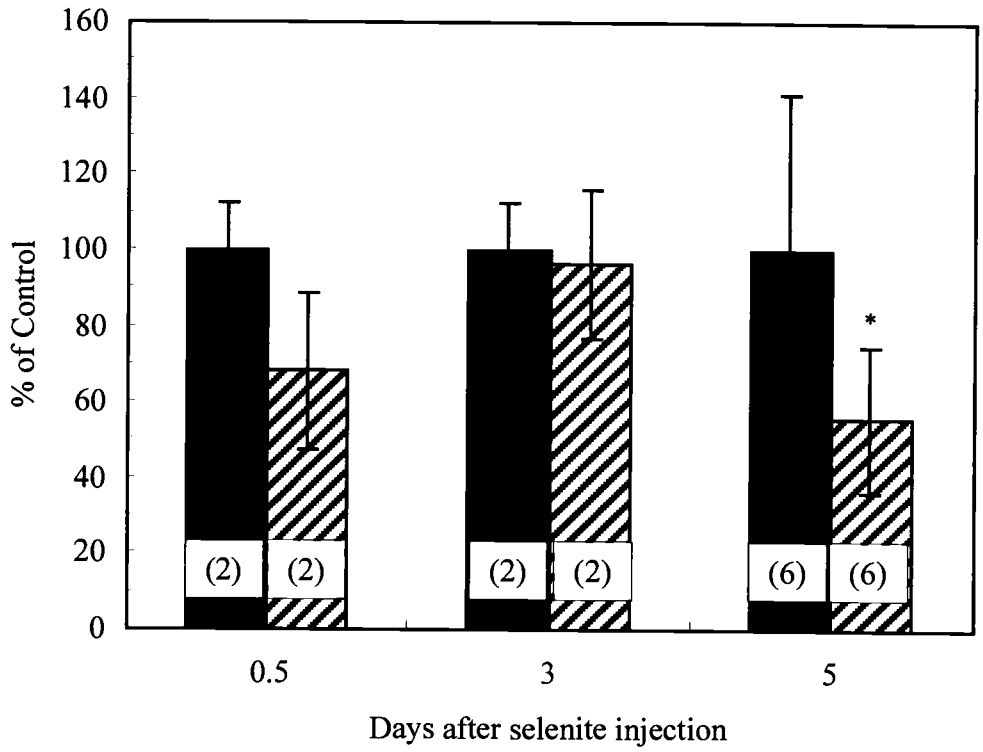

Figure 3.4: Changes in Lp82 mRNA during selenite cataract formation. Percent change in mRNA in lens epithelia from selenite cataract was compared to mRNA in control epithelia. Control mRNA was expressed as 100 %. Control mRNA, solid bar; cataractous mRNA, stippled bar. Number in parenthesis on each bar indicates the number of replications. *, statistical significance ($p<0.05$) compared to control. Error bars at means represent plus and minus one standard deviation unit.

3.5). In summary, expression of all mRNAs studied showed no marked changes during selenite cataract formation, indicating that changes in protein levels or enzyme activation were the cause of biological activity rather than increased gene expression. Decreases in mRNA levels of Lp82 and calpastatin at 5 days after selenite injection indicated an after-effect, since visible cataract usually formed at 3 days after the selenite injection.

3.1.2 Protein profiles and calpain activities in lens epithelial cells in selenite cataract

Figures 3.6 and 3.7 show lens protein profiles in selenite cataract, specifically for epithelium, cortex, and nucleus. Major proteins in these three regions of lens were the crystallins ranging from 15 to 30 kDa. Epithelial cells contained a higher concentration of higher molecular weight proteins (lane 3 in Figure 3.6), compared to whole lens (lane 2). In epithelial cells, a few bands of lower molecular weight proteins, crystallins, were degraded at 3 day after selenite injection (lane 6). Crystallins at 30, 20, and 18 kDa were extensively degraded (stippled arrows), and a band around 20 kDa appeared (solid arrow) at 3 days after selenite injection. Figure 3.7 shows proteins from lens cortex (A) and nucleus (B) in selenite cataract. Interestingly, crystallins in the cortex did not undergo extensive degradation even 5

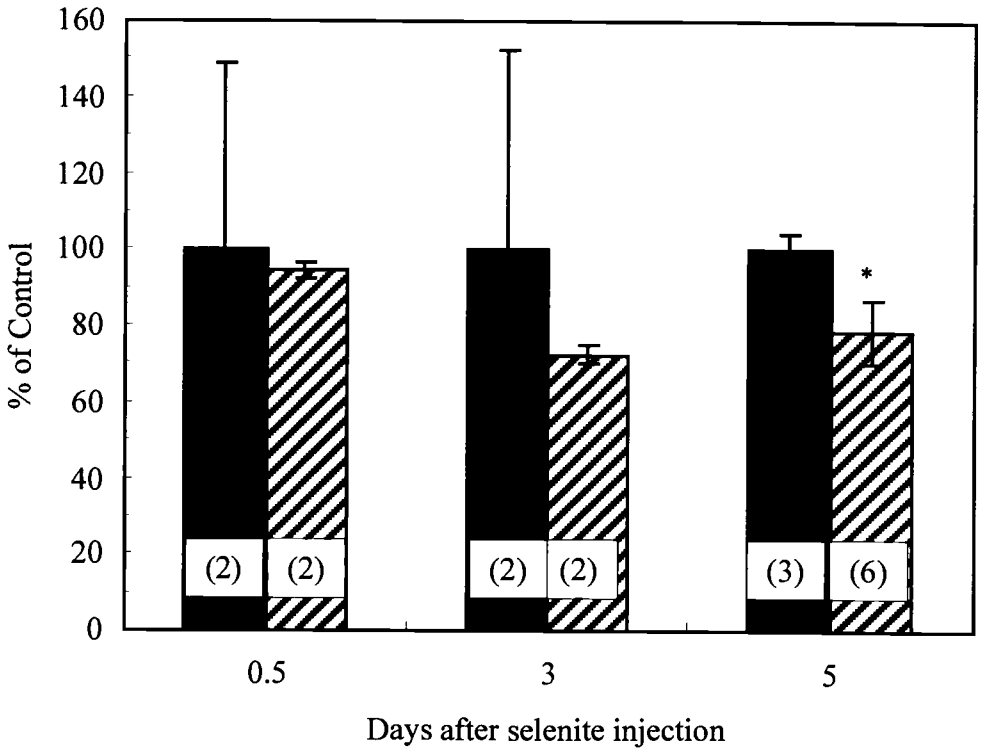

Figure 3.5: Changes in calpastatin mRNA during selenite cataract formation. Percent change in mRNA in lens epithelia from selenite cataract was compared to mRNA in control epithelia. Control mRNA was expressed as 100 %. Control mRNA, solid bar; cataractous mRNA, stippled bar. Number in parenthesis on each bar indicates the number of replications. *, statistical significance ($p<0.01$) compared to control. Error bars at means represent plus and minus one standard deviation unit.

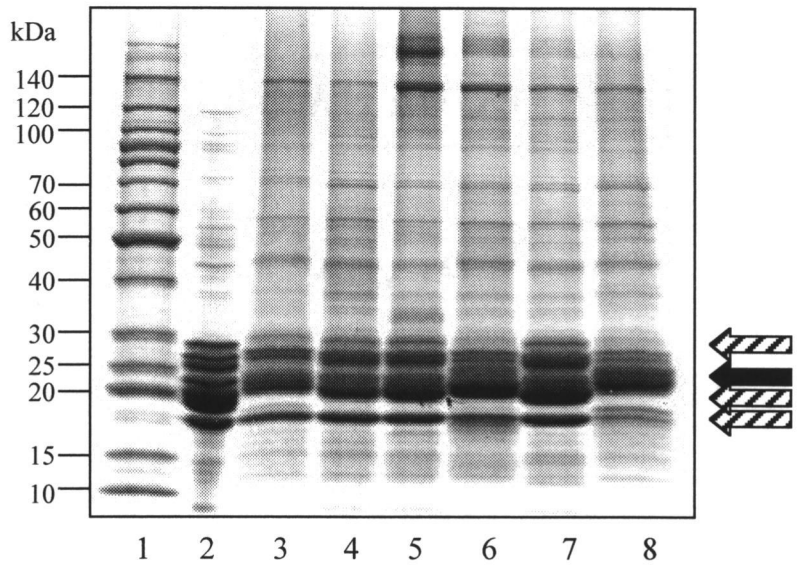

Figure 3.6: SDS-PAGE for lens epithelial proteins. 1, protein standard; 2, whole lens from 13-day old rats; 3, control epithelium at 1 day after injection; 4, selenite epithelium at 1 day after injection; 5, control epithelium at 3 day after injection; 6, selenite epithelium at 3 day after injection; 7, control epithelium at 5 day after injection; 8, selenite epithelium at 5 day after injection. Stippled arrows indicate degraded proteins, and solid arrow indicates accumulated breakdown peptides. 25 μg soluble protein was loaded into each lane.

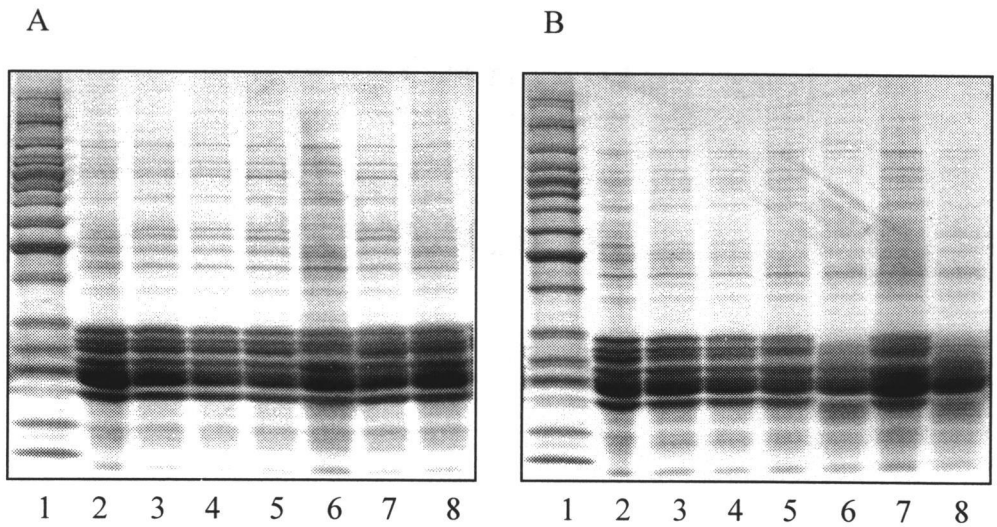

Figure 3.7: SDS-PAGE for protein in cortex (A) and nucleus (B) from lens. 1, protein standard; 2, whole lens from 13-day old rats; 3, control lens at 1 day after injection; 4, selenite lens at 1 day after injection; 5, control lens at 3 day after injection; 6, selenite lens at 3 day after injection; 7, control lens at 5 day after injection; 8, selenite lens at 5 day after injection. 25 μg soluble protein was loaded.

days after selenite injection, indicating less protease activities in cortex, compared to the epithelium and nucleus.

In order to investigate if the proteolysis occurring in lens epithelium during cataract formation was caused by activation of calpains, casein zymography was used. As shown in Figure 3.8, calpain activities were maintained until 1 day after injection, but at 3 days after injection when visible cataract was observed, proteolytic activity of Lp82 and calpain 2 was diminished (lane 6). These results suggested that both calpains were activated during cataract formation, that calpains proteolyzed proteins in epithelium, and then the calpains autolyzed themselves. At 5 days after injection, the proteolytic activities still remained at the level shown on the 3-day sample (lane 4).

3.1.3 *In vitro* oxidation of epithelial proteins by selenite

To verify the thiol-blot methodology, epithelial proteins from normal rat lens were alkylated in a high concentration of IAA. Free sulfhydryl groups in the original native proteins were visualized in the 2-D thiol-blot as a series of spots (Figure 3.9 A). Horizontal rows of spots at the same molecular weight indicated that a different number of free sulfhydryl groups were present in the same protein. Slight increases in the molecular weight of spots as they became more acidic indicated incorporation of MPB molecules into proteins (MPB molecular weight,

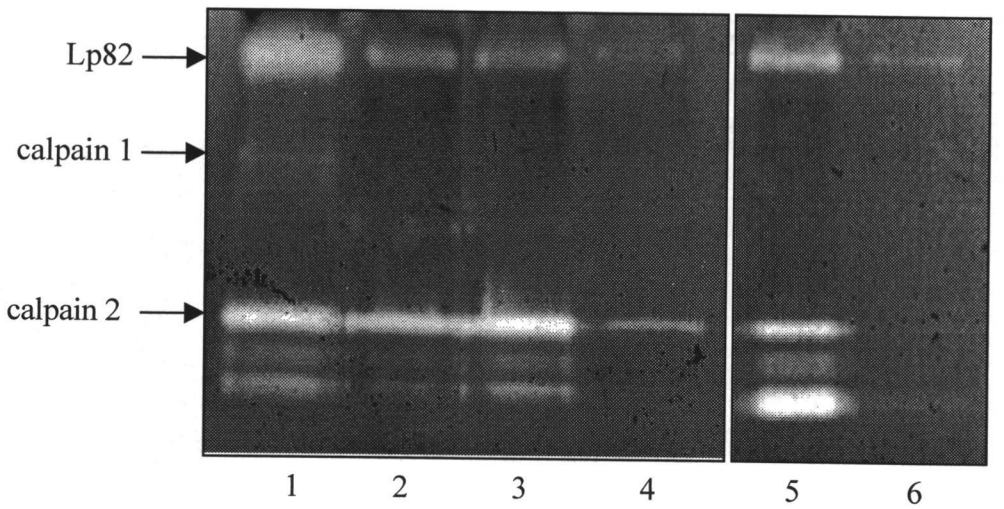

Figure 3.8: Zymogram for calpains in epithelia from rat lenses. 1, whole lens from 13-day old rats (100 μg); 2, control lens epithelium from 13-day old rats (50 μg); 3, selenite epithelium at 1 day after injection (50 μg); 4, selenite epithelium at 5 days after injection (50 μg); 5, control epithelium at 3 days after injection(30 μg); 6, selenite epithelium at 3 days after injection (30 μg).

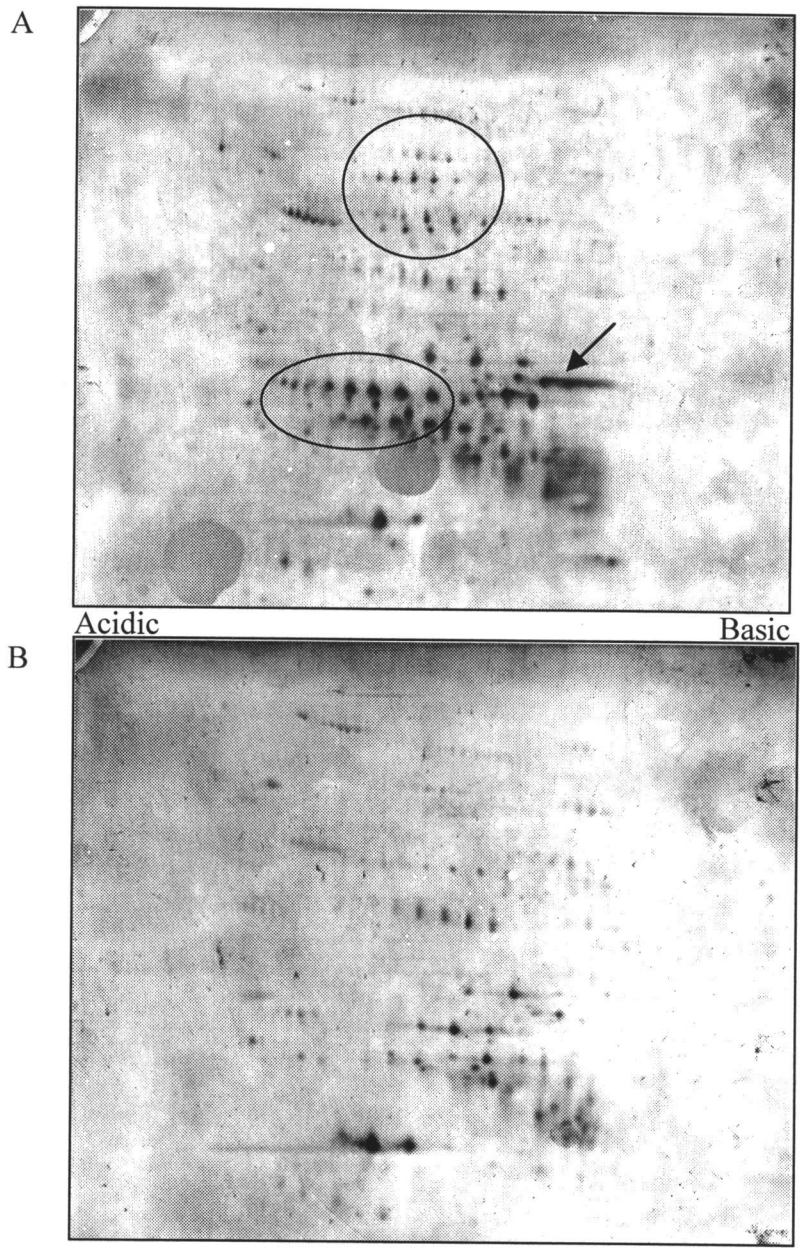

Figure 3.9: *In vitro* alkylation of epithelial proteins by iodoacetamide. (A) thiol-blot of age-matched control epithelial proteins. (B) thiol-blot of partially alkylated epithelial proteins. 25 μg of soluble proteins from 12-day-old lens were incubated with 5 mM iodoacetamide. Circles and arrow in A indicates protein groups that disappeared in B.

523.6). This indicated that different degrees of oxidation on a protein could be distinguished by our thiol-blotting procedure. When compared to the control thiol-blot without IAA incubation (Figure 3.9 A), the thiol-blot incubated with IAA (B) showed extensive loss of spots. A number of spots shown in Figure 3.9 A (circled and arrowed) were not found in panel B, which indicated that extensive loss of free sulfhydryl groups occurred after incubation with IAA. These results established that changes in the oxidative status of proteins could be visualized using the thiol-blotting procedure.

To investigate if selenite could act *in vitro* as an oxidant of proteins, epithelial proteins were incubated with a relatively high concentration of sodium selenite (100 μM). When compared to control proteins (Figure 3.10 A), a limited number of proteins were oxidized *in vitro* by selenite (Figure 3.10 B). Arrows in panel B indicate protein thiol-spots which decreased in intensity after selenite incubation. This established that selenite can oxidize free sulfhydryl groups on several proteins after *in vitro* incubation.

3.1.4 *In vivo* oxidation of epithelial proteins in selenite cataract

To determine if free sulfhydryl groups on proteins were oxidized by selenite during selenite cataract formation, the oxidation status of thiol groups on epithelial proteins from selenite cataract were measured by thiol-blotting. At only one day

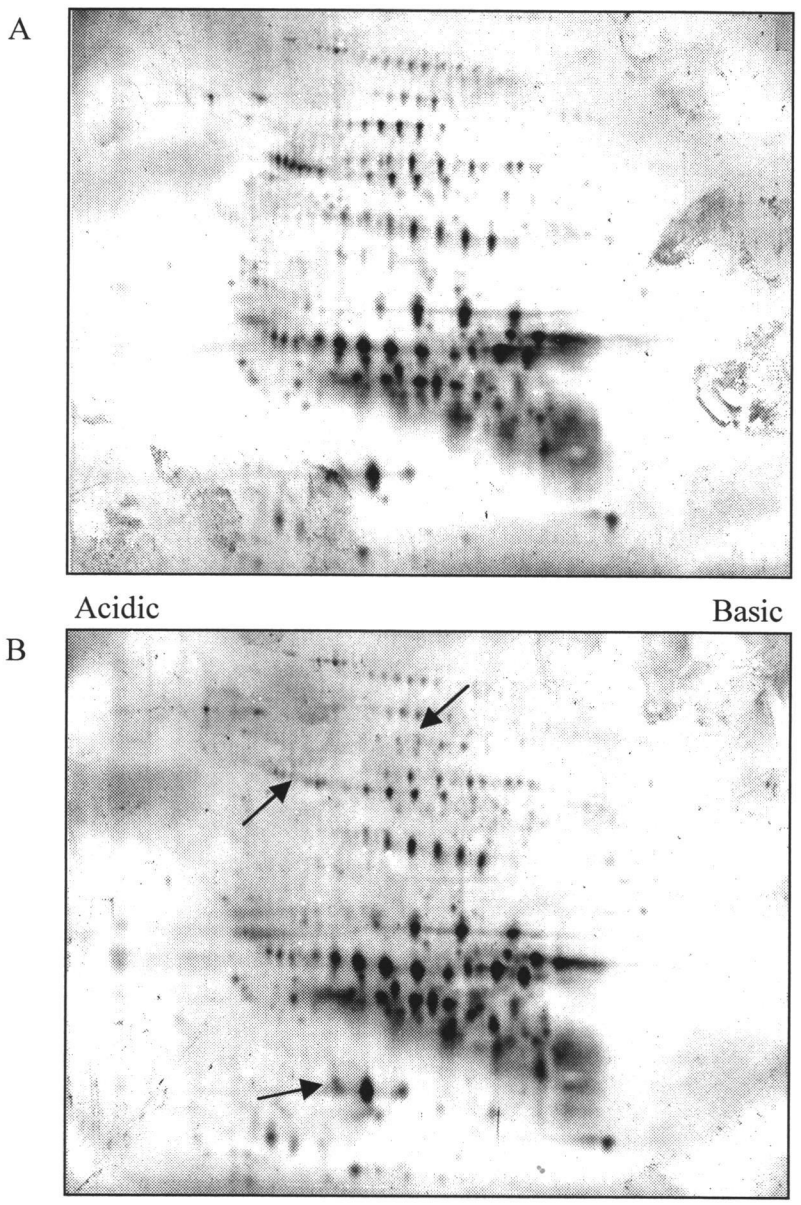

Figure 3.10: *In vitro* oxidation of epithelial proteins by selenite. (A) thiol-blot of age-matched control epithelial proteins. (B) thiol-blot of oxidized epithelial proteins. 25 µg of soluble proteins from 12-day-old lens were incubated with 100 µM sodium selenite. Arrows in B indicates protein spots showing decreases in intensity, compared to spots in A.

after injection of sodium selenite into animals, epithelial proteins, mostly crystallins, already showed proteolysis (Figure 3.11 B). Also, a series of thiol-spots near 50 kDa at pI 6.0 (circled in Figure 3.11 A) were lost in cataractous thiol-blot (Figure 3.11 B), suggesting that a protein was oxidized by selenite. However, very few proteins were oxidized at 1-day post-injection (p.i.) compared to control. Most proteins showed changes in thiol-spot intensities within a group. This indicated that during selenite cataract formation, proteins underwent changes in degree of oxidation, rather than complete oxidation.

Surprisingly, when 3-day (Figure 3.12 B) and 5-day (Figure 3.13 B) p.i. thiol-blots were compared to the 1-day p.i. thiol-blot (Figure 3.11 B), the oxidized protein spots in 1-day p.i. reappeared at 3-day and 5-day p.i. On both 3-day and 5-day thiol-blots, proteolysis was also more advanced. Interestingly, thiol-blots from cataractous epithelial showed more spots of higher molecular weight compared to blots of respective controls.

3.1.5 Identification of protein spots from thiol-blots

To identify the major spots visualized on the thiol-blots, epithelial protein from 13-day old lens was separated by 2-D gel electrophoresis, and the spots were analyzed by mass spectrometry. Figure 3.14 shows identified proteins on a 2-D gel

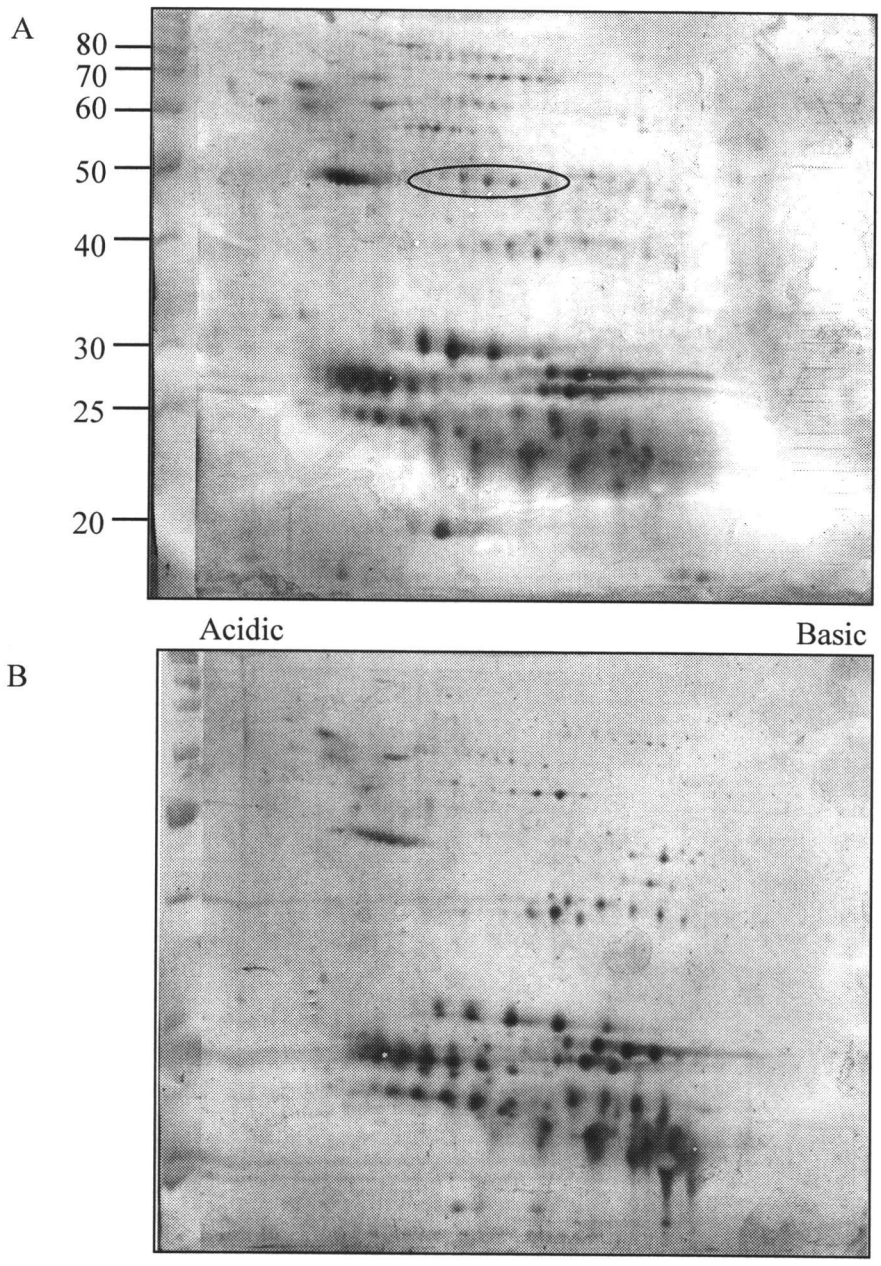

Figure 3.11: *In vivo* oxidation of epithelial proteins in selenite cataract at 1 day post injection. (A) thiol-blot of age-matched control epithelial proteins. (B) thiol-blot of cataractous epithelial proteins. 25 μg of soluble proteins was used for each blot. The circle in A indicates protein spots that disappeared in B.

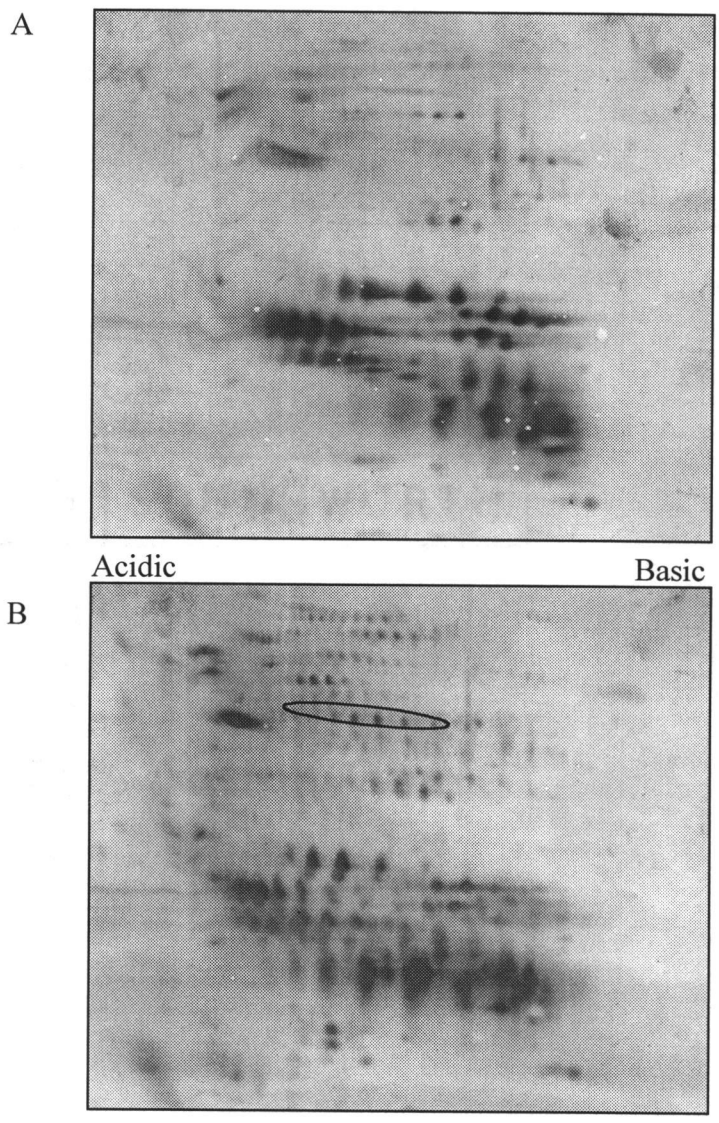

Figure 3.12: *In vivo* oxidation of epithelial proteins in selenite cataract at 3 day post injection. (A) thiol-blot of age-matched control epithelial proteins. (B) thiol-blot of cataractous epithelial proteins. 25 μg of soluble proteins was used for each blot. Circle in B indicates protein spots that reappeared at day 3, compared to the 1 day post injection sample.

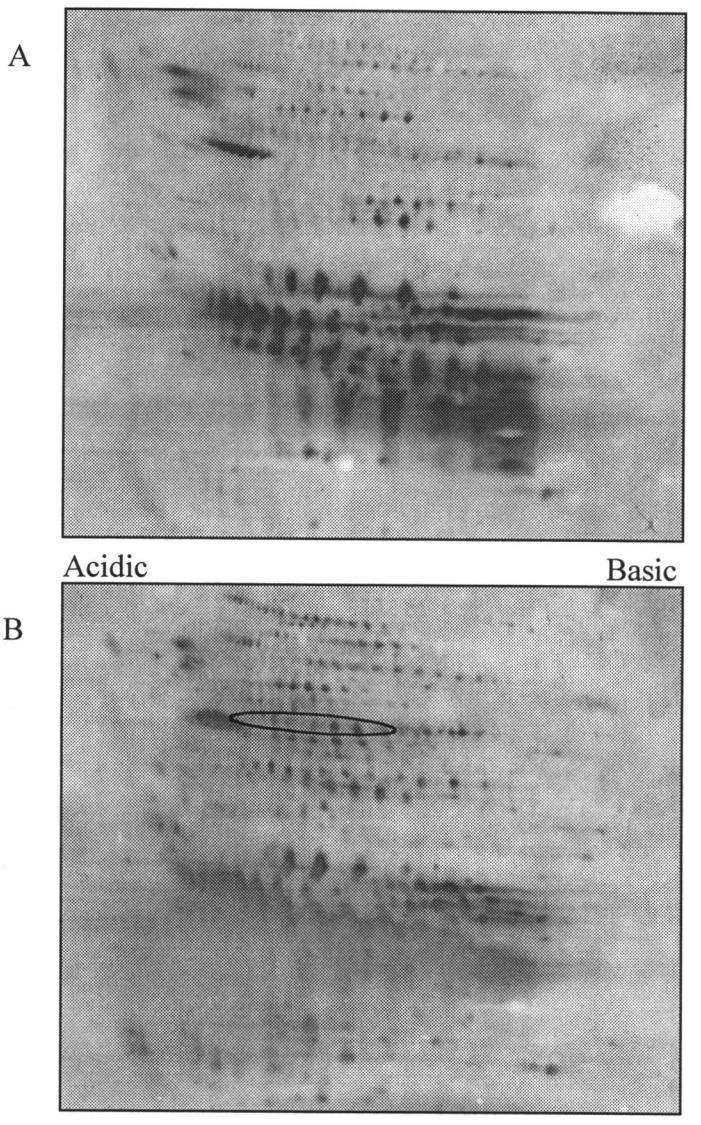

Figure 3.13: *In vivo* oxidation of epithelial proteins in selenite cataract at 5 day post injection. (A) thiol-blot of age-matched control epithelial proteins. (B) thiol-blot of cataractous epithelial proteins. 25 μg of soluble proteins was used for each blot. Circle in B indicates protein spots that reappeared at day 5, compared to the 1 day post injection sample.

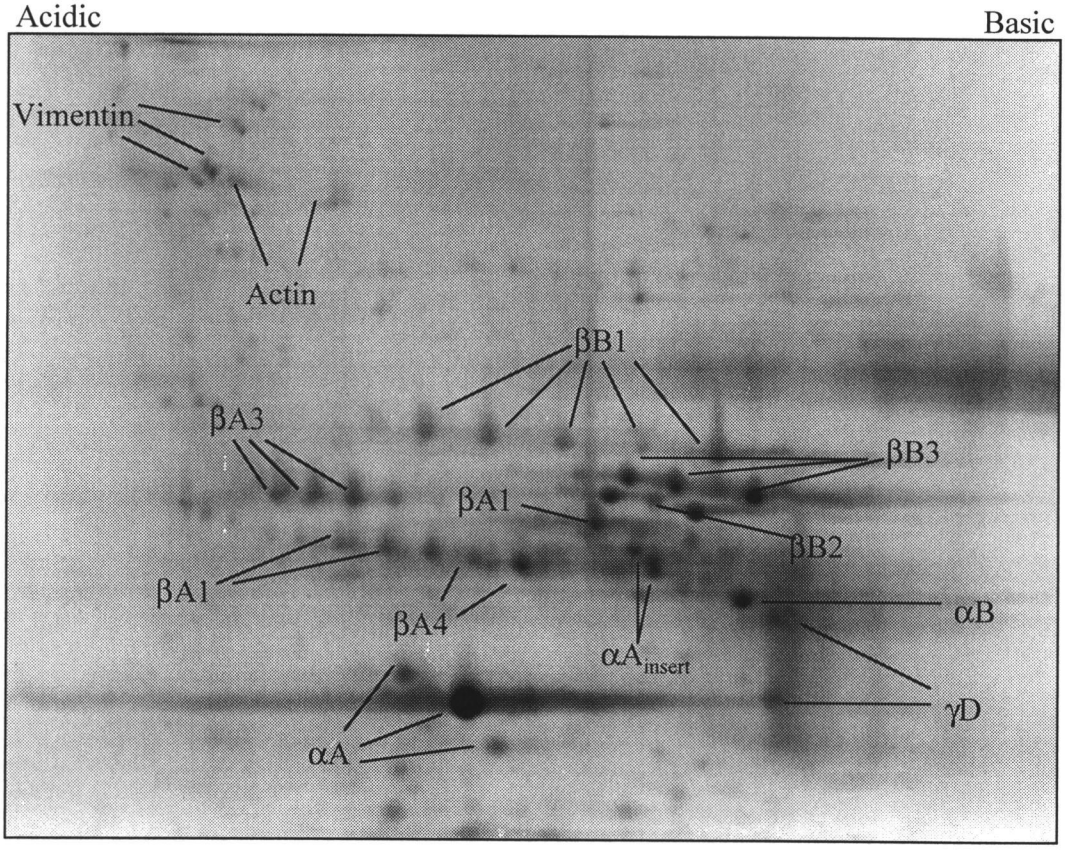

Figure 3.14: Identification of lens epithelial proteins from thiol-blot by mass spectrometry. MPB-treated epithelial soluble proteins (60 μg) from 13-day old lens were visualized by Zn staining. Identified protein spots were labeled.

image. Most of proteins identified were crystallins. Vimentin and actin were the only higher molecular weight proteins identified.

3.2 STUDIES ON CALPAINS IN LENS

3.2.1 Calpain 10 during aging and selenite cataract formation

A majority of the calpain 10 immunopositive proteins were detected near 77 and 82 kDa in the insoluble fraction of lenses from young rats (lane 4 in Figure 3.15 A). Approximately 5 times more insoluble calpain 10 was present compared to soluble calpain 10 (lane 2 in Figure 3.15 B). In an adult lens, calpain 10 was greatly diminished (lane 5) and almost no calpain 10 could be detected in soluble protein (lane 3). These results are in accordance with calpain 10 in human lenses (Ma et al., 2001), and suggested that calpain 10 may be associated with developing lens and then lost with aging.

In order to investigate if calpain 10 proteins were affected by the massive increase in cellular calcium in selenite cataract (Shearer and David, 1982), calpain 10 immunoblotting was performed from different regions of lens during selenite cataract formation. In the epithelium (Figure 3.16 A), calpain 10 protein decreased at day 3 after selenite injection and degradation of calpain 10 progressed at day 5. In the nucleus (Figure 3.16 C), calpain 10 was completely lost on day 3 when

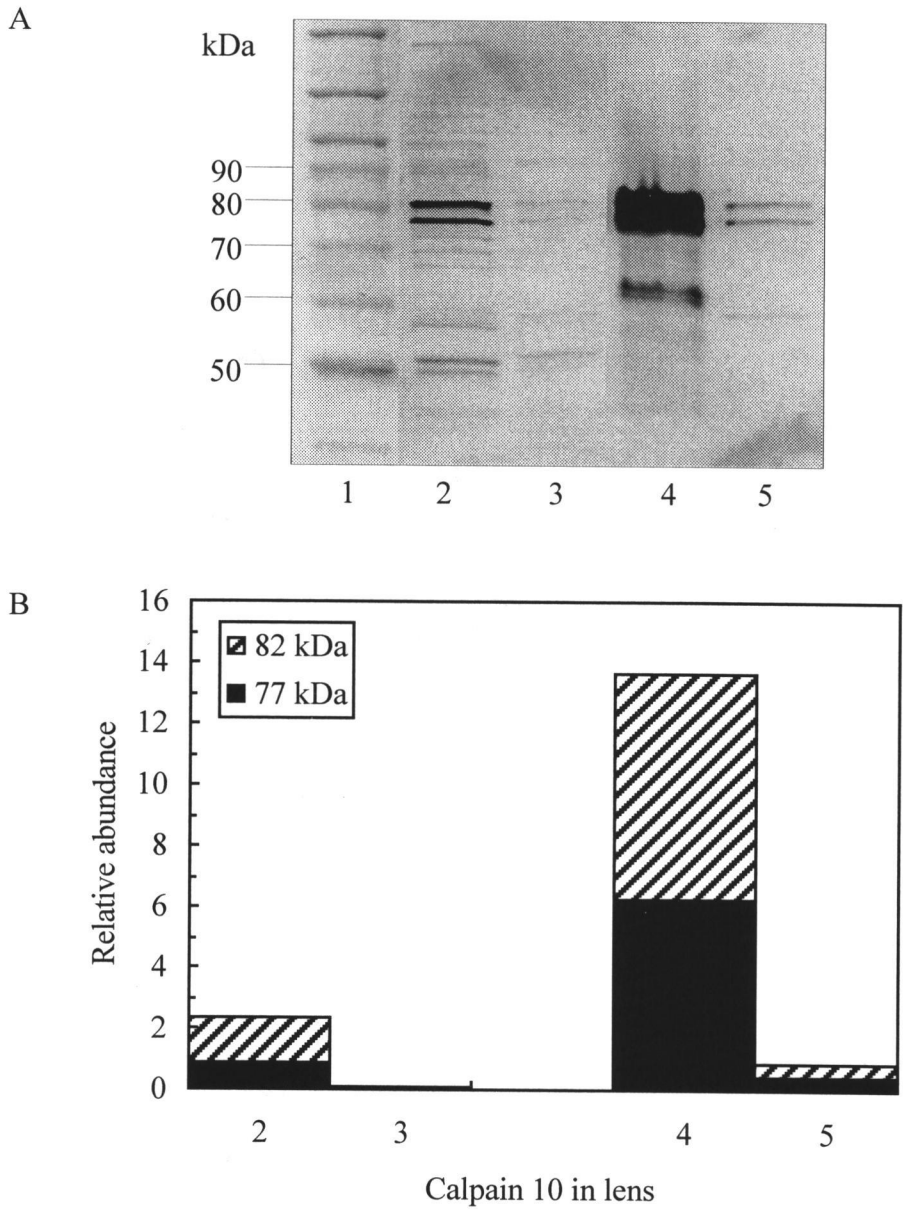

Figure 3.15: Calpain 10 in lens. (A) Western blot for calpain 10 in lens. (B) Relative abundance of immuno-reactive bands for calpain 10 in 100 μg protein. Band optimal intensities were measured from a scanned western blot using NIH image software (version 1.57). 1, protein standard; 2, lens soluble protein from young rats (100 μg); 3, lens soluble protein from aged rats (100 μg); 4, young insoluble lens protein (75 μg); 5, insoluble lens protein in aged rats (75 μg).

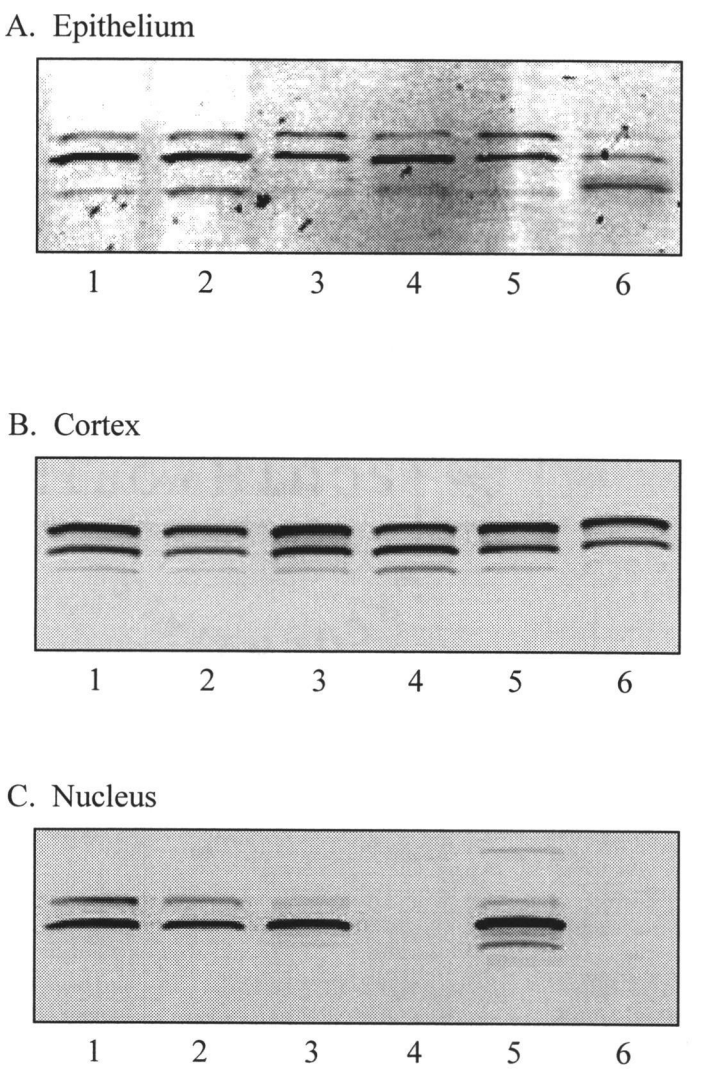

Figure 3.16: Changes in calpain 10 during selenite cataract formation. (A) Western blot for calpain 10 in the soluble proteins from lens epithelium (25 μg each lane). (B) Soluble proteins from cortex (100 μg). (C) Soluble proteins from nucleus (100 μg). 1, control lens at 1 day after selenite injection; 2, selenite lens at 1 day after injection; 3, control lens at 3 day after injection; 4, selenite lens at 3 day after injection; 5, control lens at 5 day after injection; 6, selenite lens at 5 day after injection.

nuclear cataract appeared. In contrast, calpain 10 protein levels in cortical region (Figure 3.16 B) were maintained during selenite cataract formation.

3.2.2 Hydrolysis of calpain 10 by calpain 2 and Lp82

Calpain 10 decreased in lens during selenite cataract formation (Figure 3.16). Calpain 10 does not have a calcium binding domain (Ma et al., 2001), and we have not been able to activate it with calcium (unpublished data). We questioned if calpain 10 could be a substrate for other calpains in lens. Thus, *in vitro* studies were performed to investigate if calpain 10 would be degraded by endogenous and recombinant calpain 2 and Lp82. Degradation of calpain 10 was observed after 1 hour incubation of soluble lens protein with calcium *in vitro* (Figure 3.17 A). This indicated that endogenous calpains were activated by calcium and caused degradation of calpain 10. The higher molecular band of calpain 10 immunopositive proteins was lost first at 1 hour, and after overnight incubation, lower molecular weight bands disappeared. When the cysteine protease inhibitor E64 was added, calpain 10 remained intact even after overnight incubation. Zymography (Figure 3.17 B) indicated that endogenous calpains were activated, and then autolyzed during incubation with calcium. After 1 hour incubation with calcium, intact Lp82 and calpain 2 were lost and showed residual activities from their degradation products. The degradation products were lost further after 2

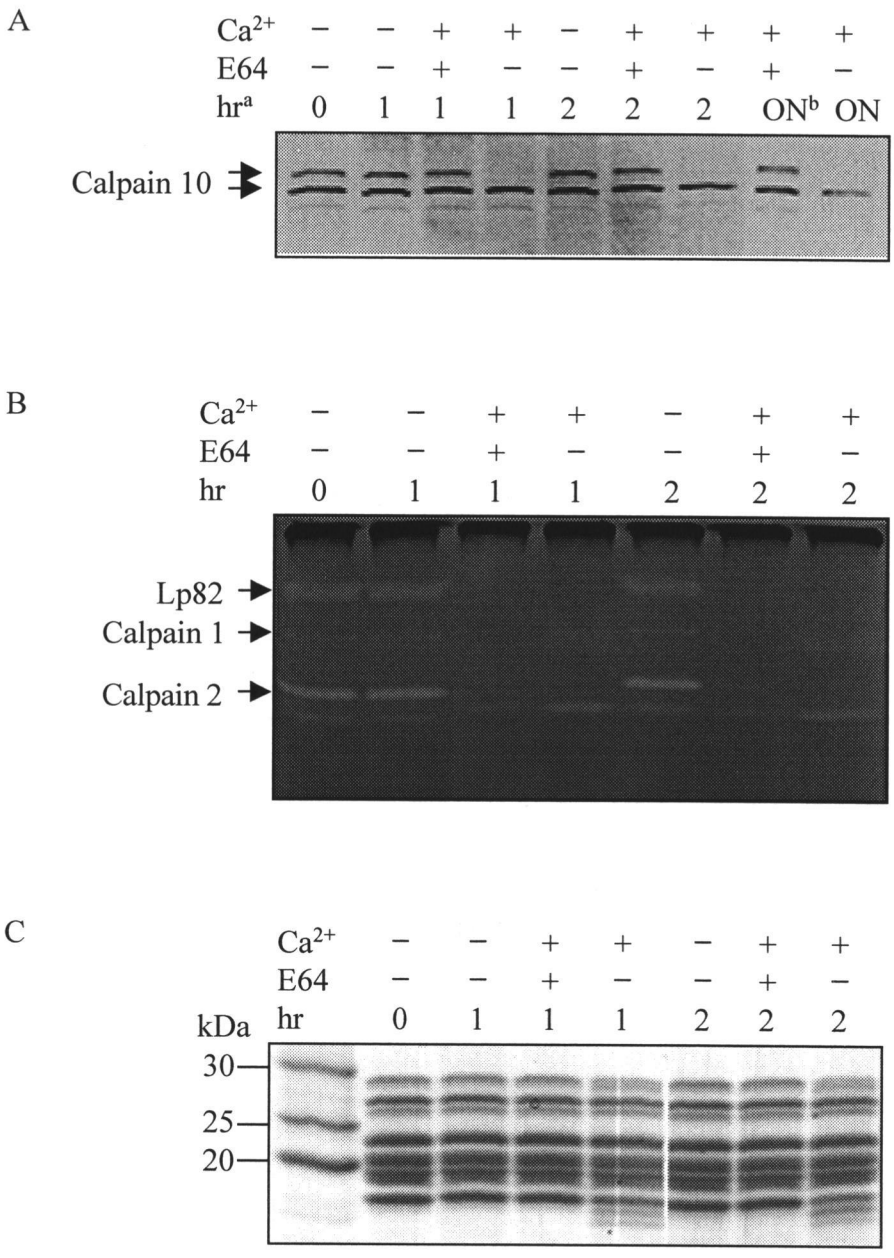

Figure 3.17: *In vitro* degradation of calpain 10 by endogenous calpains in the soluble proteins from lens fibers. (A) Western blot for calpain 10 (100 μg each lane). (B) Zymography (50 μg). (C) SDS-PAGE (10 μg). Soluble lens proteins were incubated at 37°C without Ca^{2+}, with Ca^{2+} and calpain inhibitor E64, or with Ca^{2+}. [a] incubation hour; [b] overnight.

hours. At 0 hour and 2 hours of incubation without calcium, calpains were still active. When calcium and E64 were added, calpain activity was completely inhibited as expected, indicating irreversible inhibition by E64. Lens crystallins underwent degradation, while endogenous calpains were activated in the presence of calcium (Figure 3.17 C). These results suggested that calpain 10 might be a substrate for other calcium-activated calpains in lens.

In order to distinguish which calpain in lens was responsible for calpain 10 degradation, calpain 10 in lens nuclear proteins was incubated with recombinant calpains *in vitro*. To provide the same amounts of activity for each recombinant calpain, an *in vitro* proteolysis assay was performed using modified casein as a substrate. By optimizing with proper amounts of calpain, proteolytic activity curves were obtained (Figure 2.2), and both rCalpain 2 and rLp82 showed very similar activities. For the calpain 10 hydrolysis studies, activities of calpains were in the linear range of the assay.

To eliminate the endogenous calpain activities in samples containing calpain 10, the samples were treated with IAA prior to incubation with recombinant calpain. Endogenous calpains were no longer active after alkylation of the free sulfhydryl group on the cysteine in the calpain active site (lane 1 in Figure 3.18 A). At 0 hour, both rLp82 and rCalpain 2 showed proteolytic activities (lanes 3 and 5). After 1 hour incubation with calcium, rCalpain 2 completely lost its activity (lane 6) indicating autolysis, whereas rLp82 still showed faint intact protein activity and a smear area due to activity by a degradation product (lane 4). SDS-PAGE gels

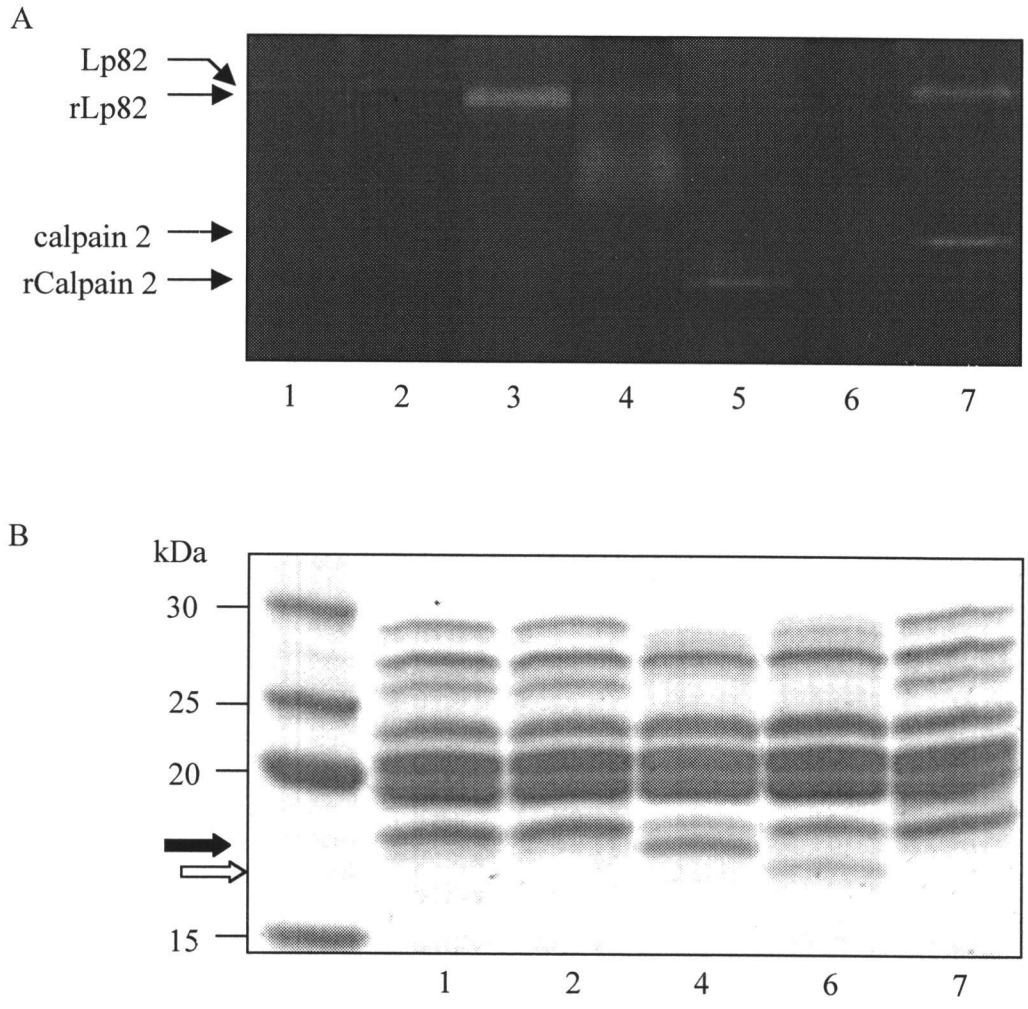

Figure 3.18: *In vitro* incubation of lens proteins with recombinant calpains, rLp82 and rCalpain 2. (A) Zymography of recombinant calpain activities after 1 hour incubation with soluble lens nuclear protein (75 μg each lane). (B) SDS-PAGE of lens crystallins incubated with recombinant calpains (10 μg each lane). Solid arrow, degradation product caused by proteolysis by rLp82; open arrow, degradation product by rCalpain 2. Before the incubation, free sulfhydryl groups in protein were alkylated with 10 mM iodoacetamide (IAA) to eliminate endogenous calpain activities. For calpain incubations at 37°C, 2 mM Ca^{2+} was added for activation. 1, IAA-treated protein from 13-day old lens at 0 hr; 2, protein + Ca^{2+} only at 1 hr; 3, rLp82 + Ca^{2+} at 0 hr; 4, protein with rLp82 + Ca^{2+} at 1 hr; 5, rCalpain 2 + Ca^{2+} at 0 hr; 6, protein with rCalpain 2 + Ca^{2+} at 1 hr; 7, normal soluble nuclear protein from 13-day old rat lens.

(Figure 3.18 B) showed that the proteolytic activity of rLp82 against crystallins (solid arrow) was different from that of rCalpain 2 (open arrow), as previously reported (Nakamura et al., 2000; Ueda et al., 2001).

Immunoblotting clearly showed that calpain 10 was a substrate for both calpain 2 and Lp82 (Figure 3.19 A). After 1 hour incubation with rLp82 or rCalpain 2 in the presence of calcium, calpain 10 immunopositive proteins were lost, indicating degradation of calpain 10. As previously reported (Fukiage et al., 2002), western blots for Lp82 (Figure 3.19 B) and calpain 2 (Figure 3.19 C) also showed that Lp82 and calpain 2 were substrates for each other. Lp82 immunopositive protein completely disappeared when incubated with rCalpain 2 (lane 5 in Figure 3.19 B). In contrast, an intact calpain 2 band still remained after incubation with rLp82 (lane 4 in Figure 3.19 C). This indicated that Lp82 was a more sensitive substrate for calpain 2 than calpain 2 was for Lp82. Both Lp82 (lane 4 in Figure 3.19 B) and calpain 2 (lane 5 in Figure 3.19 C) also showed autolysis indicated by the immunopositive degradation products.

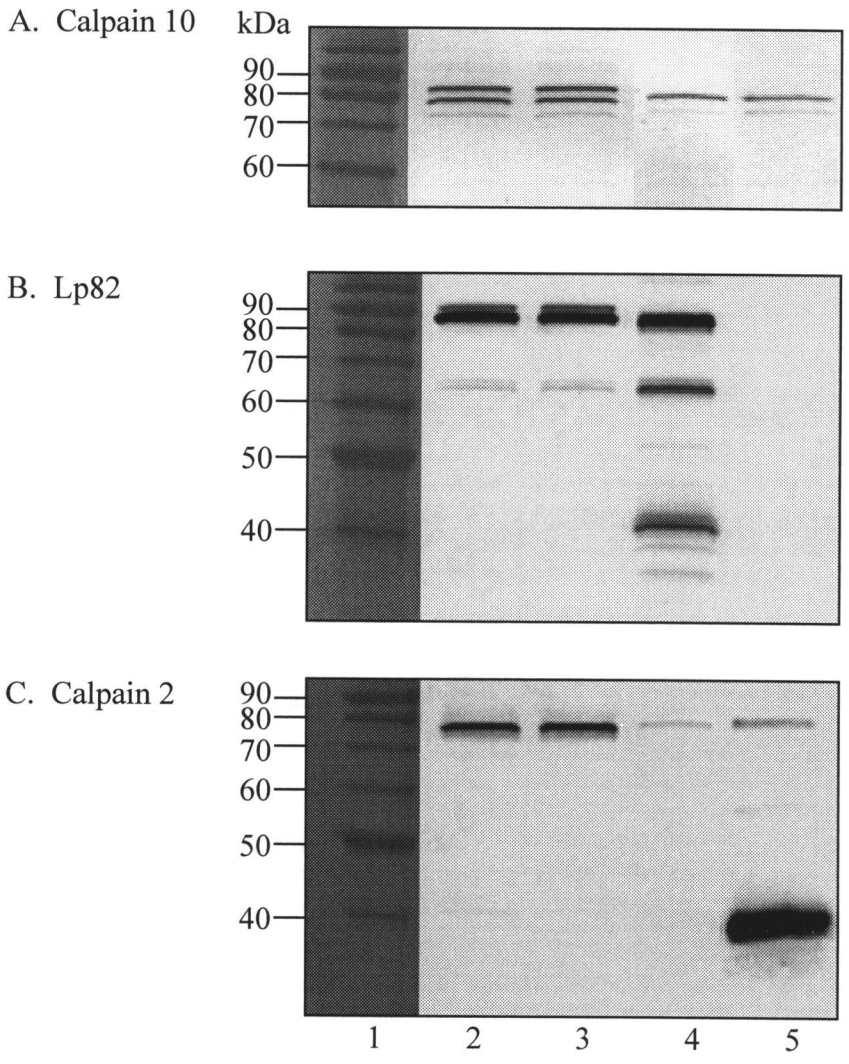

Figure 3.19: Degradation of calpains by recombinant calpains, rLp82 and rCalpain 2. (A) Western blot for endogenous calpain 10 in soluble nuclear protein from 13-day old lens. (B) Western blot for Lp82. (C) Western blot for calpain 2. Before the incubation, free sulfhydryl groups in protein were alkylated with 10 mM IAA to eliminate endogenous calpain activities. 1, protein size standard; 2, at 0 hr; 3, at 1 hr; 4, incubated with rLp82 at 1 hr; 5, incubated with rCalpain 2 at 1 hr.

3.3 STUDIES ON POST-TRANSLATIONAL MODIFICATION OF βB1-CRYSTALLIN

3.3.1 Secondary structure of truncated βB1-crystallins

In order to investigate how the removal of the N- and C-terminal extensions affects the structure and stability of βB1-crystallins, WT and Q204E βB1-crystallins were proteolyzed by calpain 2 in the presence of 2 mM calcium. Calpain 2 truncates 47 residues from the N-terminus and 5 residues from the C-terminus of WT, which results in trWT with the calculated mass of 23,040.8 (Lampi et al., 2001; small panel, Figure 3.20 B). On SDS-PAGE, both trWT and trQ204E migrated to similar positions between the 20 and 25 kDa standards (Figure 3.20 A), suggesting similar cleavage of the two proteins by calpain 2. The mass of trQ204E was 23,043.9 (Figure 3.20 B), which corresponded to the predicted mass of Q204E missing 47 amino acids from the N-terminus and missing 5 residues from the C-terminus (calculated mass of 23,041.8). MALDI mass spectrometry also confirmed the mass to be 23,045.8. Protein N-terminal sequencing confirmed cleavage of 47-residue from the N-terminus of trQ204E.

Circular dichroism measurements were performed to investigate the secondary structure of trWT and trQ204E (Figure 3.21). The average secondary structure for trWT was 10% α-helix, 41% β-structure, 20% turns, and 29% other structures. TrQ204E had 9% α-helix, 42% β-structure, 19% turns, and 29% other structures.

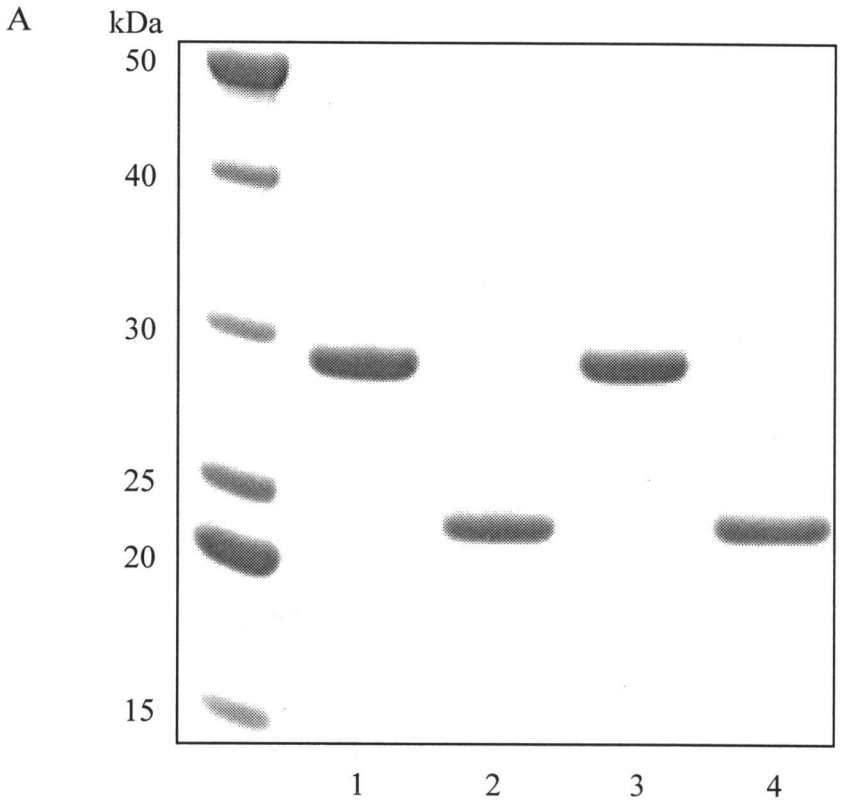

Figure 3.20 (A): SDS-PAGE of WT βB1-crystallin (1), trWT (2), Q204E (3), and trQ204E (4).

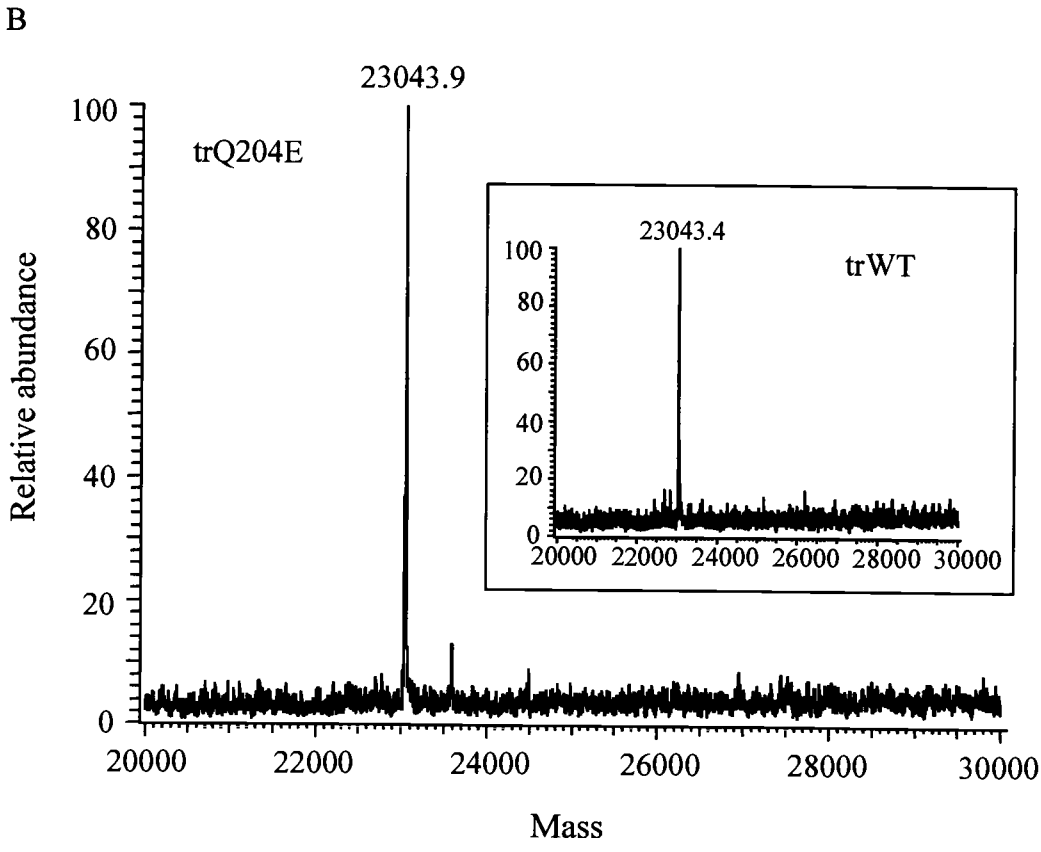

Figure 3.20 (B): Electrospray ionization mass spectra of trQ204E and trWT (insertion).

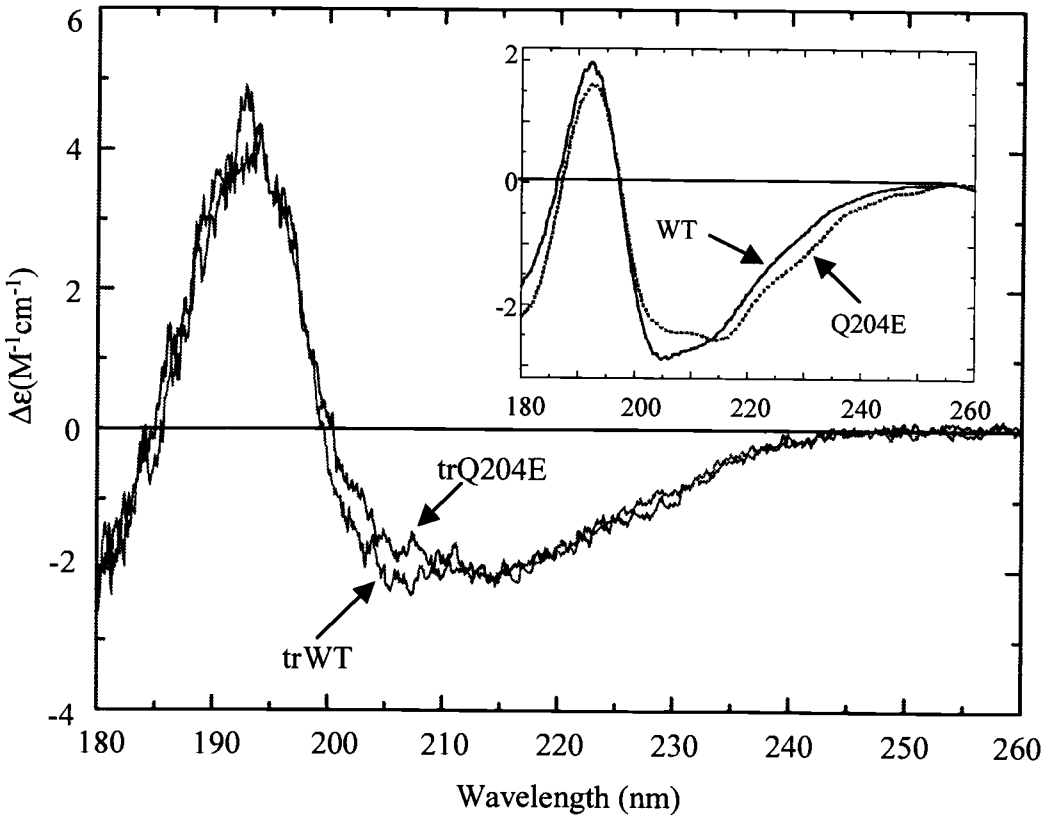

Figure 3.21: Circular dichroism of truncated βB1-crystallins at 20 μM concentration (0.48 μg/ml). Inner panel shows full-length WT (—) and Q204E (---) CD from the previous publication (Lampi et al., 2001).

These results indicated that the two proteins have very similar secondary structures. Comparison to their respective full-length proteins (small panel, Figure 3.21) showed that truncated proteins did not have significantly different structure, except for an overall decrease in α-helix content.

3.3.2 Elution of βB1-crystallins on size exclusion chromatography (SEC)

In order to study changes in elution properties of modified βB1-crystallins, SEC was performed on modified βB1-crystallins at concentrations favoring monomers and dimer formation. When compared to the gel filtration standard proteins (Figure 3.22 A), as a monomer WT eluted between 44 and 17 kDa (Figure 3.22 B), which was close to its calculated molecular weight at 28 kDa and in accordance to a previous publication (Lampi et al., 2001). As also shown in the previous publication, elution of monomeric trWT was appreciatively delayed, eluting at an apparent molecular weight between 17 and 1.35 kDa compared to the standards (Figure 3.22 C). The molecular weight measured with the mass spectrometer was 23 kDa (inner panel in Figure 3.20 B). The second peaks observed in both Figure 3.22 B and C were reported to be elution of oxidized DTT in the previous report (Lampi et al., 2001). Another interesting observation was the much earlier elution of Q204E at the same monomeric concentration as WT, with an approximate molecular weight of 158 kDa (Figure 3.23 B). As described in the previous

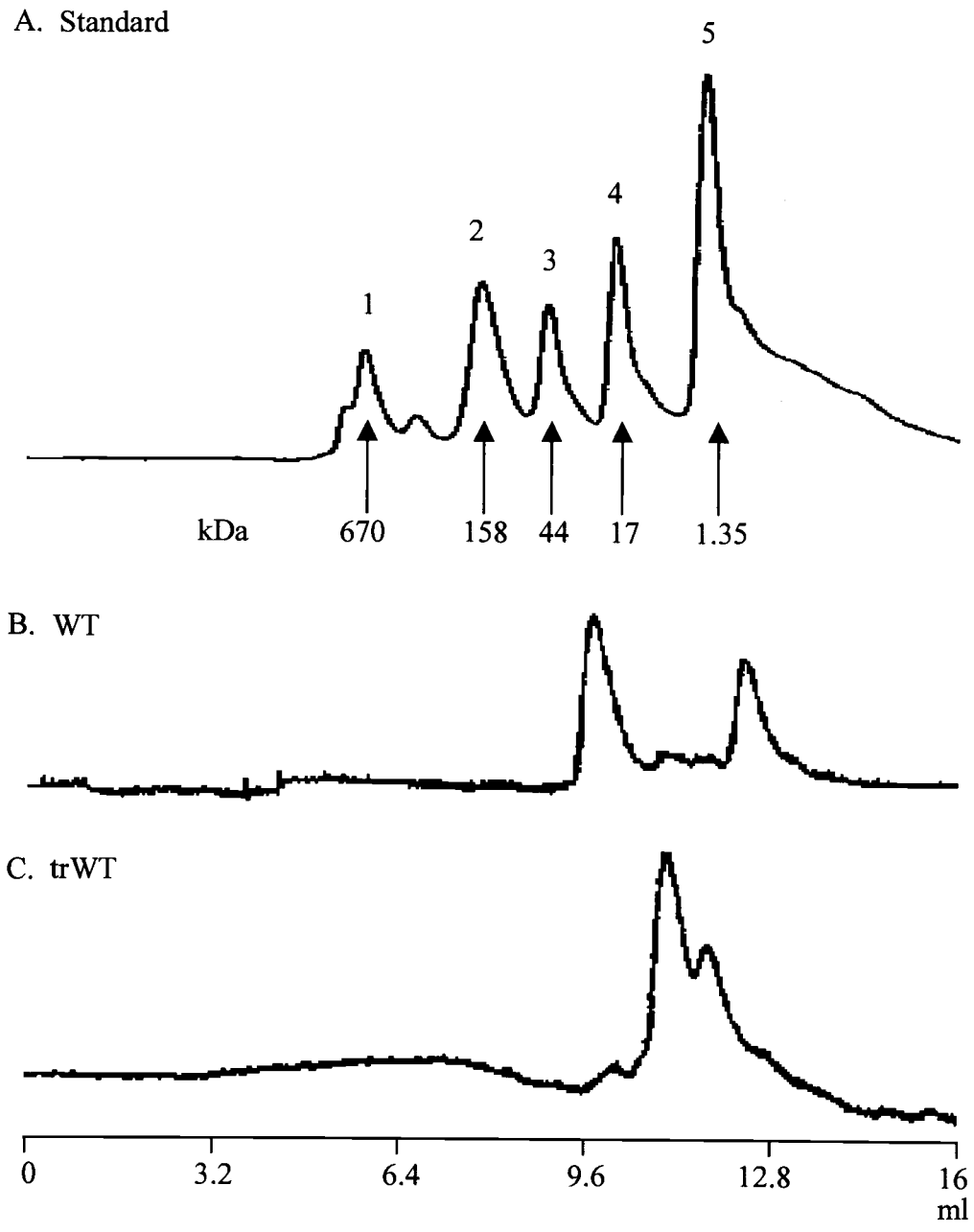

Figure 3.22: Size exclusion chromatography of βB1-crystallins. (A) Size exclusion standard proteins. 1, thyroglobulin (50 μg); 2, IgG (50 μg); 3, ovalbumin (50 μg); 4, myoglobin (25 μg); 5, vitamin B12 (5 μg). (B) WT. (C) trWT. Ten μg protein was injected onto column at 0.2 mg/ml.

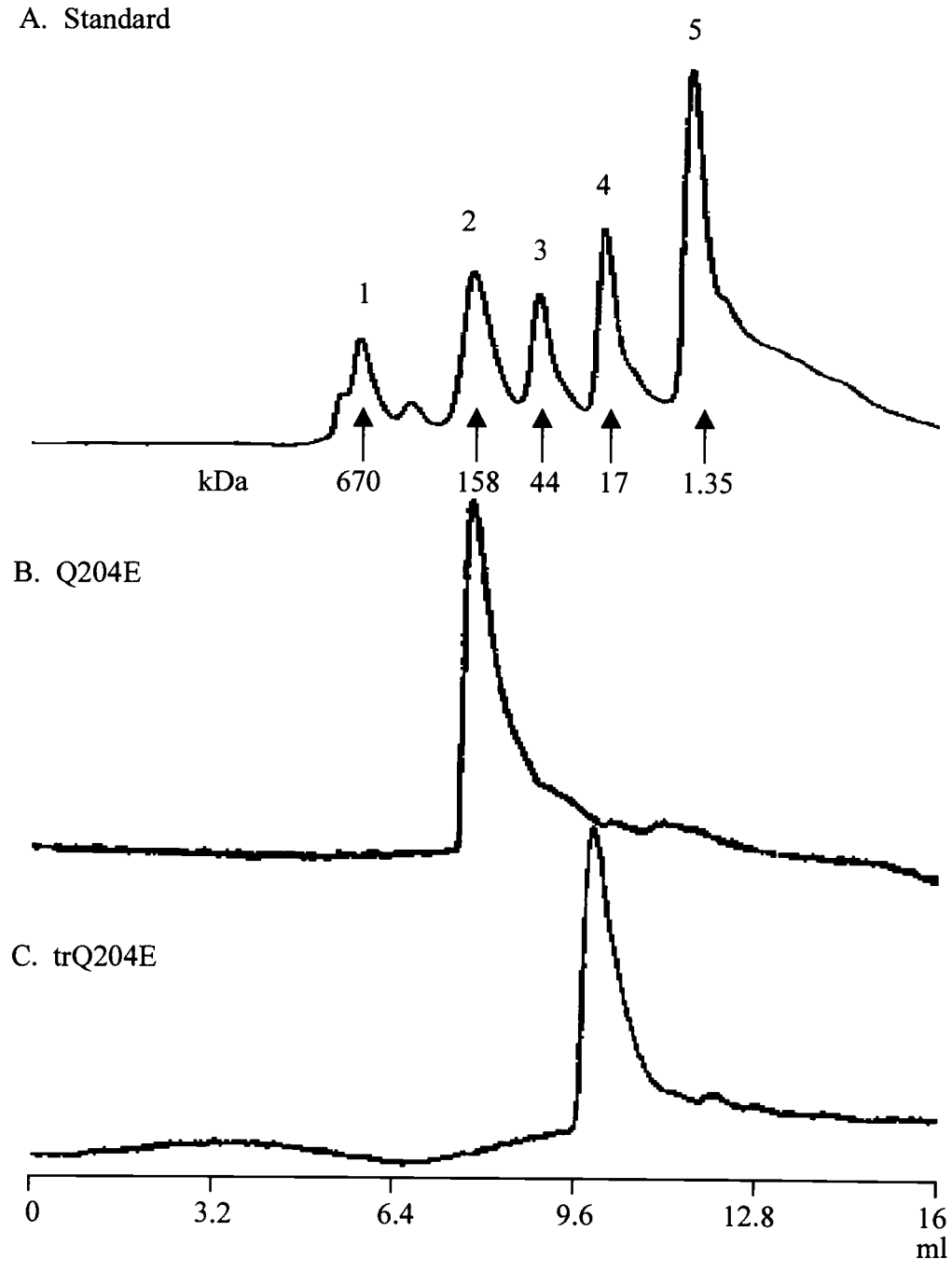

Figure 3.23: Size exclusion chromatography of deamidated βB1-crystallins. (A) Size exclusion standard proteins as shown in Figure 1. (B) Q204E. (C) trQ204E. Ten μg protein was injected onto column at 0.2 mg/ml.

publication, Q204E behaved as higher ordered aggregates, although light scattering measurements indicated that its self-association status was the same as WT at the same concentration (Lampi et al., 2001). TrQ204E eluted in a similar manner showing delayed elution between 44 and 17 kDa (Figure 3.23 C), as did trWT when compared to respective their full-length proteins. This indicated that removal of the N- and C-terminal extensions caused the truncated proteins to behave as more compact molecules compared to their respective full-length proteins.

The elution peak of WT was shifted to a higher molecular weight position at a 5-fold higher concentration (Figure 3.24 B), compared to monomeric elution peak (Figure 3.24 A). This indicated that WT eluted as a dimer. TrWT also eluted earlier at the higher concentration (Figure 3.24 D), compared to monomeric peak (Figure 3.24 C). Surprisingly, Q204E did not show a shift of elution peak even at a dimeric concentration (Figure 3.25 B), showing the same elution peak position as in monomeric elution (Figure 3.25 A). TrQ204E, however, showed a shift at dimer concentration (Figure 3.25 D), as seen in WT and trWT. This indicated that the Q204E may have a less compact folded tertiary structure or a different interaction with the gel matrix in the SEC column compared to other βB1-crystallins.

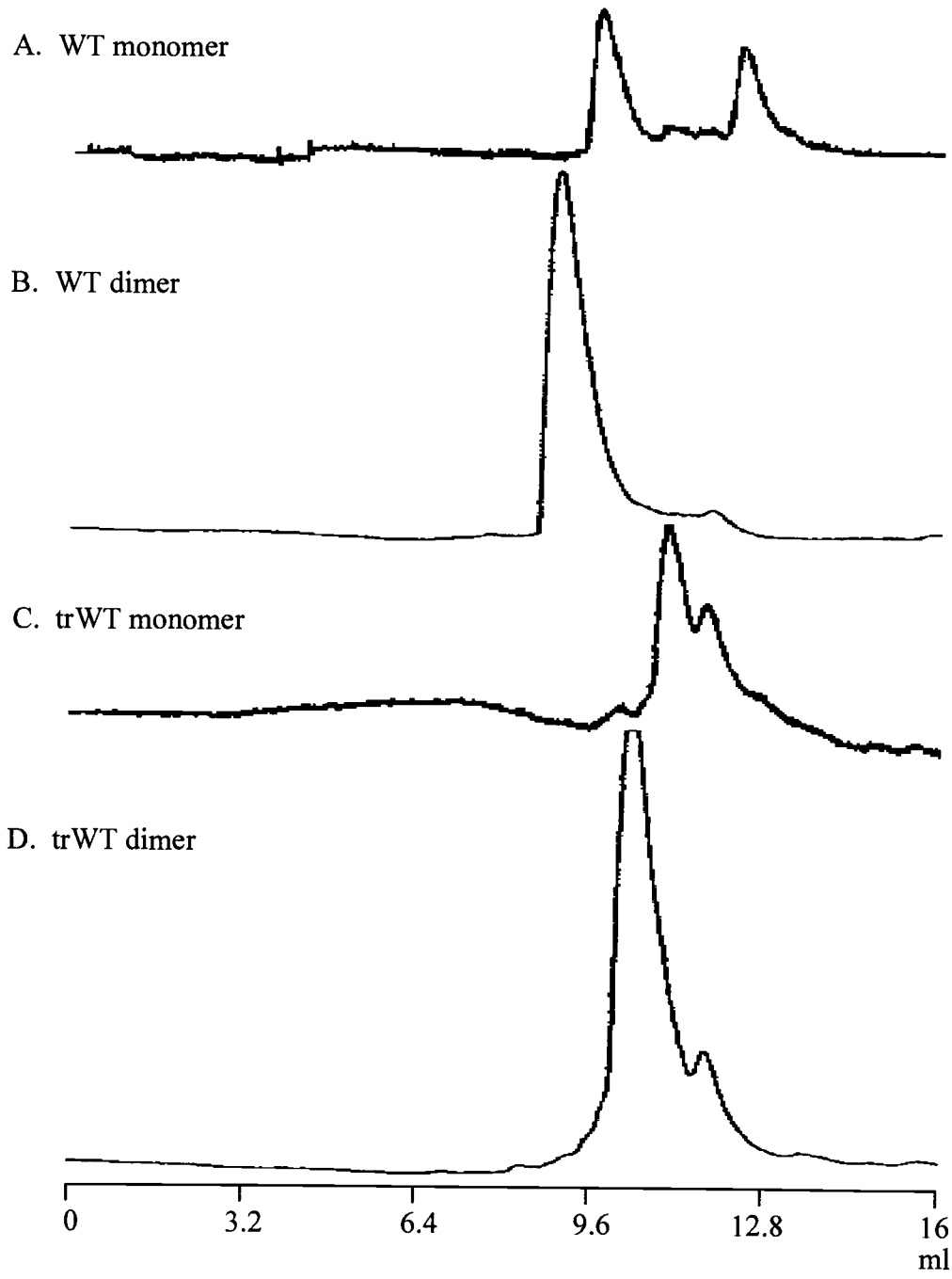

Figure 3.24: Comparison of the elution of monomeric and dimeric βB1-crystallins. (A) WT monomers (10 μg). (B) WT dimers (50 μg). (C) trWT monomers (10 μg). (D) trWT dimers (50 μg).

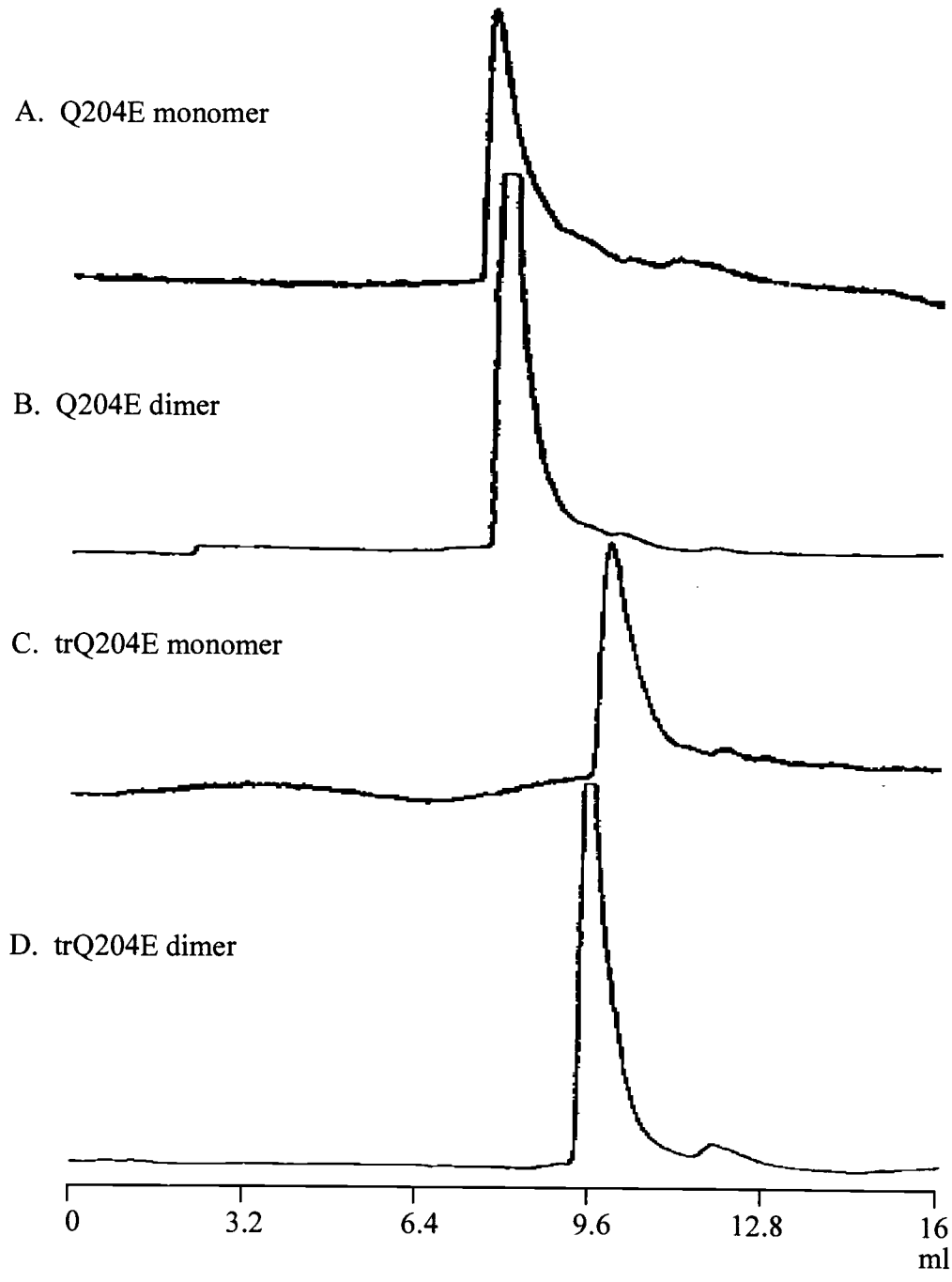

Figure 3.25: Comparison of the elution of monomeric and dimeric deamidated βB1-crystallins. (A) Q204E monomers (10 μg). (B) Q204E dimers (50 μg). (C) trQ204E monomers (10 μg). (D) trQ204E dimers (50 μg).

3.3.3 Absorption and emission spectra of βB1-crystallin

Spectrofluorimetry was used to measure structural changes in βB1-crystallin during urea-induced denaturation. The UV-absorption spectrum of WT βB1-crystallin showed maximum absorbance at 283 nm and a shoulder at 290 nm (Figure 3.26). Thus, the excitation wavelength was set at 283 nm for the fluorescence emission scan. Native βB1-crystallin showed a maximum fluorescence emission at 336 nm. Q204E, trWT and trQ204E also showed similar absorption and emission spectra compared to WT, with maximum absorption at 283 nm and maximum emission at 336 nm. At 1 μM protein concentration, the absorption and emission intensities were different among the four proteins. The order of fluorescence intensity from highest to lowest was Q204E, WT, trQ204E and trWT.

3.3.4 Fluorescence emission spectra for unfolding βB1-crystallins

To study the stability of βB1-crystallins in a denaturing environment, the proteins were incubated in various concentrations of urea. Protein unfolding and refolding were detected by measuring tryptophan fluorescence. Fluorescence emission spectra of βB1-crystallin in increasing concentrations of urea showed a red-shift as the maximum fluorescence wavelength increased from 336 to 353 nm

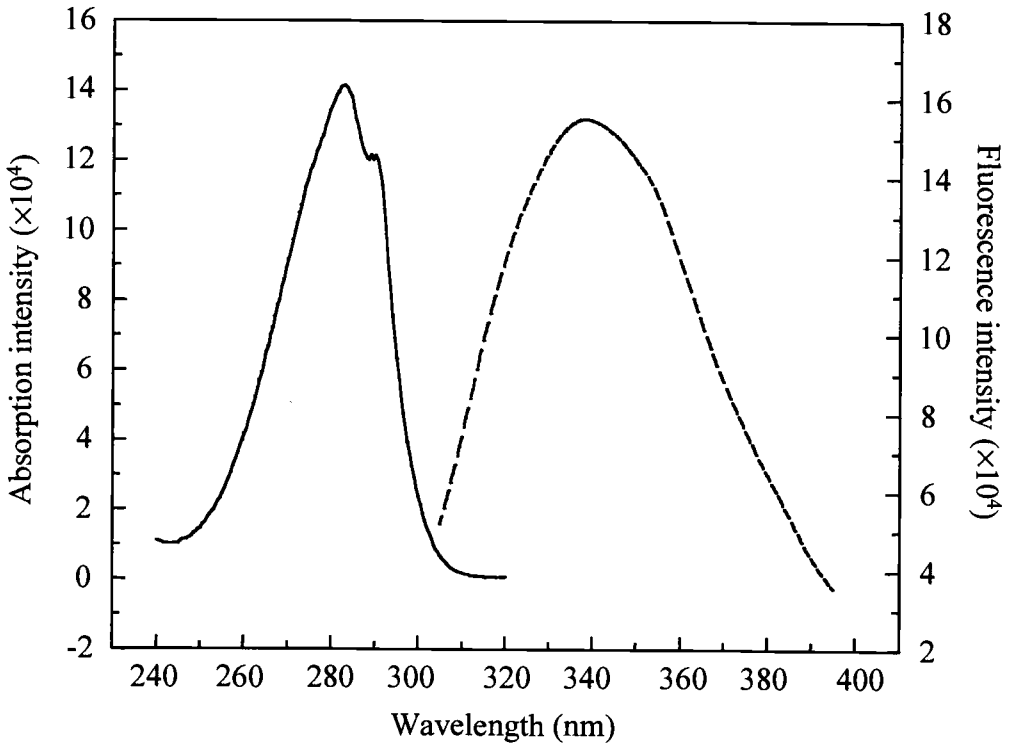

Figure 3.26: Absorption (—) and emission (---) spectra of WT βB1-crystallin at 1 μM concentration (27.9 μg/ml). For the UV-absorption spectrum, absorbance was measured from 240 to 320 nm with emission wavelength at 336 nm. For the fluorescence emission spectrum, the protein was excited at 283 nm and the emission was measured from 300 to 400 nm.

(Figure 3.27), indicating protein unfolding. As WT βB1-crystallin denatured in increasing urea concentrations, the fluorescence intensity increased. βB1-crystallin was fully denatured in a high concentration of 7.5 M urea. Higher concentrations of 18 μM WT showed the same pattern of denaturation in urea as at 1 μM (data not shown).

3.3.5 Unfolding/Refolding of WT and Q204E

Fluorescence emission was compared between WT and Q204E at 357 nm, where the maximum difference was observed between the native and fully denatured βB1-crystallin emission spectra (Figure 3.28). As proteins denatured by urea were refolded in non-denaturing buffer, the refolding fluorescence spectrum superimposed on the unfolding spectrum. This indicated reversible protein denaturation and renaturation in urea. Q204E showed a decrease in folded protein starting at 3 M urea, while WT started to unfold at 4 M urea. WT showed a one-step transition yielding 50% unfolding at 5.86 M, whereas Q204E showed a two-step transition showing 50% unfolding with the first transition at 4.06 M and the second transition at 7.19 M urea.

Using CD measurements, both WT (Figure 3.29 A) and Q204E (Figure 3.29 B) showed similar unfolding patterns compared to fluorescence data. The 50% unfolding for WT was at 5.86 M, and for Q204E it was at 4.15 and 7.05 M urea.

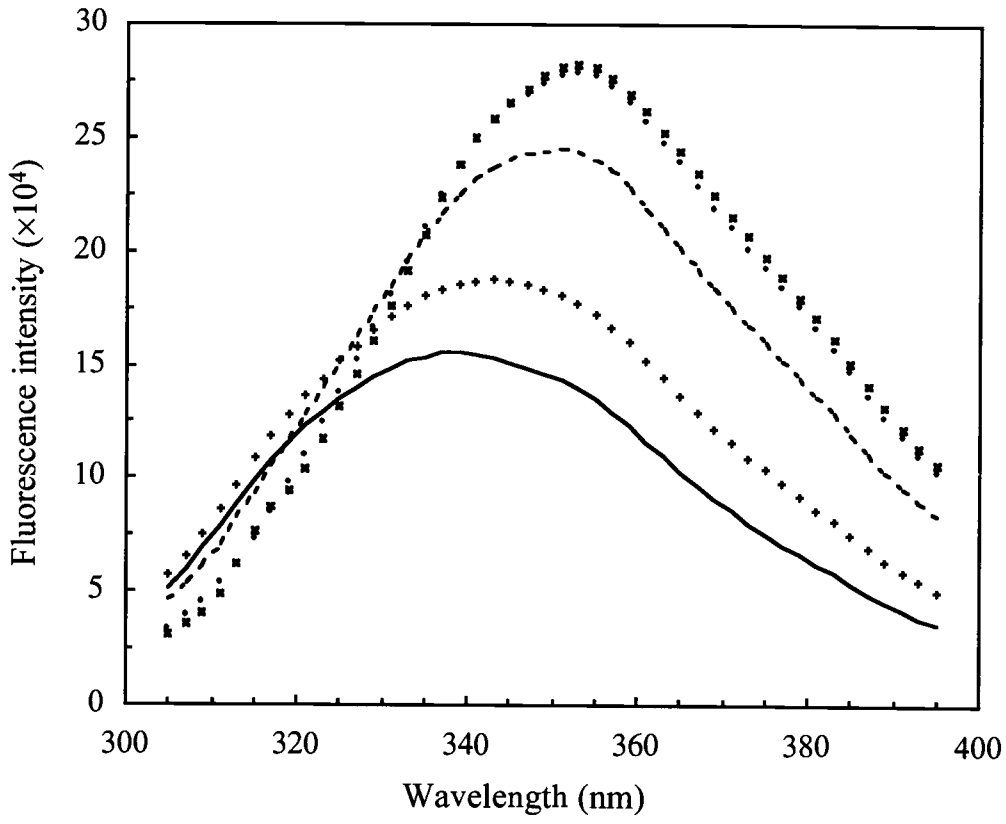

Figure 3.27: Urea-induced denaturation of WT as measured by fluorescence spectroscopy. WT (1 μM) was incubated in various concentrations of urea overnight at 25°C. 0 M urea, —; 3 M, + + +; 5 M, ---; 6.5 M, •••; 7.5 M × × ×. The fluorescence emission was measured from 300 to 400 nm with excitation at 283 nm.

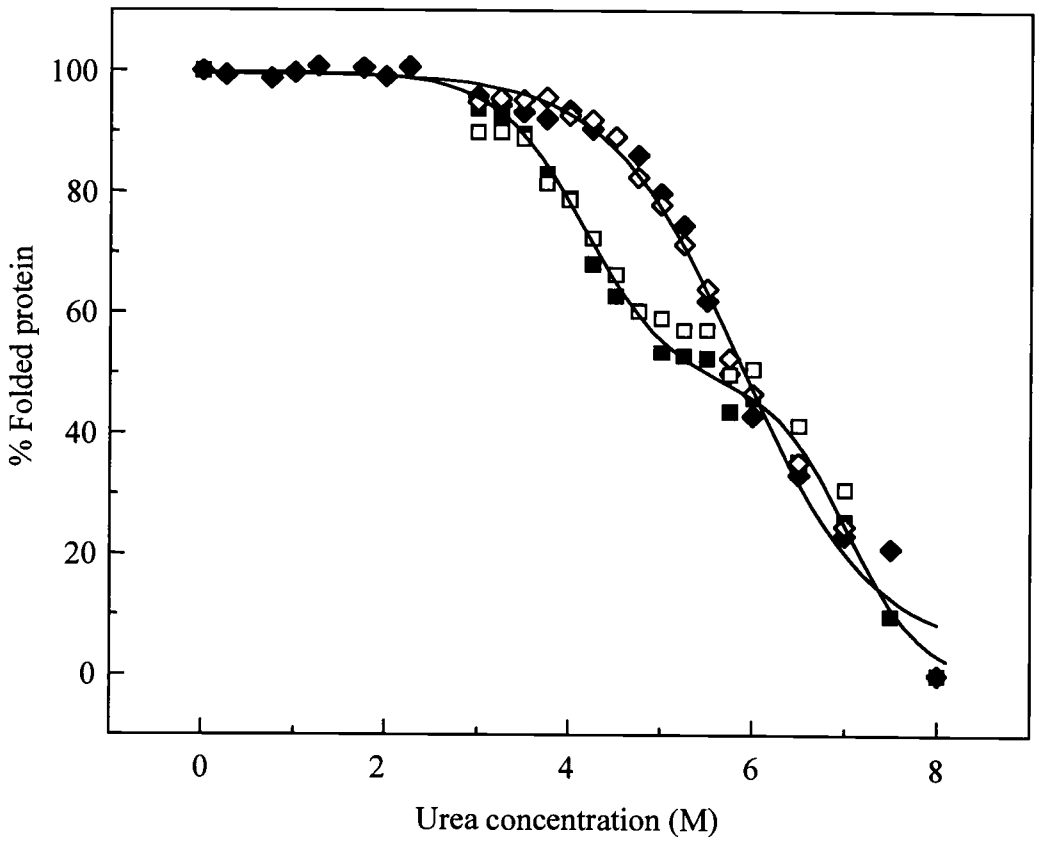

Figure 3.28: Stability of WT (diamond) and Q204E (square) βB1-crystallins in urea as measured by fluorescence spectroscopy. Unfolding (filled symbols) or refolding (open symbols) proteins at 1 μM were excited at 283 nm. Fluorescence emission intensity at 357 nm was used to construct the plot.

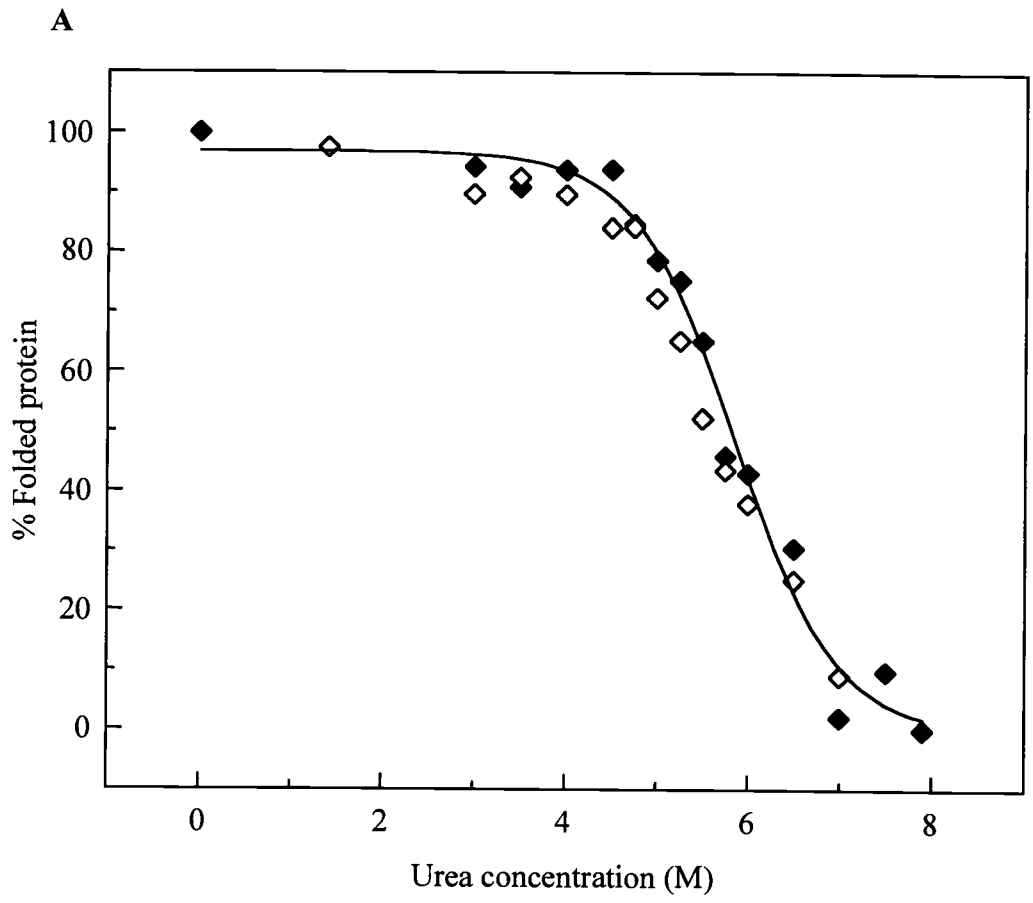

Figure 3.29 (A): Stability of WT βB1-crystallin (diamond) in urea measured by CD. Unfolding (filled symbols) and refolding (open symbols) were monitored. Ten μM protein (0.28 mg/ml) were used, and the ellipticity at 218 nm was used to construct the graph.

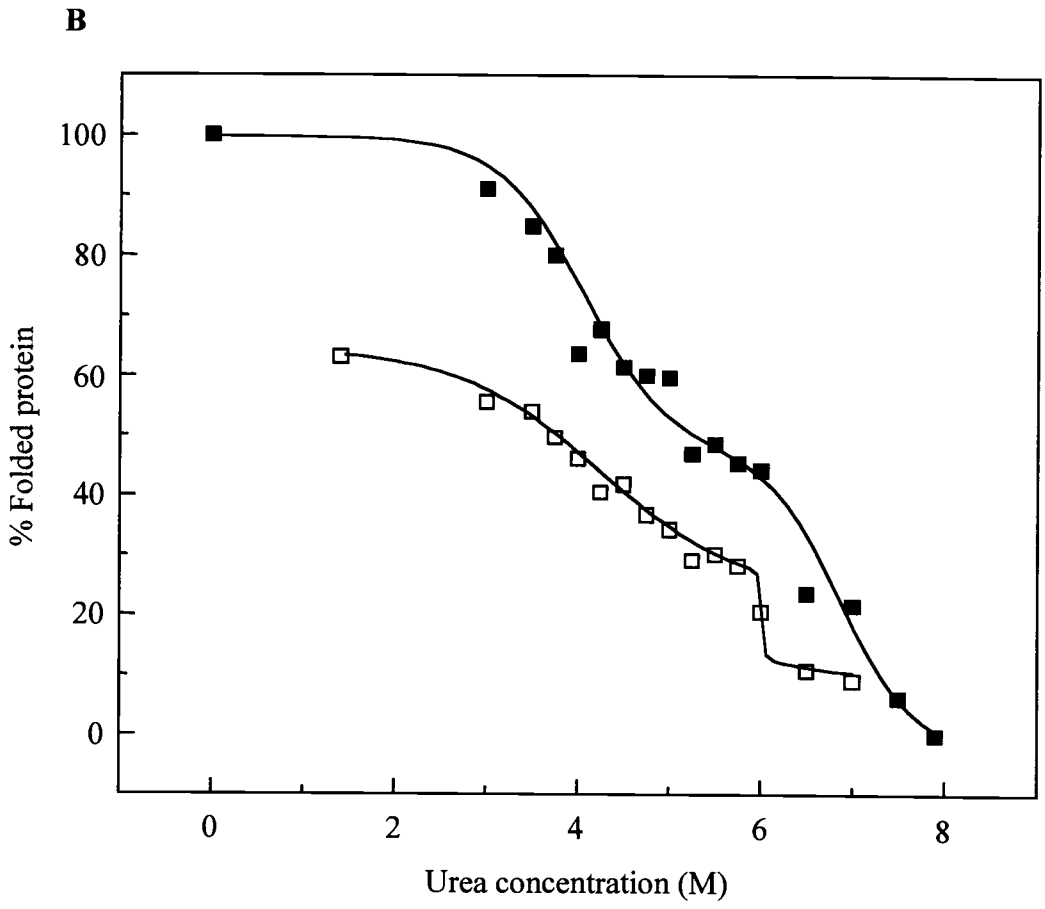

Figure 3.29 (B): Stability of Q204E βB1-crystallin (square) in urea measured by CD. Unfolding (filled symbols) and refolding (open symbols) were monitored. Ten μM protein (0.28 mg/ml) were used, and the ellipticity at 218 nm was used to construct the graph.

However, Q204E was not able to refold completely when the denatured protein was diluted in buffer without urea, whereas the WT refolding curve was superimposed on the unfolding curve. Figure 3.29 C shows that refolding protein is more denatured than the unfolding protein at 3 M urea.

3.3.6 Unfolding/refolding of truncated βB1-crystallins

To investigate if truncation of the extensions would influence stability of βB1-crystallin, N- and C-terminal extensions from WT and Q204E were cleaved by calpain 2. Both trWT and trQ204E showed reversible denaturation by urea (Figure 3.30). Truncation of the extensions did not change stability of proteins compared to full-length proteins. Similar to respective full-length proteins, trWT underwent 50% unfolding at 5.76 M urea with a one-step transition, and trQ204E showed a two-step transition at 4.09 and 6.49 M.

3.3.7 Stability of truncated βB1-crystallins in heat

In order to study the role of the N- and C-terminal extensions in βB1-crystallin stability, trWT and trQ204E were incubated at 55°C. Figure 3.31 shows

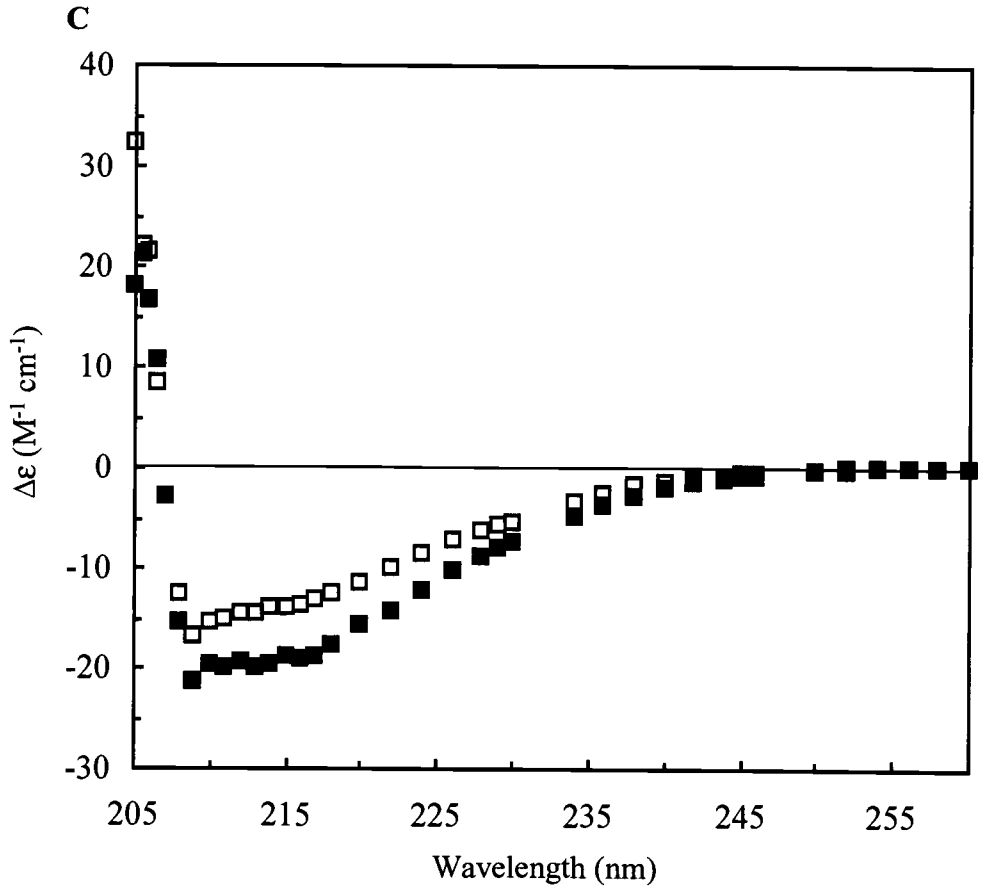

Figure 3.29 (C): Whole CD spectra of unfolding (filled square) and refolding (open square) Q204E in 3 M urea.

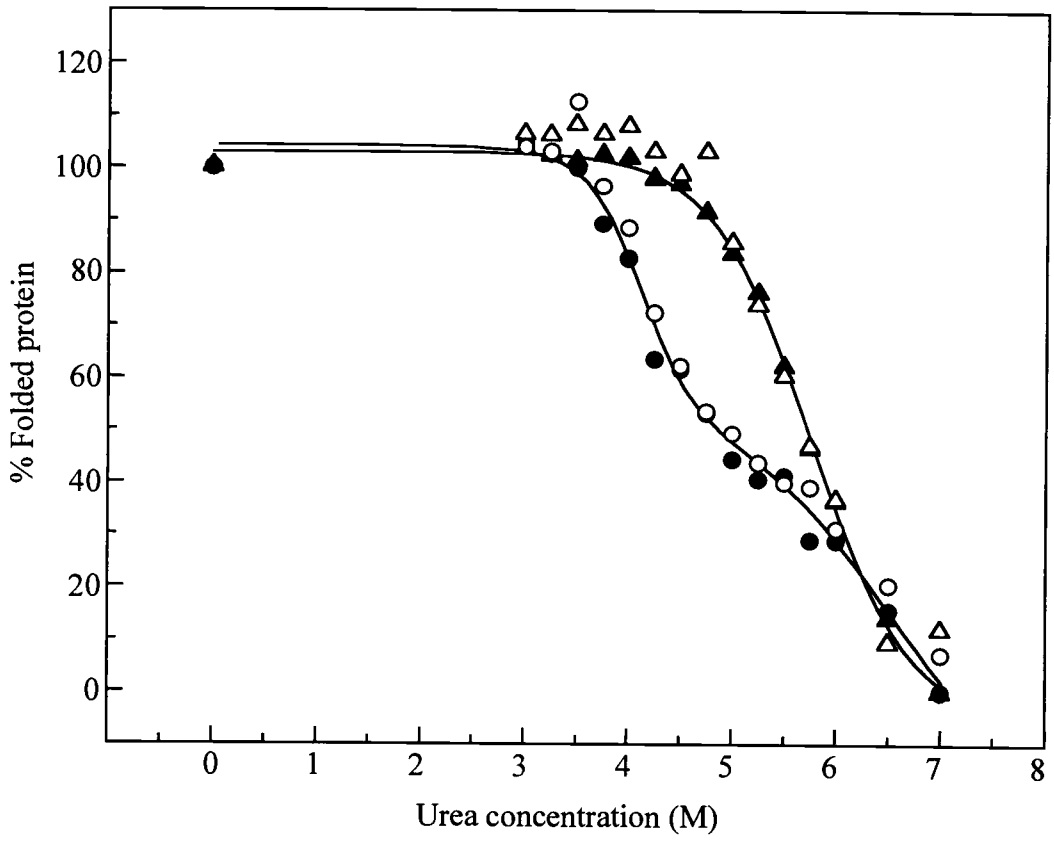

Figure 3.30: Stability of trWT and trQ204E βB1-crystallins in urea measured by fluorescence spectroscopy. Unfolding (filled symbols) and refolding (open symbols) of trWT (triangle) and trQ204E (circle) were monitored. The same conditions as described in Figure 5 were used. For truncation of WT and Q204E, proteins were incubated with calpain 2 in buffer containing 2 mM calcium at 37°C for 1 - 2 hours.

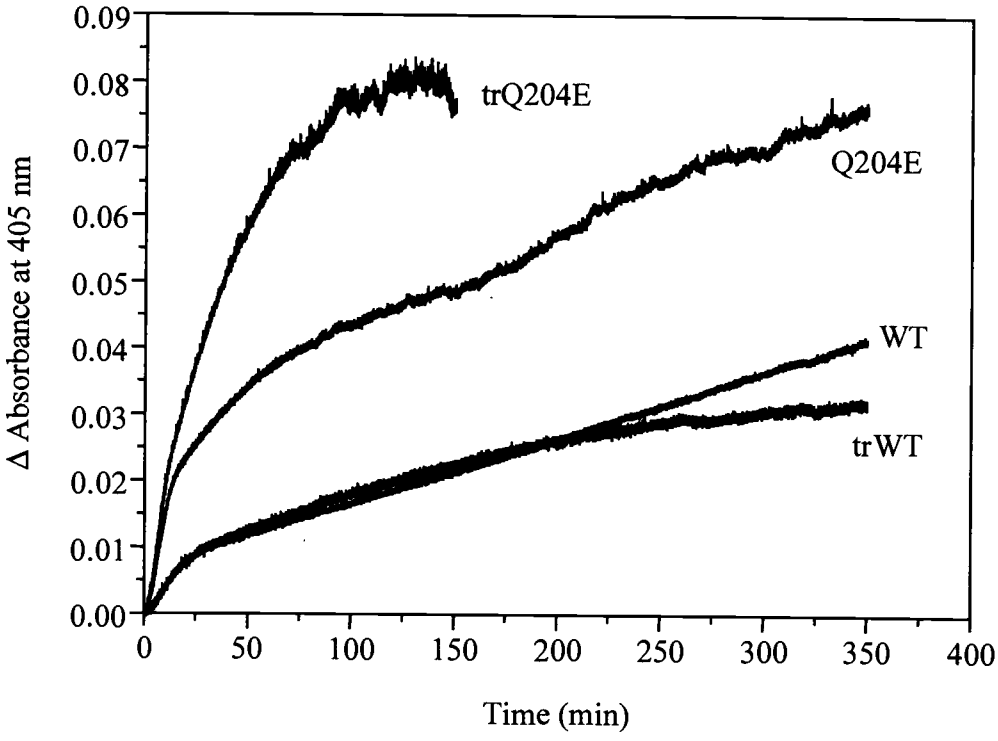

Figure 3.31: Stability of trWT and trQ204E βB1-crystallins to heating. Turbidity curves were obtained by measuring absorbance at 405 nm while heating 3.6 μM proteins at 55°C (WT& Q204E, 0.1 mg/ml; trWT & trQ204E, 0.08 mg/ml).

aggregation of βB1-crystallins during heating as measured by absorbance at 405 nm. WT was fairly stable at 55°C. TrWT was as stable as WT. As described in Lampi et al., (2002), Q204E was less heat-stable than WT. TrQ204E aggregated/precipitated more rapidly than Q204E and the other proteins.

3.3.8 Interaction of truncated βB1-crystallins with αA-crystallin in heat

To investigate how the extensions affect interaction of βB1-crystallin with a molecular chaperone αA-crystallin (αA) in a denaturing environment, the βB1-αA complex was incubated at 55°C. When equal molar amounts of αA were added to trWT, aggregation was prevented until 500 min (trWT+αA in Figure 3.32 A), demonstrating the chaperone activity of αA. However, prolonged heating caused trWT-αA complex to precipitate, suggesting failure of the αA-crystallin chaperone function. With a 2:1 molar ratio of αA to trWT, precipitation of trWT was prevented by αA (trWT+2αA in Figure 3.32 A). WT was effectively chaperoned by 1:1 molar ratio amount of αA (Lampi et al., 2002).

Figure 3.32 B shows profiles for the soluble and insoluble protein fractions after heat incubation. Proteins found in insoluble fraction indicate aggregation. When trWT alone was heated, a majority of protein remained in the soluble fraction (lane 1), with a fairly small amount of trWT found in insoluble fraction, indicating

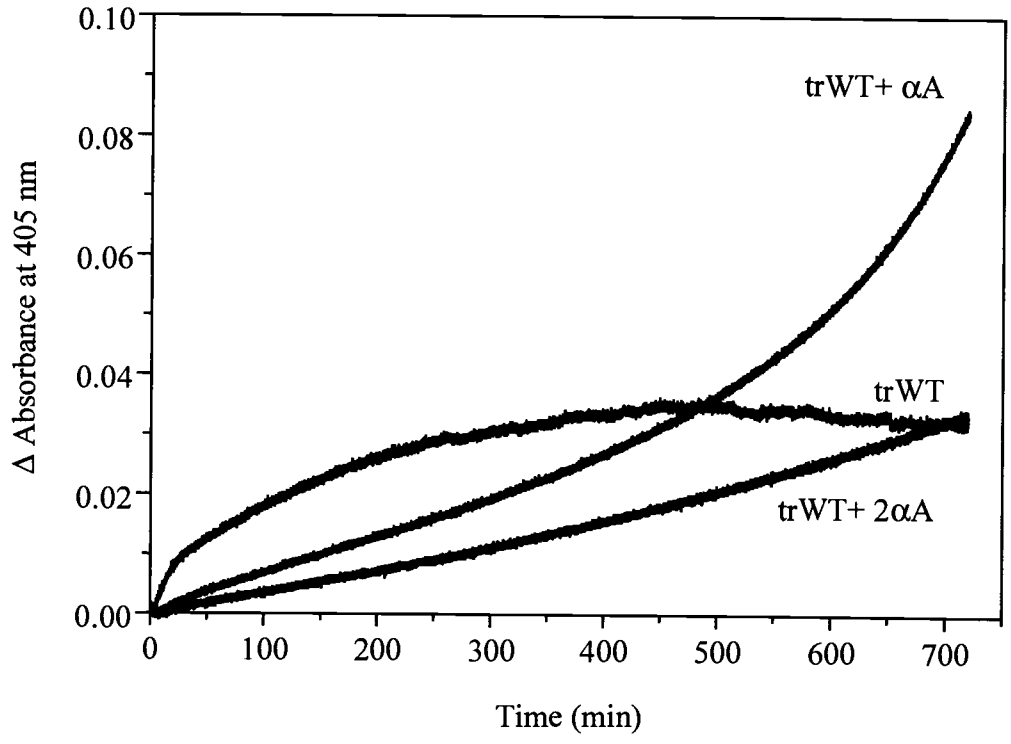

Figure 3.32 (A): Interaction of trWT with αA-crystallin during heating. TrWT was heated without or with a 1:1 or 2:1 molar ratio of αA to trWT and compared to heating trWT alone.

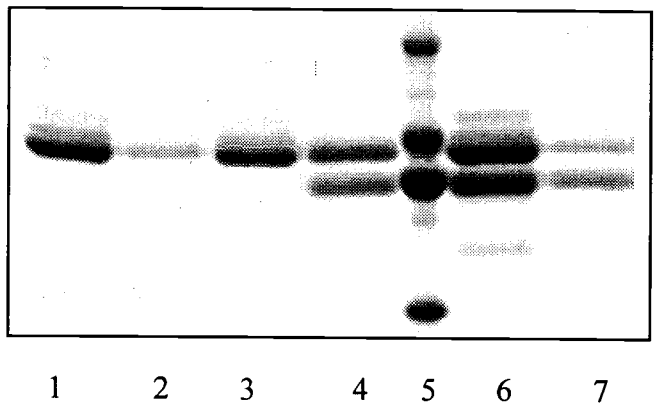

Figure 3.32 (B): SDS-PAGE of trWT with αA-crystallin from (A) after heating. Lanes 1 & 2, trWT soluble & insoluble fractions; lanes 3 & 4, trWT+ αA soluble & insoluble; 5, molecular weight standards; lanes 6 & 7, trWT+2 αA soluble & insoluble.

aggregation (lane 2). When 1:1 ratio of trWT and αA was heated, only trWT was found in the soluble fraction (lane 3), while both trWT and αA were found in insoluble fraction, indicating aggregation of the trWT-αA complex (lane 4). With a 1:2 ratio of trWT to αA, a majority of the complex remained in the soluble fraction, indicating that αA was able to chaperone trWT (lane 5). Only a small amount of complex was found in insoluble fraction (lane 6).

TrQ204E showed more aggregation when complexed with αA at a 1:1 ratio (trQ204E+αA in Figure 3.33 A). TrQ204E alone, or with a 1:1 ratio of αA, was found exclusively in the insoluble fractions (lanes 2 and 4 in Figure 3.33 B). A trace amount of trQ204E remained in soluble fraction (lane 3). The 2:1 ratio of αA to trQ204E did not completely prevent aggregation (trQ204E+2αA in Figure 3.33 A), and more trQ204E and αA were found in insoluble fraction (lane 6 in Figure 3.33 B). When a 4:1 ratio αA was present, a majority of proteins stayed in the soluble fraction (trQ204E+4αA in Figure 3.33 A and lane 7 and 8 in Figure 3.33 B).

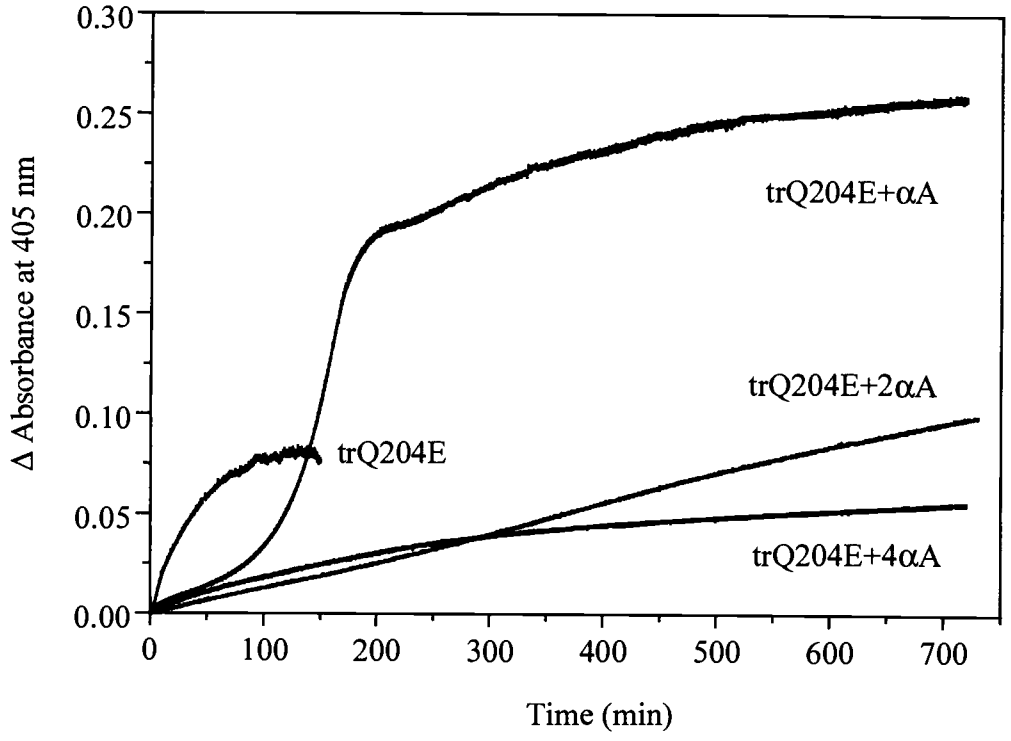

Figure 3.33 (A): Interaction of trQ204E with αA-crystallin during heating. TrQ204E was heated at 55°C without or with a 1:1, 2:1 or 4:1 ratios of αA to trQ204E.

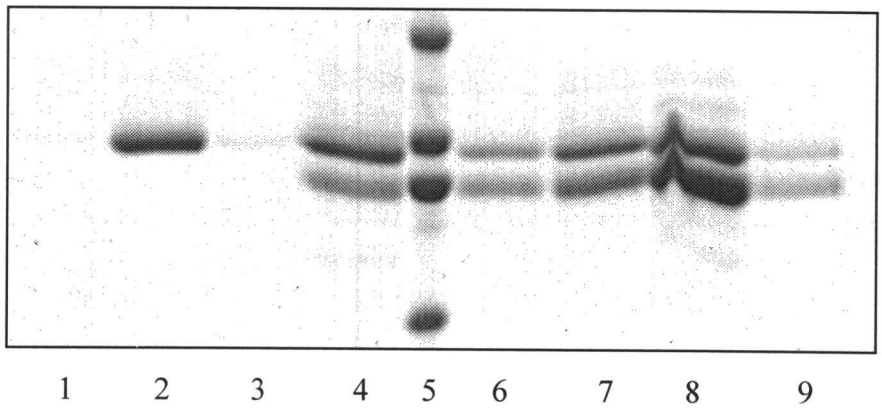

Figure 3.33 (B): SDS-PAGE of trQ204E with αA-crystallin after heating. Lanes 1 & 2, trQ204E soluble & insoluble fractions; 3 &4, trQ204E+ αA soluble & insoluble; 5, molecular weight standards; lanes 6 & 7, trQ204E+2 αA soluble & insoluble; lanes 8 & 9, trQ204E+4 αA soluble & insoluble.

4 DISCUSSION

4.1 EPITHELIAL CHANGES IN SELENITE CATARACT

4.1.1 Apoptosis in selenite cataract

Apoptosis in lens epithelial cells was accelerated in selenite cataract (Tamada et al., 2000), and apoptosis was proposed as a mechanism for selenite cataract formation. Histologically, cleavage of double stranded DNA during apoptosis was elevated in epithelial cells in selenite cataract. This was detected by the terminal deoxynucleotidyl transferase-mediated dUTP nick end labeling (TUNEL) assay. In addition, apoptotic epithelial cells induced by selenite showed disappearance of the nuclear membrane and condensation of karyoplasm or chromatin observed by transmission electron microscopy.

Other evidence for apoptosis in selenite cataract was activation of caspase 3 (Tamada et al., 2000). This was measured by breakdown of poly(ADP-ribose) polymerase (PARP). Caspase 3 is known as one of cascade enzymes playing a key role in apoptosis (Miura et al., 1993; Nicholson et al., 1995), and caspase 3 is known to cleave PARP. Calpains were also found to be involved in the apoptosis process in other tissues, and calpain inhibitors blocked apoptosis (Squier et al., 1994; Martin et al., 1995). In selenite cataract, calpain 2 and Lp82 were activated

(Figure 3.8), and calpain-specific breakdown fragments of α-spectrin and vimentin were observed (Tamada et al., 2000). In the present studies, selenite cataract did not cause appreciable changes in the levels of mRNAs of calpains and caspase 3 during the course of cataract formation. Decreases in transcripts of Lp82 and calpastatin were observed (Figures 3.4 and 3.5), but these changes occurred after apoptotic events, calpain activation and cataract formation. Calpain activation (Figure 3.8) and increased number of apoptotic cells (Tamada et al., 2000) were observed within 3 days after selenite injection, and cataracts were usually visualized at day 3. This indicated that the decreased expression of Lp82 and calpastatin might not be a direct response to selenite insult or apoptotic process, but rather after-effect of calpain activation or cell damage. Thus, the competitive RT-PCR data suggested that the increased activities of calpain 2 and caspase 3 in selenite cataract occurred at the level of enzyme activation rather than up-regulation of mRNAs.

Recently it was reported that three genes showed major changes in expression during selenite cataract formation: decrease in cytochrome c oxidase subunit I (COX-I) by 3- to 5-fold, and gastric inhibitory polypeptide by 2- to 6-fold, and increase in early growth response protein-1 (Egr-1) by 5- to 6-fold (Nakajima et al., 2002). COX-I is an enzyme involved in the electron transport system in mitochondrial membranes, and the mRNA is transcribed from mitochondrial DNA (D'Aurelio et al., 2001). The mRNA level for *Cox-I* decreased progressively during neuronal cell death, followed by decreased protein activity (Abe et al., 1996), and

Cox-1 expression was down-regulated in apoptotic cells (Ragno et al., 1998). EGR-1 is a zinc finger transcription factor that couples extracellular signals to long-term responses by altering expression of *Egr-1* target genes (Cibelli et al., 2002). EGR-1 is also known to be essential for induction of apoptosis (Wyllie, 1992), and *Egr-1* mRNA expression was acutely elevated during nitrogen oxide-induced apoptosis in human neuroblastoma cells (Cibelli et al., 2002).

Li et al. (1995b) reported that lens tissue cultures tested with calcium ionophore showed lens epithelial cell apoptosis followed by cataract formation. In this study, mRNA of *c-fos* encoding a transcription activation factor was rapidly up-regulated, and the high level of mRNA was sustained. This indicated a possible involvement of c-Fos protein for mediating changes in gene expression that lead to apoptosis of the observed lens epithelial cells. The above studies suggested that apoptosis of lens epithelial cells may be a contributing pathway in cataract formation.

4.1.2 Proteolysis of lens epithelial proteins during selenite cataract formation

During selenite cataract formation, we found that proteolysis of epithelial crystallins was pronounced. Proteolysis of higher molecular weight proteins in the epithelium was not as prominent as in crystallins. Since crystallins are the predominant components in the lens comprising up to 90% of the soluble protein (Hope, Chen, and Hejtmancik, 1994), their abundancy may facilitate crystallins as

substrates for activated proteases. Two calpains, calpain 2 and Lp82, exhibit major activities in young lenses from rats (David and Shearer, 1986; Fukiage et al., 1997b; Shearer, et al., 1999), mice (Ma et al., 1999; Nakamura, et al., 2000), rabbit (Ma et al., 1998), and cows (Yoshida et al., 1985; Ueda et al., 2001). Involvement of calpains in cataract formation has been studied *in vivo* (David and Shearer, 1986; Ma et al., 1997; Nakamura et al., 2000) and *in vitro* (Fukiage et al., 1998; Nakamura et al., 1999; Nakamura, et al., 2000). In cataract studies, an increase in calpain activities was coupled with a massive increase in cellular calcium (Shearer and David, 1982; Hightower, David, and Shearer, 1987; Fukiage et al., 1998). The free calcium level was elevated to over 100 μM in nucleus from the selenite cataract lens, compared to 0.5 μM calcium in the normal lens nucleus (Hightower, David, and Shearer, 1987). In addition, by using calcium ionophore, nuclear cataract could be induced *in vitro* (Fukiage et al., 1998). When calpain inhibitors were added to lenses cultured with calcium ionophore, cataract formation was delayed (Azuma, David, and Shearer, 1991; Azuma, David, and Shearer, 1992; Fukiage et al., 1997a; Fukiage et al., 1998; Shearer et al., 1991). Insolubilized crystallins from selenite cataract lenses were compared to crystallins proteolyzed by calpain 2 *in vitro* and insolubilized. Similar cleavage sites were observed (David, and Shearer, 1993; David, Shearer, and Shih, 1993; David, Wright, and Shearer, 1992; Shearer et al., 1995). In human senile cataract, lens calcium was significantly higher compared to normal lenses (Dilsiz, Olcucu, and Atas, 2000), and a calcium-dependent proteolytic activity was reported in human lens

epithelium (Karlsson et al., 1999). In addition, *in vitro* culture of human lenses with calcium ionophore caused cortical opacification, and resulted in a calpain-specific breakdown product of vimentin (Sanderson, Marcantonio, and Duncan, 2000). These observations suggest that calcium-activated calpains in lens may play a key role during cataract formation.

4.1.3 Oxidation of epithelial proteins during selenite cataract formation

2-D gel electrophoresis followed by thiol-blotting was shown in the present studies to be a sensitive method for visualizing the oxidative status of proteins. The surprising finding from our study was that most of free sulfhydryl groups on lens epithelial proteins were not oxidized during selenite cataract formation. *In vitro*, these proteins did lose free sulfhydryl groups when exposed to either an alkylator, IAA (Figure 3.9 B) or an oxidant, selenite (Figure 3.10 B). Previously David and Shearer (1984b) reported a decrease in reduced glutathione by 44% in whole lenses with selenite cataract. However, in their studies, there was no significant increase in oxidized glutathione (GSSG) or oxidized proteins (PSSP) in whole lens, which was similar to the current findings in epithelium.

In contrast, an increase in protein disulfide content has been reported in human cataracts (Augusteyn, 1981; Harding, 1991d). Crystallin oxidation and aggregation occurs preferentially in nucleus of lenses. The nucleus contains the oldest lens

proteins and less reduced glutathione is present. During human cataractogenesis, especially nuclear cataract, the lens proteins unfold and free sulfhydryls that were buried become reactive (Harding, 1991d). These free sulfhydryls then react to form mixed disulfides with glutathione and cysteine, and disulfide-crosslinked protein aggregates. The total protein thiol decreases progressively as the protein disulfide content increases in human cataracts (Hum, and Augusteyn, 1987). Liang and Pelletier (1987) also reported that the reaction of native crystallins with oxidized glutathione provoked a conformational change.

Interestingly, disulfide bonds in rat lens proteins appeared to be intramolecular in normal aging lenses (Hum, and Augusteyn, 1987a) rather than intermolecular as found in human lenses (Hum, and Augusteyn, 1987b). Combined with our results, these observations suggest that proteins in rat lens may be well-protected and more resistant to sulfhydryl oxidation. The excessive amount of reduced glutathione (Giblin et al., 1985; Spector, 1991; Reddan et al., 1999) may play an immediate defense role against the oxidizing insult of selenite in lens epithelium during selenite cataract formation. If oxidation of epithelial proteins occurs in selenite cataract, it may be limited to a very specific class of proteins. Generalized oxidation of many types of protein sulfhydryl groups in the epithelium is not a mechanism for selenite cataract formation.

4.2 CALPAIN 10 IN LENS

4.2.1 Calpain 10 protein in tissues and localization in lens

In the present study, calpain 10 was found to be highly concentrated in water-insoluble fraction of lens. This suggested that majority of cellular calpain 10 may be insoluble in the cytosol or associated with membranes or cytoskeletal proteins. Calpain 10 protein was also found in other rat tissues such as brain, heart, kidney, liver, lung, skeletal muscle, spleen, stomach, and retina (Ma et al., 2001). This indicates that calpain is another ubiquitous calpain along with calpains 1 and 2. Immunohistochemical studies (Ma et al., 2001) revealed that calpain 10 was located mainly in the cytoplasm of the epithelium and bow region of the newborn mouse lens, but much lower levels were found in cortex and nucleus. In human lens, calpain 10 was also concentrated in epithelium, but interestingly, in the outer fiber cells, calpain 10 was concentrated at the plasma membrane. Similarly, in skeletal muscle from young mouse, calpain 10 was predominantly detected at the muscle fiber membrane, the sarcolemma. These observations may explain why calpain 10 was found to be concentrated in water-insoluble fraction.

Another interesting observation was the para-nuclear localization of calpain 10 in cultured lens epithelial cells (Ma et al., 2001). Although histochemical staining showed that calpain 10 was not associated with DNA, calpain 10 was present in the nucleus in a punctate arrangement as well as in cytosol. Interestingly, when

cellular calcium was elevated by treatment with calcium ionophore, calpain 10 staining increased in cell nucleus and decreased in cytoplasm. This observation suggested that calpain 10 may bind to nuclear components involved in a calcium-dependent signal transduction.

4.2.2 Changes in calpain 10 with age

Another finding from the present study was that calpain 10 level in rat lens decreased with age. Human lenses also showed a decrease in calpain 10 proteins during aging. Calpain 10 was concentrated in the epithelium and bow region of lens where cell turnover and differentiation occurred. Decrease in calpain 10 during aging or in fully differentiated fiber cells indicated that calpain 10 may be involved in development of lens and lost with aging or differentiation. However, the precise function of calpain 10 in the cell is not yet known, and further studies need to be done to clarify the role of calpain 10.

4.2.3 Proteolysis of calpain 10 in selenite cataract

During selenite cataract formation, calpain 10 protein was completely lost in lens nucleus where cataract was formed. However, it was not clear if calpain 10

was activated during cataract formation or was degraded by other proteases. Calpain 10 is an atypical calpain with calcium-binding domain replaced by T domain (Braun et al., 1999), but the function of the T domain is not known. Calpain 10 was not activated by calcium and did not show proteolytic activity when measured by assays used for typical calpains (unpublished results). Thus, with an assumption that calpain 10 does not have a calcium-dependent proteolytic activity, we investigated if calpain 10 could be degraded by other calpains in lens. *In vitro* hydrolysis studies showed that calpain 10 was a substrate for both calpain 2 and Lp82. From these results, another question rose: which calpain proteolyzes calpain 10 during selenite cataract formation? In selenite cataract, calcium accumulated predominantly in nuclear region of lens (Shearer and David, 1982), and cataract was mainly formed in the nucleus. This suggests that calpain in lens nucleus may play a significant role during selenite cataract formation or degradation of calpain 10. Indeed, calpain 10 was completely lost in the nucleus of selenite cataract at 3 days (lane 4 in Figure 3.16 C), whereas in epithelium intact calpain 10 was still present at 5 day (lane 6 in Figure 3.16 A). Previously, Ma et al. (1998) reported different regional distributions of calpain 2 and Lp82 in lens. Calpain 2 was most abundant in epithelium, while Lp82 was most abundant in nucleus. In addition, Lp82 had a longer half-life compared to calpain 2 when their activities were assayed *in vitro* under the same conditions (Ueda et al., 2001). Based on the observations above, we concluded that calpain 10 in lens nucleus was degraded by

Lp82 during selenite cataract formation, and that calpain 10 activation may not be the cause of selenite cataract.

4.3 POST-TRANSLATIONAL MODIFICATION OF βB1-CRYSTALLIN

4.3.1 Altered protein behavior by modifications to βB1-crystallin

Replacement of a single amino acid, glutamine to glutamic acid caused a dramatic change in tertiary structure of the βB1-crystallin molecule, as observed by size exclusion chromatography (SEC). Deamidated βB1-crystallin monomers behaved in a gel filtration column as a trimer or tetramer (Figure 3.23 B). This indicated that introducing the charged glutamate residue into a hydrophobic domain caused a change in the shape of the βB1-crystallin molecule. This result also suggested that the negative charge from glutamic acid may interfere with the hydrophobic interaction between domains in βB1-crystallin and render the molecule less compact. However, it is not clear why dimeric Q204E behaved similar to a monomer in SEC.

When the N- and C-terminal extensions were removed, βB1-crystallin eluted later on SEC than expected (Figure 2.22 C), which suggested that truncation caused the molecule to become more compact. This result is in agreement with nuclear magnetic resonance (NMR) data showing that the terminal extensions in WT βB1-

crystallin are highly flexible (Lampi et al., 2002). By truncation of the highly mobile extensions, βB1-crystallin may become more compact, and/or βB1-crystallin lost hydrophilicity contributed by the extensions. More hydrophobic surfaces may have been exposed, allowing trWT to interact more strongly with the gel matrix than WT. Removal of the extensions from Q204E also delayed elution in SEC compared to full-length Q204E, indicating that the extensions contributed to tertiary structure of deamidated βB1-crystallin. Interestingly, trQ204E eluted earlier compared to trWT elution, but showed very similar elution compared to full-length WT, indicating effects of both modifications. After truncation, the molecule became more compact. After deamidation, the molecule became less compact. When truncation and deamidation occurred together, the effect of truncation cancelled out the effect of deamidation in doubly modified trQ204E. Thus, trQ204E apparently behaved as WT in SEC.

4.3.2 Decreased stability of βB1-crystallin by deamidation

The SEC studies showed that deamidation altered βB1-crystallin behavior on the gel filtration column, and a previous publication suggested that deamidation of βB1-crystallin might alter protein stability (Lampi et al., 2001). This hypothesis was proven to be correct in the present experiments using urea and heat to perturb protein structures. Altered protein stability was supported by observing

denaturation of Q204E in lower urea concentrations compared to that of WT, as measured by fluorescence spectroscopy and CD. Interestingly, Q204E exhibited a two-step transition during urea-induced denaturation, while WT showed a one-step transition.

Production of Q204E introduced a negative charge in the globular domain of βB1-crystallin where hydrophobic interactions occur between domains (Lampi et al., 2001). We speculate that the negative charge disturbed the hydrophobic environment and that the protein became more prone to unfolding by denaturants such as heat or urea. Electron paramagnetic resonance (EPR) data also supported this speculation (Kim et al., 2002), showing that the N-terminal domain of Q204E was less stable, compared to WT. This indicated that a negative charge on C-terminal domain affected stability of N-terminal domain. These data suggest a possible mechanism for the two-step transition of Q204E. Urea denatures the N-terminal domain first, followed by denaturation of the C-terminal domain. This idea is feasible if an intra-molecular, hydrophobic interaction occurs between the two globular domains of βB1-crystallin. A negative charge produced by deamidation on the C-terminal domain of Q204E may interfere with the hydrophobic interaction between the domains, and the N-terminal domain may no longer have hydrophobic support from the C-terminal domain for its stability. Deprivation of a hydrophobic partner may cause the N-terminal domain to be more vulnerable to a denaturant such as urea.

Although deamidation caused instability, it did not affect cleavage site specificity for calpain 2 during truncation of the N- and C-terminal extensions. Protein N-terminal sequencing analysis, ESI-MS, and MALDI-MS confirmed that both WT (Lampi et al., 2001, Shih et al., 2001) and Q204E (Figure 3.20 A & B) were cleaved at the same cleavage sites by calpain 2.

In fluorescence and CD studies, relatively low concentrations of 1 and 10 μM proteins were used to determine the stability of proteins without association with other molecules. Unexpectedly, Q204E failed to show reversible denaturation and renaturation in the CD studies, showing more denaturation in the refolding spectrum than in the unfolding spectrum. This suggested that upon refolding, a portion of Q204E might aggregate. Indeed, the aggregation of dimeric 27 μM Q204E was observed in an EPR study (Kim et al., 2002). These observations indicated that Q204E may undergo a different unfolding mechanism compared to WT. Unfolding of a certain portion or of a specific domain may accelerate aggregation of partially unfolded Q204E molecules.

4.3.3 Structure and stability of truncated βB1-crystallins

Another important finding from the current study was that the N- and C-terminal extensions did not contribute to stability of the βB1-crystallin monomers. Both trWT and trQ204E showed very similar denaturation patterns in urea compared to

their full-length proteins, indicating that deamidation has more effect on stability than truncation. The reason for the lack of effect of truncation on stability may be due to overall conservation of secondary structure (Figure 3.21). In truncated βB1-crystallins, the total amount of helical structure decreased, but the amount of β-sheet structure was similar compared to the full-length WT and Q204E (Lampi et al., 2001). This suggested the hydrophobic globular domains of βB1-crystallin were maintained in the absence of the terminal extensions. This was supported by the fact that both truncation and deamidation on βB1-crystallin did not cause a synergistic effect on urea-stability. Concurrent modifications had nearly the same effect as deamidation alone. Similarly, in chick lens βB1-crystallin, no change was observed in dimerization, structure, or heat stability by substitution of the conserved pro-ala-pro-ala region in the N-terminal extension or by deletion of 16 residues from the C-terminal extension (Coop et al., 1998). Therefore, we concluded that stability of βB1-crystallin depends on maintaining the hydrophobic cores in the globular domains, rather than maintaining the hydrophilic terminal extensions.

Another interesting finding was that when the terminal extensions were removed, the secondary structural differences between WT and Q204E decreased. TrWT and trQ204E had almost identical CD spectra. Nuclear magnetic resonance (NMR) studies on the N- and C-terminal extensions in WT βB1-crystallin revealed high flexibility, while in deamidated βB1-crystallin, Q204E, the N-terminal extension was less flexible (Lampi et al., 2002). This suggested that the

hydrophilic N-terminal extension in Q204E may have an ionic interaction with glutamic acid-204 in the C-terminal domain. These observations indicated that the less flexible N-terminal extension of Q204E may contribute to changes in secondary structure of Q204E.

The extensions in β-crystallins were suggested to stabilize proteins or to facilitate self-association or dimerization in the βA3/A1-crystallins (Hope, Chen & Hejtmancik, 1994) and in βB2-crystallin aggregates (Trinkl, Glockshuber & Jaenicke, 1994). However, other studies showed that the N-terminal extension was not involved in homo- or hetero-dimerization of βA3/A1-crystallins (Werten et al., 1996, and Sergeev, Wingfield, & Hejtmancik, 2000). Nalini et al. (1994) demonstrated by X-ray crystallography that the N-terminal extension in βB2-crystallin played a major role in directing interactions between tetramers. In their study, one of the N-terminal extensions showed interaction with a hydrophobic area on the N-terminal globular domain of another tetramer. In aged lens, βB1-crystallin loses the N-terminal extension. Truncated βB1-crystallin is mostly associated with the βL fraction on gel filtration chromatography, whereas full-length βB1-crystallin is present in βH fraction (Ajaz et al., 1997). Recent studies with truncated βB1-crystallins also support the idea that extensions may affect association of proteins. Lampi et al. (2001) and Bateman, Lubsen & Slingsby (2001) showed delayed elution of truncated βB1-crystallin dimers during size exclusion chromatography, suggesting that loss of the extensions changed association with the column matrix. At certain concentrations over 5 mg/ml, truncation of βB1-crystallin promoted

aggregation compared to WT βB1-crystallin (Bateman, Lubsen & Slingsby, 2001). This indicates that the extensions in βB1-crystallin may be involved in oligomerization rather than stability.

4.3.4 Stability of βB1-crystallin

βB1-crystallin contains eight trytophan and nine tyrosine residues. These contribute to the maximum absorption at 283 nm for the tryptophan residues and to the shoulder at 290 nm for tyrosine residues. The fluorescence emission of WT is mostly due to tryptophan residues. All of the aromatic amino acids were retained in the modified βB1-crystallin proteins used in the present study. Deamidation on the C-terminal domain, truncation of 47 residues from the N-terminus, and truncation of 5 amino acids from the C-terminus do not affect the pattern of UV-absorption and fluorescence emission in comparison to WT. This suggests that the tryptophans have a similar surrounding environment and indicates that overall structure of these modified proteins were similar to WT. Differences in both absorption and emission intensities among WT and the modified proteins indicated slight changes in conformation of proteins, resulting in different degrees of fluorescence quenching from tryptophans.

Among β-crystallins, βB2-crystallin has a high sequence homology to βB1-crystallin, for which the 3-D structure has already been studied. When βB2-

crystallin and βB1-crystallin sequences were aligned, the aromatic amino acids were well conserved showing 55% homology. Sequence alignment also showed that several tyrosine and phenylalanine residues in βB2-crystallin were replaced with tryptophan in βB1-crystallin yielding more tryptophan in βB1-crystallin. Based on βB2-crystallin crystallography structure, most tryptophans in βB1 would be located in the inner part of C-terminal domain, while a few would be located on the C-terminal domain surface. WT βB1-crystallin is fully denatured in a fairly high concentration of urea, 7.5 M, compared to βB2-crystallin which is fully denatured at 5 M urea (Trinkl, Glockshuber, and Jaenicke, 1994). Increased fluorescence intensity in the unfolding state may indicate exposure of tryptophan in a less quenching environment. WT βB1-crystallin seems to be denatured by urea without an intermediate step, while βB2-crystallin dimer showed two transitions. During the first transition, βB2-crystallin dimers dissociated yielding monomers with the N-terminal domain unfolded. Then, during the second transition, the partially unfolded βB2-crystallin became completely unfolded by unfolding of the C-terminal domain (Wieligmann, Mayr, and Jaenicke, 1999). The protein concentration used for βB1-crystallin fluorescence studies was 1 μM where proteins are most likely monomers. At 18 μM concentration where proteins are likely dimers, WT βB1-crystallin still had similar fluorescence emission to that at 1 μM, which showed a one-step transition. Thus, both of N- and C-terminal domains in WT βB1-crystallin may be denatured in urea simultaneously.

In summary, deamidation of glutamine-204 in a hydrophobic region of βB1-crystallin caused instability, while loss of the N- and the C-terminal extensions of βB1-crystallin did not affect stability. Therefore, for stability of βB1-crystallin, hydrophobic domains must be preserved. Perturbation of the hydrophobic cores by a post-translational modification such as deamidation may lead to destabilization of protein and formation of cataract.

4.3.5 Heat-stability of βB1-crystallins

In a non-equilibrium stability study using heat denaturation, Q204E showed more accelerated aggregation/precipitation compared to WT (Lampi et al., 2002). Q204E required more αA-crystallin to prevent heat aggregation. These results suggested that two factors may influence the stability of WT βB1-crystallin. First, undisrupted hydrophobic cores in the N- and C-terminal globular domains are necessary for solubility. Secondly, the flexible extensions promote solubility. To test the validity of these two ideas, full-length βB1-crystallins were proteolyzed by calpain 2. This resulted in truncation of the N- and C-terminal extensions. The stability of truncated βB1-crystallins was then tested.

When the terminal extensions were removed, trWT showed similar aggregation to WT during heating, suggesting that the extensions were not critical for solubility. However, trWT required more αA-crystallin compared to WT to prevent further

aggregation. This indicated that the presence of flexible terminal extensions were critical to maintaining solubility of trWT-αA complex. Truncated and deamidated βB1-crystallin (trQ204E) showed the most precipitation in heat and required much higher amounts of αA-crystallin to maintain the trQ204E-αA complex in solution. These results indicated that truncation and deamidation caused a synergistic effect on βB1-crystallin stability during heating.

Therefore, the extensions in βB1-crystallin were critical for maintaining the solubility of βB1-αA complex during heating. This indicated that the terminal extensions were important for interaction with other crystallins and for maintaining the solubility of crystallin complexes. This could have important implications *in vivo*, where αA-crystallin undergoes loss of chaperone function with age (Kramps et al., 1978; Groenen et al., 1994; Takemoto, 1995).

5 CONCLUSIONS

In current studies, we found that expression of calpains, calpastatin, and caspase 3 did not change in epithelium during selenite cataract formation, although activation of calpains and caspase 3 did occur. Thus, activation of these enzymes at the protein level may cause epithelial apoptosis or cell damage during selenite cataract formation. Surprisingly, epithelial proteins were very resistant to sulfhydryl oxidation. The proteins were vulnerable to proteolysis, indicating a significant role of calpains in the epithelium during cataract formation.

During selenite cataract formation, calpain 10 was degraded gradually in epithelium and rapidly in the nucleus. When calpain 10 was incubated with activated calpain 2 or Lp82, calpain 10 underwent degradation, indicating that calpain 10 may be a substrate for calpain 2 and Lp82. From this observation, we concluded that degradation of calpain 10 in selenite cataract was a result of proteolytic activity by calpain 2 and Lp82 rather than by calpain 10 autolysis.

Deamidation on βB1-crystallin caused a dramatic decrease in stability in urea and heat. Surprisingly, the terminal extensions on βB1-crystallin did not appear to be critical for protein stability. However, truncation of the extensions caused altered solubility when associated with the molecular chaperone, αA-crystallin, upon heating. Concurrent truncation and deamidation caused a synergistic effect on heat instability and altered association with αA-crystallin. These results

indicated that the terminal extensions on βB1-crystallin are essential for association with other crystallins and for solubility of the aggregates. Therefore, we concluded that proteolysis and deamidation of crystallins were crucial factors contributing to cataract formation by disrupting protein stability and association with other crystallins.

BIBLIOGRAPHY

Abe, K., Kawagoe, J., Itoyama, Y., and Kogure, K. (1996) Isolation of an ischemia-induced gene and early disturbance of mitochondrial DNA expression after transient forebrain ischemia. *Adv. Neurol.* 71, 485-503.

Ajaz, M. S., Ma, Z., Smith, D. L., and Smith, J. B. (1997) Size of human lens β-crystallin aggregates is distinguished by N-terminal truncation of βB1, *J. Biol. Chem.* 272, 11250-11255.

Alcala, J., and Maisel, H. (1985) Biochemistry of lens plasma membranes and cytoskeleton, in *The Ocular Lens* (Maisel, H., Ed.), pp 169-222, Marcel Dekker, Inc., New York.

Anderson, R. S., Shearer, T. R., and Claycomb, C. K. (1986) Selenite-induced epithelial damage and cortical cataract. Curr. Eye Res. 5, 53-61.

Augusteyn, R. C. (1981) Protein modification in cataract: Possible oxidative mechanisms, in *Mechanisms of cataract formation in the human lens* (Duncan, G., Ed.), pp71-115, Academic Press, New York.

Azuma, M., David, L. L., and Shearer, T. R. (1991) Cysteine protease inhibitor E64 reduces the rate of formation of selenite cataract in the whole animal. *Curr. Eye Res.* 10, 657-666.

Azuma, M., David, L. L., and Shearer, T. R. (1992) Superior prevention of calcium ionophore cataract by E64d. *Biochim. Biophys. Acta* 1180, 215-220.

Azuma, M., Fukiage, C., David, L. L., and Shearer, T. R. (1997) Activation of calpain in lens: A review and proposed mechanism. *Exp. Eye Res.* 64, 529-538.

Bateman, O. A., Lubsen, N. H., and Slingsby, C. (2001) Association behaviour of human βB1-crystallin and its truncated forms. *Exp. Eye. Res.* 73, 321-331.

Bax, B., Lapatto, R., Nalini, V., Driessen, H., Lindley, P. F., Mahadevan, D., Blundell, T. L., and Slingsby, C. (1990) X-ray analysis of βB2-crystallin and evolution of oligomeric lens proteins. *Nature* 347, 776-780.

Bayer, E. A., Safars, M., and Wilchek, M. (1987) Selective labeling of sulfhydryls and disulfides on blot transfers using avidin-biotin technology: Studies on purified proteins and erythrocyte membranes. *Anal. Biochem.* 161, 262-271.

Becquet, F., Courtois, Y., and Goureau, O. (1997) Nitric oxide in the eye: Multifaceted roles and diverse outcomes. *Surv. Ophthalmol.* 42, 71-82.

Berman, E. R. (1991) Lens, in *Biochemistry of the eye*, pp 201-290, Plenum Press, New York.

Blunt, D. S., and Takemoto, L. (2000) Inhibition of selenite cataract by S-diethylsuccinyl glutathione isopropyl ester. *Curr. Eye Res.* 20, 341-345.

Boyle, D. L., Blunt, D. S., and Takemoto, L. J. (1997) Confocal microscopy of cataracts from animal model systems: Relevance to human nuclear cataract. *Exp. Eye Res.* 64, 565-572.

Boyle, D. L., and Takemoto, L. J. (1997) Confocal microscopy of human lens membranes in aged normal and nuclear cataracts. *Invest. Ophthalmol. Vis. Sci.* 38, 2826-2832.

Braun, C., Engel, M., Theisinger, B., Welter, C., and Seifert, M. (1999) CAPN 8: isolation of a new mouse calpain-isoenzyme. *Biochem. Biophys. Res. Commun.* 260, 671-675.

Bunce, G. F., Hess, J. L., and Batra, R. (1984) Lens calcium and selenite-induced cataract. *Curr. Eye Res.* 3, 315-320.

Cenedella, R. J. (1987) Direct chemical measurement of DNA synthesis and net rates of differentiation of rat lens epithelial cells in vivo: applied to the selenium cataract. *Exp Eye Res.* 44, 677-690.

Chakrapani, B., Yedavally, S., Leverenz, V., Giblin, F. J., and Reddy, V. N. (1995) Simultaneous measurement of reduced and oxidized glutathione in human aqueous humor and cataracts by electrochemical detection. *Ophthalmic Res.* 27, 69-77.

Cheng, H. M., and Chylack, Jr., L. T. (1985) Lens metabolism, in *The Ocular Lens* (Maisel, H., Ed.), pp 169-222, Marcel Dekker, Inc., New York.

Chylack, Jr., L. T. (1981) Sugar cataracts – possibly the beginning of medical anti-cataract therapy, in *Mechanisms of cataract formation in the human lens* (Duncan, J., Ed.), pp237-252, Academic Press, New York.

Clark, J. I., Matsushima, H., David, L. L., and Clark, J. M. (1999) Lens cytoskeleton and transparency: a model. *Eye* 13, 417-424.

Clark, J. I., and Steele, J. E. (1992) Phase-separation inhibitors and prevention of selenite cataract. *Proc. Natl. Acad. Sci.* 89, 1720-1724.

Cibelli, G., Policastro, V., Rossler, O. G., and Thiel, G. (2002) Nitric oxide-induced programmed cell death in human neuroblastoma cells is accompanied by the synthesis of Egr-1, a zinc finger transcription factor. *J. Neurosci. Res.* 67, 450-460.

Compton, L. A., Mathews, C. K., and Johnson, W. C. Jr. (1987) The conformation of T4 bacteriophage dihydrofolate reductase from circular dichroism. *J. Biol. Chem.* 262, 13039-13043.

Coop, A., Goode, D., Sumner I., and Crabbe, M. J. (1998) Effects of controlled mutations on the N- and C-terminal extensions of chick lens beta B1 crystallin. *Graefes. Arch. Clin. Exp. Ophthalmol.* 236, 146-150.

D'Aurelio, M., Pallotti, F., Barrientos, A., Gajewski, C. D., Kwong, J. Q., Bruno, C., Beal, M. F., and Manfredi, G. (2001) In vivo regulation of oxidative phosphorylation in cells harboring a stop-codon mutation in mitochondrial DNA-encoded cytochrome c oxidase subunit I. *J. Biol. Chem.* 276, 46925-46932.

David, L. L., Lampi, K. J., Lund, A. L., and Smith, J. B. (1996) The sequence of human βB1-crystallin cDNA allows mass spectrometric detection of βB1 protein missing portions of its N-terminal extension. *J. Biol. Chem.* 271, 4273-4279.

David, L. L., and Shearer, T. R. (1984a) State of sulfhydryl in selenite cataract. *Toxicol. Appl. Pharmacol.* 74, 109-115.

David, L. L., and Shearer, T. R. (1984b) Calcium-activated proteolysis in the lens nucleus during selenite cataractogenesis. *Invest. Ophthalmol. Vis. Sci.* 25, 1275-1283.

David, L. L., and Shearer, T. R. (1986) Purification of calpain II from rat lens and determination of endogenous substrates. *Exp. Eye Res.* 42, 227-238.

David, L. L., and Shearer, T. R. (1993) β-Crystallins insolubilized by calpain II *in vitro* contain cleavage sites similar to β-crystallins insolubilized during cataract. *FEBS Lett.* 324, 265-270.

David, L. L., Shearer, T. R., and Shih, M. (1993) Sequence analysis of lens β-crystallins suggests involvement of calpain in cataract formation. *J. Biol. Chem.* 268, 1937-1940.

David, L. L., Vamum, M. D., Lampi, K. J., and Shearer, T. R. (1989) Calpain II in human lens. *Invest. Ophthalmol. Vis. Sci.* 30, 269-275.

David, L. L., Wright, J. W., and Shearer, T. R. (1992) Calpain II induced insolubilization of lens beta-crystallin polypeptides may induce cataract. *Biochim. Biophys. Acta* 1139, 210-216.

Delaye, M., and Tardieu, A. (1983) Short-range order of crystallin proteins accounts for eye lens transparency. *Nature* 302, 415-417.

Derham, B. K., and Harding, J. J. (1999) α-crystallin as a molecular chaperone. *Prog. Ret. Eye Res.* 18, 463-509.

Dilsiz, N., Olcucu, A., and Atas, M. (2000) Determination of calcium, sodium, potassium and magnesium concentrations in human senile cataractous lenses. *Cell Biochem. Funct.* 18, 259-262.

Drew, B., and Leeuwenburgh, C. (2002) Aging and the role of reactive nitrogen species. *Ann. N. Y. Acad. Sci.* 959, 66-81.

Fukiage, C., Azuma, M., Nakamura, Y., Tamada, Y., Nakamura, M., and Shearer, T. R. (1997a) SJA6017, a newly synthesized peptide aldehyde inhibitor of calpain: Amelioration of cataract in cultured rat lenses. *Biochim. Biophys. Acta.* 1361, 304-312.

Fukiage, C., Azuma, M., Nakamura, Y., Tamada, Y., and Shearer, T. R. (1997b) Calpain-induced light scattering by crystallins from three rodent species. *Exp. Eye Res.* 65, 757-770.

Fukiage, C., Azuma, M., Nakamura, Y., Tamada, Y., and Shearer, T. R. (1998) Nuclear cataract and light scattering in cultured lenses from guinea pig and rabbit. *Curr. Eye Res.* 17, 623-635.

Fukiage, C., Nakajima, E., Ma, H., Azuma, M., and Shearer, T. R. (2002) Characterization and regulation of lens-specific calpain Lp82. *J. Biol. Chem.* 277, 20678-20685.

Giblin, F. J. (2000) Glutathione: A vital lens antioxidant. *J. Ocul. Pharmacol. Ther.* 16, 121-135.

Giblin, F. J., McCready, J. P., Reddan, J. R., Dziedzic, D. C., and Reddy, V. N. (1985) Detoxification of hydrogen peroxide by cultured rabbit lens epithelial cells: Participation of the flutathione redox cycle. *Exp. Eye Res.* 40, 827-840.

Graw, J. (1997) The crystallins: Genes, proteins and diseases. *Biol. Chem.* 378, 1331-1348.

Groenen, P., Merck, K., de Jong, W., and Bloemendal, H. (1994) Structure and modifications of the junior chaperone α-crystallin: From lens transparency to molecular pathology. *Eur. J. Biochem.* 225, 1-19.

Gupta, S. K., and Joshi, S. (1994) Role of naproxen as anti-oxidant in selenite cataract. *Ophthalmic Res.* 26, 226-231.

Hanson, R. A. S., Hasan, A., Smith, D. L., and Smith, J. B. (2000) The major in vivo modifications of the human water-insoluble lens crystallins are disulfide bonds, deamidation, methionine oxidation and backbone cleavage. *Exp. Eye Res.* 71, 195-207.

Harding, J. (1991a) The normal lens, in *Cataract: biochemistry, epidemiology, and pharmacology*, pp1-70, Chapman & Hall, New York.

Harding, J. (1991b) Experimental opacification of the lens *in vivo* and *in vitro*, in *Cataract: biochemistry, epidemiology, and pharmacology*, pp125-194, Chapman & Hall, New York.

Harding, J. (1991c) The aging lens, in *Cataract: biochemistry, epidemiology, and pharmacology*, pp71-82, Chapman & Hall, New York.

Harding, J. (1991d) Human cataract, in *Cataract: biochemistry, epidemiology, and pharmacology*, pp195-217, Chapman & Hall, New York.

Hightower, K. R., David, L. L., and Shearer, T. R. (1987) Regional distribution of free calcium in selenite cataract: Relation to calpain II. *Invest. Ophthalmol. Vis. Sci.* 28, 1702-1706.

Hiraoka, T., Clark, J. I., Li, X. Y., and Thurston, G. M. (1996) Effect of selected anti-cataract agents on opacification in the selenite cataract model. *Exp. Eye Res.* 62, 11-19.

Hope, J. N., Chen, H. C., and Hejtmancik, J. F. (1994) βA3/A1-crystallin association: Role of the N-terminal arm. *Protein Eng.* 7, 445-451.

Horikawa, Y., Oda, N., Cox, N. J., Li, X., Orho-Melander, M., Hara, M., Hinokio, Y., Lindner, T. H., Mashima, H., Schwarz, P. E. H., del Bosque-Plata, L., Horikawa, Y., Oda, Y., Yoshiuchi, I., Colilla, S., Polonsky, K. S., Wei, S., Concannon, P., Iwasaki, N., Schulze, J., Baier, L. J., Bogardus, C., Groop, L., Boerwinkle, E., Hanis, C. L., and Bell, G. I. (2000) Genetic variation in the gene encoding calpain-10 is associated with type 2 diabetes mellitus. *Nat. Genet.* 26, 163-175.

Huang, L. L., Hess, J. L., and Bunce, G. E. (1990) DNA damage, repair, and replication in selenite-induced cataract in rat lens. *Curr. Eye Res.* 9, 1041-1050.

Huang, L. L., Zhang, C. Y., Hess, J. L., and Bunce, G. E. (1992) Biochemical changes and cataract formation in lenses from rats receiving multiple, low doses of sodium selenite. *Exp. Eye Res.* 55, 671-678.

Huang, Y., and Wang, K. K. W. (2001) The calpain family and human disease. *Trends Mol. Med.* 7, 355-362.

Hum, T. P., and Augusteyn, R. C. (1987a) The nature of disulphide bonds in rat lens proteins. *Curr. Eye Res.* 6, 1103-1108.

Hum, T. P., and Augusteyn, R. C. (1987b) The state of sulfhydryl groups in proteins isolated from normal and cataractous human lenses. *Curr. Eye Res.* 6, 1091-1101.

Ito, Y., Cai, H., Terao, M., and Tomohiro, M. (2001a) Preventive effect of diethyldithiocarbamate on selenite-induced opacity in cultured rat lenses. *Ophthalmic Res.* 33, 52-59.

Ito, Y., Nabekura, T., Takeda, M., Nakao, M., Terao, M., Hori, R., and Tomohiro, M. (2001b) Nitric oxide participates in cataract development in selenite-treated rats. *Curr. Eye Res.* 22, 215-220.

Karlsson, J.-O., Anderson, M., Kling-Petersen, A., and Sjostrand, J. (1999) Proteolysis in human lens epithelium determined by a cell-permeable substrate. *Invest. Ophthalmol. Vis. Sci.* 40, 261-264.

Kim, Y. H., Kapfer, D. M., Boekhorst, J., Lubsen, N. H., Bachinger, H. P., Shearer, T. R., David, L. L., Feix, J. B., and Lampi, K. J. (2002) Deamidation, but not truncation, decreases the urea-stability of a lens structural protein, βB1-crystallin. *Biochemistry* submitted.

Lampi, K. J., Kim, Y. H., Bachinger, H. P., Boswell, B., Lindner, R. A., Carver, J. A., Shearer, T. R., David, L. L., and Kapfer, D. M. (2002) Decreased heat stability and increased chaperone requirement of modified human βB1-crystallins. *Mol. Vis.* Submitted.

Lampi, K. J., Ma, Z., Hanson, S. R. A., Azuma, M., Shih, M., Shearer, T. R., Smith, D. L., Smith, J. B., and David L. L. (1998) Age-related changes in human lens crystallins identified by two-dimensional electrophoresis and mass spectrometry. *Exp. Eye Res.* 67, 31-43.

Lampi, K. J., Oxford, J. T., Bachinger, H. P., Shearer, T. R., David, L. L., and Kapfer, D. M. (2001) Deamidation of human βB1 alters the elongated structure of the dimer. *Exp. Eye Res.* 72, 279-288.

Li, W.-C., Kuszak, J. R., Dunn, K., Wang, R. R., Wang, G. M., Spector, A., Leib, M., Cotliar A. M., Weiss, M., Espy, J., Howard, G., Farris, R.L., Auran, J., Donn, A., Hofeldt, A., Mackay, C., Merriam, J., Mittl, R., and Smith, T. R. (1995a) Lens

epithelial cells apoptosis appears to be a common cellular basis for non-congenital cataract development in humans and animals. *J. Cell Biol.* 130, 169-181.

Li, W.-C., Kuszak, J. R., Wang, G.-M., Wu, Z.-Q., and Spector, A. (1995b) Calcimycin-induced lens epithelial cell apoptosis contributes to cataract formation. *Exp. Eye Res.* 61, 91-98.

Liang, J. N., and Pelletier, M. R. (1987) Spectroscopic studies on the mixed disulphide formation of lens crystallin with glutathione. *Exp. Eye Res.* 45, 197-206.

Lindley, P. F., Narebor, M. E., Summers, L. J., and Wistow, G. J. (1985) The structure of lens proteins, in *The Ocular Lens* (Maisel, H., Ed.), pp 123-167, Marcel Dekker, Inc., New York.

Lund, A. L., Smith, J. B., and Smith, D. L. (1996) Modifications of the water-insoluble human lens α-crystallins. *Exp. Eye Res.* 63, 661-672.

Ma, H., Fukiage, C., Azuma, M., and Shearer, T. R. (1998a) Cloning and expression of mRNA for calpain Lp82 from rat lens: Splice variant of p94. *Invest. Ophthalmol. Vis. Sci.* 39, 454-461.

Ma, H., Fukiage, C., Kim, Y. H., Duncan, M. K., Reed, N. A., Shih, M., Azuma, M., and Shearer, T. R. (2001) Characterization and expression of calpain 10. *J. Biol. Chem.* 276, 28525-28531.

Ma, H., Hata, I., Shih, M., Fukiage, C., Nakamura, Y., Azuma, M., and Shearer, T. R. (1999) Lp82 is the dominant form of calpain in young mouse lens. *Exp. Eye Res.* 68, 447-456.

Ma, H., Shih, M., Fukiage, C., Azuma, M., Duncan, M. K., Reed, N. A., Richard, I., Beckmann, J. S., and Shearer, T. R. (2000b) Influence of specific regions in Lp82 calpain on protein stability, activity, and localization within lens. *Invest. Ophthalmol. Vis. Sci.* 41, 4232-4239.

Ma, H., Shih, M., Hata, I., Fukiage, C., Azuma, M., and Shearer, T. R. (1998b) Protein for Lp82 calpain is expressed and enzymatically active in young rat lens. *Exp. Eye Res.* 67, 221-229.

Ma, H., Shih, M., Hata, I., Fukiage, C., Azuma, M., and Shearer, T. R. (2000a) Lp85 calpain is an enzumatically active rodent-specific isozyme of lens Lp82. *Curr. Eye Res.* 20, 183-189.

Ma, H., Shih, M., Throneberg, D. B., David, L. L., and Shearer, T. R. (1997) Changes in Calpain II mRNA in young rat lens during maturation and cataract formation. *Exp. Eye Res.* 64, 437-445.

Ma, Z., Hanson, S. R .A., Lampi, K. J., David, L. L., Smith, D. L., and Smith, J. B. (1998) Age-related changes in human lens crystallins identified by HPLC and mass spectrometry. *Exp. Eye Res.* 67, 21-30.

Martin, S. J., O'Brien, G. A., Nishioka, W. K., McGahon, A. J., Mahboubi, A., Saido, T. C., and Green, D. R. (1995) Proteolysis of fodrin (non-erythroid spectrin) during apoptosis. *J. Biol. Chem.* 270, 6425-6428.

Matsushima, H., David, L. L., Hiraoka, T., Clark, J. I. (1997) Loss of cytoskeletal proteins and lens cell opacification in the selenite cataract model. *Exp. Eye Res.* 64, 387-395.

McAvoy, J. W. (1981) Developmental biology of the lens, in *Mechanisms of cataract formation in the human lens* (Duncan, G., Ed.), pp7-46, Academic Press, New York.

Mitton, K. P., Hess, J. L., and Bunce, G. E. (1997) Free amino acids reflect impact of selenite-dependent stress on primary metabolism in rat lens. *Curr. Eye Res.* 16, 997-1005.

Miura, M., Zhu, H., Rotello, R., Hartwieg, E. A., and Yuan, J. (1993) Induction of apoptosis in fibroblasts by IL-1 beta-converting enzyme, a mammalian homolog of the C. elegans cell death gene ced-3. *Cell* 75, 653-660.

Nakajima, T., Nakajima, E., Fukiage, C., Azuma, M., and Shearer, T. R. (2002) Differential gene expression in the lens epithelial cells from selenite injected rats. *Exp. Eye Res.* 74, 231-236.

Nakamura, Y., Fukiage, C., Ma, H., Shih, M., Azuma, M., and Shearer, T. R. (1999) Decreased sensitivity of lens-specific calpain Lp82 to calpastatin inhibitor. *Exp. Eye Res.* 69, 155-162.

Nakamura, Y., Fukiage, C., Shih, M., Ma, H., David, L. L., Azuma, M., and Shearer, T. R. (2000) Contribution of calpain Lp82-induced proteolysis to experimental cataractogenesis in mice. *Invest. Ophthalmol. Vis. Sci.* 41, 1460-1466.

Nalini, V., Bax, B., Driessen, H., Moss, D. S., Lindley, P. F., and Slingsby, C. (1994) Close packing of an oligomeric eye lens beta-crystallin induces loss of symmetry and ordering of sequence extensions. *J. Mol. Biol.* 236, 1250-1258.

Nicholson, D. W., Ali, A., Thornberry, N. A., Vaillancourt, J. P., Ding, C. K., Gallant, M., Gareau, Y., Griffin, P. R., Labelle, M., Lazebnik, Y. A., et al. (1995) Identification and inhibition of the ICE/CED-3 protease necessary for mammalian apoptosis. *Nature* 376, 37-43.

Ostadalova, I., Babicky, A., and Kopoldova, J. (1988) Selenium metabolism in rats after administration of toxic doses of selenite. *Physiol. Bohemosolv.* 37, 159-164.

Ottonello, S., Foroni, C., Carta, A., Petrucco, S., and Maraini, G. (2000) Oxidative stress and age-related cataract. *Ophthalmologica* 214, 78-85.

Patmore, L., and Duncan, G. (1981) The physiology of lens membranes, in *Mechanisms of cataract formation in the human lens* (Duncan, G., Ed.), pp193-217, Academic Press, New York.

Rafferty, N. S. (1985) Lens morphology, in *The Ocular Lens* (Maisel, H., Ed.), pp 1-60, Marcel Dekker, Inc., New York.

Ragno, S., Estrada-Garcia, I., Butler, R., and Colston, M. J. (1998) Regulation of macrophage gene expression by *Mycobacterium tuberculosis*: Down-regulation of mitochondrial cytochrome c oxidase. *Infect. Immun.* 66, 3952-3958.

Rao, G. N., Sadasivudu, B., and Coltier, E. (1983) Studies on glutathione S-transferase, glutathione peroxidase and glutathione reductase in human normal and cataractous lenses. *Ophthalmic Res.* 15, 173-179.

Reddan, J. R., Giblin, F. J., Kadry, R., Leverenz, V. R., Pena, J. T., and Dziedzic, D. C. (1999) Protection from oxidative insult in glutathione depleted lens epithelial cells. *Exp. Eye Res.* 68, 117-127.

Rogers, K. R., Morris, C. J., and Blake, D. R. (1991) Oxidation of thiol in the vimentin cytoskeleton. *Biochem. J.* 275, 789-791.

Sanderson, J., Marcantonio, J. M., and Duncan, G. (2000) A human lens model of cortical cataract: Ca^{2+}-induced protein loss, vimentin cleavage and opacification. *Invest. Ophthalmol. Vis. Sci.* 41, 2255-2261.

Sergeev, Y. V., Wingfield, P. T., and Hejtmancik, J. F. (2000) Monomer-dimer equilibrium of normal and modified βA3-crystallins: Experimental determination and molecular modeling. *Biochemistry* 39, 15799-15806.

Shearer, T. R., Azuma, M., David, L. L., and Murachi, T. (1991) Amelioration of cataracts and proteolysis in cultured lenses by cysteine protease inhibitor E64. *Invest. Ophthalmol. Vis. Sci.* 32, 533-540.

Shearer, T. R., and David, L. L. (1982) Role of calcium in selenite cataract. *Curr. Eye Res.* 2, 777-784.

Shearer, T. R., David, L. L., and Anderson, R. S. (1986) Selenite decreases phase separation temperature in rat lens. *Exp. Eye Res.* 42, 503-506.

Shearer, T. R., David, L. L., and Anderson, R. S. (1987) Selenite cataract: A review. *Curr. Eye Res.* 6, 289-300.

Shearer, T. R., Ma, H., Fukiage, C., and Azuma, M. (1997) Selenite nuclear cataract: Review of the model. *Mol. Vis.* 3, 8.

Shearer, T. R., Ma, H., Shih, M., Fukiage, C., and Azuma, M. (2000) Calpains in the lens and cataractogenesis. *Methods Mol. Biol.* 144, 277-285.

Shearer, T. R., Ma, H., Shih, M., Hata, I., Fukiage, C., Nakamura, Y., and Azuma, M. (1998) Lp82 calpain during rat lens maturation and cataract formation. *Curr. Eye Res.* 17, 1037-1043.

Shearer, T. R., Shih, M., Azuma, M., and David, L. L. (1995) Precipitation of crystallins from young rat lens by endogenous calpain. *Exp. Eye Res.* 61, 141-150.

Shih, M., David, L. L., Lampi, K. J., Ma, H., Fukiage, C., Azuma, M., and Shearer, T. R. (2001) Proteolysis by m-calpain enhances in vitro light scattering by crystallins from human and bovine lenses. *Curr. Eye Res.* 22, 458-469.

Slingsby, C., and Clout, N. J. (1999) Structure of the crystallins. *Eye* 13, 395-402.

Spector, A. (1984) The search for a solution to senile cataracts. *Invest. Ophthalmol. Vis. Sci.* 25, 130-146.

Spector, A. (1991) The lens and oxidative stress. In: *Oxidative stress: Oxidants and antioxidants* (Sies, H., Ed.), pp. 529-558. Academic Press, New York.

Squier, M. K., Miller, A. C., Malkinson, A. M., and Cohen, J. J. (1994) Calpain activation in apoptosis. *J. Cell. Physiol.* 159, 229-237.

Takemoto, L. (2001) Deamidation of Asn-143 of γS crystallin from protein aggregates of the human lens. *Curr. Eye Res.* 22, 148-153.

Takemoto, L., and Boyle, D. (1998) Deamidation of specific glutamine residues from αA crystallin during aging of the human lens. *Biochemistry* 37, 13681-13685.

Takemoto, L., and Boyle, D. (2000) Increased deamidation of asparagine during human senile cataractogenesis. *Mol. Vis.* 6, 164-168.

Takemoto, L., Fujii, N., and Boyle, D. (2001) Mechanism of asparagine deamidation during human senile cataractogenesis. *Exp. Eye Res.* 72, 559-563.

Tamada, Y., Fukiage, C., Nakamura, Y., Azuma, M., Kim, Y. H., and Shearer, T. R. (2000) Evidence for apoptosis in the selenite rat model of cataract. *Biochem. Biophys. Res. Commun.* 275, 300-306.

Trinkl, S., Glockshuber, R., and Jaenicke, R. (1994) Dimerization of βB2-crystallin: The role of the linker peptide and the N- and C-terminal extensions. *Protein Sci.* 3, 1392-1400.

Truscott, R. J., Marcantonio, J. M., Tomlinson, J., and Duncan, G. (1989) Calcium-induced cleavage and breakdown of spectrin in the rat lens. *Biochem. Biophys. Res. Commun.* 162, 1472-1477.

Ueda, Y., Fukiage, C., Shih, M., Shearer, T. R., and David, L. L. (2002) Mass measurements of C-terminally truncated α-crystallins from two-dimensional gels identify Lp82 as a major endopeptidase in rat lens. *Mol. Cell Proteomics* 1, 357-365.

Ueda, Y., McCormack, A. L., Shearer, T. R., and David, L. L. (2001) Purification and characterization of lens specific calpain (Lp82) from bovine lens. *Exp. Eye Res.* 2001, 73, 625-637.

Vérétout, F., Delaye, M., and Tardieu, A. (1989) Molecular basis of eye lens transparency. Osmotic pressure and X-ray analysis of α-crystallin solutions. *J. Mol. Biol.* 205, 713-728.

Wang, Z., Bunce, G. E., and Hess, J. L. (1993) Selenite and Ca^{2+} homeostasis in the rat lens: Effect on Ca-ATPase and passive Ca^{2+} transport. *Curr. Eye Res.* 12, 213-218.

Werten, P. J. L., Carver, J. A., Jaenicke, R., and de Jong, W. W. (1996) The elusive role of the N-terminal extension of βA3- and βA1-crystallin. *Protein Eng.* 9, 1021-1028.

Wieligmann, K., Mayr, E.-M., and Jaenicke, R. (1999) Folding and self-assembly of the domains of βB2-crystallin from rat eye lens. *J. Mol. Biol.* 286, 989-994.

Yilmaz, G., Turan, B., Celebi, N., Yilmaz, N, and Demirel Yilmaz, E. (2000) Prevention of selenite-induced opacification and biochemical changes in the rat pup lens through amiloride pretreatment. *Curr. Eye Res.* 20, 454-461.

Yoshida, H., Murachi, T., Tsukahara, I. (1985) Distribution of calpain I, calpain II, and calpastatin in bovine lens. *Invest. Ophthalmol. Vis. Sci.* 26, 953-956.